Hungarian University of Agriculture and Life Sciences

NEAR INFRARED SPECTROSCOPY FOR THE QUALITY ASSESSMENT OF DAIRY PRODUCTS

Mariem Majadi
Budapest
2025

PhD School/ Program

Name:	Doctoral School of Food Science
Field:	Food Science
Head:	**Lívia Simon Sarkadi, DSc**
	Department of Nutrition
	Institute of Food Science and Technology
	Hungarian University of Agriculture and Life Sciences

Supervisors:

Zoltan Kovacs, PhD

Department of Food Measurements and Process Control, Institute of Food Science and Technology, Hungarian University of Agriculture and Life Sciences

András Szabó, DSc

Institute of Physiology and Animal Nutrition, Department of Animal Physiology and Health, Hungarian University of Agriculture and Life Sciences

The applicant met the requirement of the Ph.D. regulations of the Hungarian University of Agriculture and Life Sciences and the thesis is accepted for the defense process.

....

Head of Doctoral School Supervisor

TABLE OF CONTENTS

LIST OF ABBREVIATIONS

ALA: α-linolenic acid

ANN: Artificial Neural Networks

ANOVA: Analysis Of Variance

ATR-FTIR: Attenuated Total Reflectance-Fourier Transform Infrared

aw: water activity

BHT: Butylated Hydroxytoluene

BPNN: Back-Propagation Neural Network

CIE: Commission Internationale de la Éclargie

CLA: Conjugated Linoleic Acid

CP: Conducting Polymers

CRM: Certified Reference Material

C-S: Closest Sensors

CV: Cross-Validation

DD- SIMCA: Data-Driven Soft Independent Modeling by Class Analogy

DeTr: de-trending

TMR: Total Mixed Ration

DHA: Docosahexaenoic Acid

DIM: Days In Milk

E-nose: Electronic nose

EPA: Eicosapentaenoic Acid

FAs: Fatty Acids

FID: Flame Ionization Detectors

IDF: International Dairy Federation

ISO: International Organisation for Standardisation

KS: Kolmogorov–Smirnov

LAB: Lactic Acid Bacteria

LDA: Linear Discriminant Analysis

LV: Latent Variables

LVF: Linear Variable Filter

MIR: Mid- Infrared

MSC: Multiplicative Scatter Correction

MUFAs: Monounsaturated fatty acids

NIR: Near-Infrared

NIRS: Near-Infrared Spectroscopy

OC-PLS: One-Class Partial Least Squares

PCA: Principal Component Analysis

PCA-LDA: Principal Component Analysis -based Linear Discriminant Analysis

PCs: Principal Components

PDO: Protected Designation of Origin

PGI: Protected Geographical Indication

PLS-DA: Partial Least Squares-Discriminant Analysis

PLSR: Partial Least Squares Regression

PUFAs: Polyunsaturated Fatty Acids

R^2C: Coefficient of Determination

R^2CV: Coefficient of Determination for Cross-Validation

R^2pr: Coefficient of Determination for Prediction

RF: Random Forest

RMSEC: Root Means Square Error of Calibration

RMSECV: Root Means Square Error of Cross-Validation

RMSEP: Root Means Square Error of Prediction

SCC: Somatic Cell Count

SFAs: Saturated Fatty Acids

Sgolay 2-21-0: Savitzky–Golay second derivative with a 21-point window

SH°: Soxhlet–Henkel degrees

SNV: Standard Normal Variate

SPORT-LDA: Sequential Preprocessing through ORThogonalization Linear Discriminant Analysis

SVM: Support Vector Machines

SVR: Support Vector Regression

TBC: Total Bacterial Count

TSG: Traditional Specialty Guaranteed

v/v: volume per volume

VOCs: Volatile Organic Compounds

WPCs: whey protein concentrates

1. INTRODUCTION

The dairy industry has experienced remarkable technological advancements and considerable growth in recent decades (Barkema et al., 2015). Consumers are becoming more-and-more attracted towards safe, nutritious and high-quality food products, and are willing to pay more than the normal price (Di Rosa et al., 2017). Food quality is typically defined by traceable origin, known chemical composition, appropriate physical characteristics, acceptable sensory evaluation, safety and health measures regarding microbiological properties and toxic contamination, all of which are affected by processing and storage (Hew et al., 2024; Ray, 2023). Ensuring food quality has led to the demand for efficient and accurate analytical methods to promote fair competition among producers and safeguard consumer rights.

Global milk production is expected to grow at an annual rate of 1.7% and to reach 981 million metric tons by 2028 (Bista et al., 2021). Milk consumption is rising rapidly, especially in densely populated and low-income regions where it is the primary protein source due to limited access to other protein-rich foods (Sager et al., 2018). However, challenges such as milk's perishable nature, transportation difficulties, and inadequate refrigeration highlight the need for improved processing efficiency in the dairy industry (Wang et al., 2021; Kapaj & Deci, 2017). To overcome these issues, methods like evaporation and drying are commonly used to extend milk's shelf life by producing milk powders (Zouari et al., 2019). Powdered and liquid milk share similar nutrional benefits but differ in characteristics that suit specific applications. Liquid milk has a creamy texture and shorter shelf life, so it is more suitable for immediate consumption and usage in beverages, frozen desserts and fermented food products. In contrast, powdered milk is characterized by its extended shelf life and lack of refrigeration requirements, hence it is suited for long-term storage, industrial uses, and precise formulations. Its versatility has made it a key ingredient in various dairy and processed foods, including ice cream, yogurt, chocolate, bakery products, and sauces (Tirgarian et al., 2023; Augustin et al., 2003). The quality of milk powders are influenced by their chemical, physical, and functional properties, which are closely interconnected (Schuck, 2011). Key quality indicators consist of the amino acid composition, protein behaviour under varying pH and temperature, insolubility index, titratable acidity, and fat content. Processing conditions such as pH and temperature, significantly affect viscosity and protein stability. Extreme conditions can potentially cause defects like high insolubility index, which can lead to product rejection (Sutariya et al., 2017). Nutritional value, including amino acid profiles, is crucial for applications such as infant formulas and fortified foods (Sharma et al., 2012), while fat content impacts shelf life and

functionality in products like chocolate (Hoppe et al., 2008). Monitoring these parameters ensures optimal quality and application suitability.

Milk, in addition to being a valuable source of protein, contains fat that plays a pivotal role in shaping the nutritional, physical and sensory attributes of milk products (Kholif & Olafadehan, 2022). Milk fat is one of the most complex naturally occurring fats, comprising over 400 distinct fatty acids (Kokić et al., 2024; Tóth et al., 2019). Among these, conjugated linoleic acid isomers (CLA, C18:2) and Omega-3 (ω-3) polyunsaturated fatty acids (PUFAs), particularly, α-linolenic acid (ALA; 18:3 ω-3), eicosapentaenoic acid (EPA; 20:5 ω-3) and docosahexaenoic acid (DHA; 22:6 ω-3) are recognized for their health benefits, including improved cardiovascular health, reduced inflammation and enhanced immune function (Shahidi & Ambigaipalan, 2018; Gebreyowhans et al., 2019). Milk and dairy products contribute approximately 15% of the total fat intake and 25% of the saturated fatty acids (SFAs) consumed in Western diets. Cow's milk fat contains around 2.8-3.7% of PUFAs. However, EPA, DHA and CLA are found in small quantities (Bodkowski et al., 2024; Butler et al., 2019). The FA profile of milk and milk products is influenced by various factors, including breed, season, lactation stage, and most significantly, diet (Magan et al., 2021; Lerch et al., 2015). Enhancing the amount of health-promoting FAs can be achieved through strategic animal feeding practices. These include supplementing diets with vegetable oils, oilseeds and marine lipids (fish oil, marine algae), employing different feed sources (pasture, grass hay and grass silage) and adjusting the feed-to-concentrate ratio (Bodkowski et al., 2024). Such approaches allow for the optimization of milk fat's nutritional profile, amplifying its health-promoting attributes.

Milk is a highly multifunctional product, commonly processed into various forms, with fermented products like yogurt and cheese being the most consumed. The quality of these products is influenced by raw milk composition, fermentation conditions and the type of starter culture used (Rațu et al., 2023). Even slight variations in these parameters can profoundly influence the quality of the final product, altering its sensory characteristics, chemical composition and the shelf life (Alvarez-Hess et al., 2024). These variations have underscored the importance of authenticating the origin of raw and fermented products. This is particularly critical for high-value certified products, such as organic, Protected Designation of Origin (PDO), Protected Geographical Indication (PGI), and Traditional Speciality Guaranteed (TSG) dairy items, which follow strict dietary protocols for certification and premium status (Chaudhary et al., 2022).

Dairy research continues to advance focusing on innovative strategies in areas such as livestock nutrition, milk quality assessment, disease control and the formulation of functional dairy products. This field is inherently multidisciplinary, integrating insights from chemistry, physics,

microbiology, enzymology to address the complexities of milk and its derivatives (Priyashantha & Vidanarachchi, 2024). Researchers are exploring novel methods for milk processing, animal diet management and product manufacturing that prioritize safety, enhance functional and nutritional properties, while maintaining proper traceable origin and chemical composition (Moatsou, 2024). However, milk is an intricate biological substance, with its constituents existing in a dynamic equilibrium. Its complexity underscores the variability in the properties and shelf life of dairy products (Nasralla et al., 2022). Treatments that fail to account for these characteristics risk destabilizing milk and introducing defects in the final products, emphasizing the need for careful and scientifically grounded approaches in dairy innovation. To this end, considerable efforts have been attempted to develop reliable techniques for authenticating and detecting defects. Traditional chromatographic methods focus on analysing milk biomarkers, including fatty acid profiles, volatile compounds, and isotopes (Coppa et al., 2015). Additionally, molecular-based approaches such as genomics, proteomics, and metabolomics have proven valuable in ensuring product authenticity (Haider et al., 2024). However, these techniques often come with limitations, including being time-intensive, destructive, and requiring skilled operators. These challenges highlight the ongoing need for efficient, non-destructive, and user-friendly methods to advance dairy product quality and safety.

Near-Infrared Spectroscopy (NIRS) is a highly accurate and versatile analytical technique that measures the absorption of near-infrared light (800-2500 nm) by a sample, capturing molecular vibrations of compounds containing C-H, N-H, and O-H groups (X. Yang et al., 2020). NIR spectrometers come in various forms, including benchtop, portable, and handheld models, enabling a wide range of applications both on-line and off-line (Yakubu et al., 2022). Over the past decades, NIRS has been extensively used in dairy products analysis, with applications categorized into fraud detection, authentication, and composition analysis. It is fundamental in identifying adulteration practices such as water addition, non-dairy fat substitution, or the use of milk from other species or regions, verifying cow feeding practices and geographic origin, and predicting or quantifying milk composition (Hebling e Tavares et al., 2022; de la Roza-Delgado et al., 2017). This versatility highlights NIRS as a critical tool in guaranteeing the quality, authenticity, and safety of dairy products.

In summary, while many studies have investigated the use of NIRS for authenticating raw milk, there remains a significant research gap regarding its use for fermented milk products and cheese. Specifically, the influence of diverse animal diets on the sensory and chemical properties of the above-mentioned dairy products has not been extensively studied. This a critical area of interest, as diet can profoundly affect the quality and characteristics of these products. Similarly, although

NIRS has been applied to evaluate milk powder quality, there has been limited focus on its application to reconstituted milk due to greater variability, analytical challenges, and less regulatory or industrial focus on the reconstituted product. Detecting defects arising from improper reconstruction represents an underexplored avenue where NIRS could provide significant benefits. Furthermore, the application of NIRS to non-traditional dairy sources, such as camel and mare milk, remains sparse, despite the cultural and nutritional importance of these milk types in various regions and among certain ethnic communities. Addressing these gaps could expand the scope and utility of NIRS in the dairy industry, offering new insights into product quality and authenticity.

2. OBJECTIVES

The main aim of this research was to explore the potential of NIRS and E-nose in identifying and addressing quality deviations/differences across selected dairy food matrices. To achieve this goal, we have established specific research aims designed to systematically investigate and demonstrate the capabilities of NIRS and E-nose:

1. **Evaluation of the quality of reconstituted cow, camel and mare milk samples using NIRS and chemometric techniques:**

   The aim was to thoroughly characterize reconstituted milk samples derived from different animal sources, such as cows, mares, and camels. This involved developing robust prediction models to accurately assess critical quality parameters such as composition and functional attributes. Additionally, the aim was to create classification models to differentiate between reconstituted milk based on their spectral profiles. This included distinguishing among milk samples originating from different species as well as identifying variations arising from diverse reconstruction conditions. By integrating these models, we sought to ensure accurate identification and quality assessment of reconstituted milk, thereby enhancing product standardization and authenticity verification. This focused approach aimed to demonstrate the versatility and efficacy of NIRS in addressing challenges related to dairy product quality while expanding its application to lesser-studied matrices such as mare and camel milk.

2. **Identifying key factors that distinguish fermented milk based on feeding type and probiotic potential with e-nose and NIRS techniques:**

   The aim was to create robust models for fermented milk samples, classified by feeding type and probiotic potential, using data from two distinct techniques: NIRS and e-nose. Additionally, the aim was to identify the key sensors and specific wavelengths that contributed the most to the performance of the classification models. By identifying these factors, we aimed to achieve a better understanding of two key aspects: (1) the difference in the volatile profile and chemical composition between control and experimental fermented milk samples, regardless of the fermentation strain. This enabled a better understanding of how fermentation impacts milk composition independent of the probiotic strain. (2) The strain-specific variations in the chemical and volatile profile between control and experimental samples. This allowed to explore how each probiotic strain uniquely affects the milk's molecular changes and volatile compounds.

3. Evaluation of the impact of cattle feed on cheese ripening process by NIRS

Our objective was to evaluate the effect of cow diets on the ripening characteristics of cheese by employing the NIRS technology to detect chemical changes throughout the ripening process. Using these datasets, we aimed to develop robust classification models that account for variations in feeding type and ripening duration. In addition, we aimed to identify the key wavelengths that contributed most significantly to the accuracy and performance of these models. This analysis offered a more thorough understanding of two key aspects: (1) by examining the chemical compositions of control and experimental cheese samples over a 12-week ripening period, independent of temperature, we sought to understand how dietary changes influence the ripening process and contribute to the development of the cheese distinctive characteristics (2) we aimed to uncover feed-specific effects by revealing how each type of feed uniquely shapes molecular changes in the fresh cheese samples.

3. LITERATURE REVIEW

3.1. Introduction to Near-Infrared Spectroscopy: fundamentals, advantages, limitations and key applications

3.1.1. Fundamentals

In 1800, William Herschel discovered "radiant heat," now known as near-infrared (NIR) radiation, by observing temperature increases beyond the visible red spectrum of sunlight using a blackened bulb thermometer (Agelet & Hurburgh, 2010). However, NIR radiation's analytical applications only emerged over 150 years later due to the limited availability of commercial devices and the complexity of interpreting NIR spectra. Interest in NIR spectroscopy grew in the 1960s, thanks to Karl Norris's pioneering work in analysing moisture and fat in food products (Pasquini, 2018). NIR spectroscopy offered faster and more efficient alternatives to traditional methods, such as moisture determination, which previously relied on time-consuming heating and weighing techniques (Dias et al., 2024).

NIRS is a light-based technology used in various applications (Pellicer & Bravo, 2011). Light is a form of electromagnetic radiation characterized by its wavelength, frequency, and energy. These properties are interconnected, with the energy of light being directly proportional to its frequency and inversely proportional to its wavelength, meaning shorter wavelengths carry higher energy. Light can be arranged according by these properties to form the electromagnetic spectrum (Agelet & Hurburgh, 2010). The infrared region of this spectrum covers wavelengths from 1 nm to 750 nm, corresponding to frequencies between 300 GHz and 400 THz. This region is further subdivided into three distinct zones: the far-infrared (FIR, 300 GHz to 30 THz or 1 nm to 10 μm), the mid-infrared (MIR, 30 THz to 120 THz or 10 μm to 2.5 μm), and the near-infrared (NIR, 120 THz to 400 THz or 2500 nm to 750 nm) (Okparanma et al., 2018). These divisions are based on the varying energy levels and interactions of light within each region. Figure 1 shows the different regions in the electromagnetic spectrum.

When light interacts with a material, molecules can absorb light of certain wavelengths if the energy matches what is needed to transition a molecule from a vibrational state to a higher one. The nature of these interactions varies across different infrared regions, influencing the type of molecular vibrations induced and the absorption characteristics (Parson, 2015). For instance, the far-infrared (FIR) region, which has the lowest energy, is predominantly taken up by heavy atoms such as those in inorganic and organometallic compounds. The mid-infrared (MIR) region, with moderate energy, is widely utilized in organic chemical analyses (Agelet & Hurburgh, 2010).

The near infrared (NIR) region, the most energetic part of the infrared spectrum, is uniquely suited for detecting overtones and combination transitions, known as “forbidden transitions”. These transitions occur with significantly lower probability than the primary transitions typically observed in IR and Raman spectroscopy. Consequently, samples exhibit a lower absorption index in the NIR region, allowing NIR radiation to penetrate deeper into the sample surface, ranging from a few millimetres to a few centimetres and analyse larger sample volume (Grabska et al., 2021).

Spectra generated in the near region comprise overtones, higher-order vibrational transitions to excited energy states, and combination bands resulting from simultaneous molecular vibrations (Aouadi et al., 2020). NIR spectra reveal up to four overtones, though the fourth overtone is weak and typically disregarded. These overtones and bands arise from the absorption of light by various functional groups, including methylene C-H, methyl C-H, carbonyl associated C-H, aromatic C-H, methoxy C-H, N-H from primary and secondary amides, N-H from amides (primary, secondary, and tertiary), N-H of amine salts, O-H (alcohols and water), S-H, and C=O groups (Weyer et al., 2006).

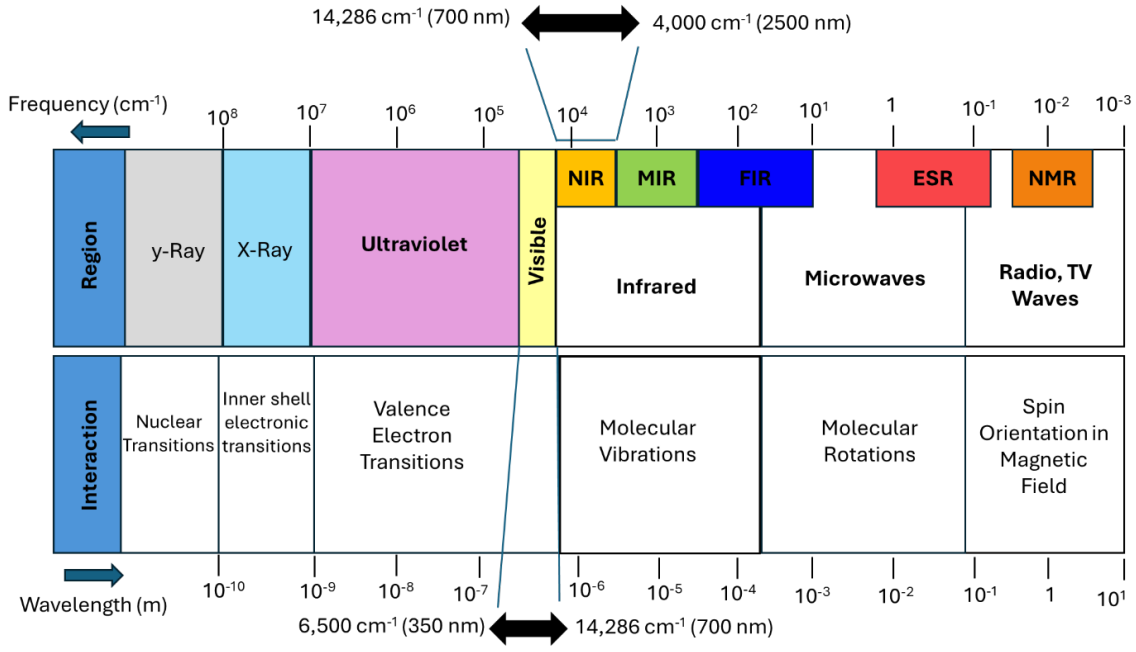

Figure 1. The spectrum of electromagnetic radiation. From (Okparanma et al., 2018)

NIR spectroscopy provides qualitative information through the wavelengths of absorption bands, which shift based on the atomic mass and chemical bond strength involved in anharmonic vibrational modes, such as overtones or combinations of fundamental vibrations. Heavier atoms increase absorption wavelengths, while stronger bonds decrease them, making NIRS highly

sensitive for detecting structural changes (Pasquini, 2018). Quantitative data are derived from absorption intensities, which correlate with the amount of absorbing substances. However, in solid samples, scattering disrupts the linear correlation between absorbance and concentration, necessitating the control of particle size distribution and the use of mathematical corrections to interpret raw spectra (S. Singh et al., 2021). For short concentration ranges, a linear relationship is identified using the logarithmic value of the reciprocal reflectance ratio between the sample and a 100% reflecting reference material (Wei & Seng, 2021).

The Beer-Lambert law, describing the linearity of absorbance and concentration, applies only to non-scattering samples with consistent light paths. Scattering samples, affected by sample appearance and dimensions, deviate from this law, requiring adjustments in NIRS data acquisition to ensure accuracy (Kiteto & Mecha, 2024).

NIR data can be acquired using five primary measurement modes: **reflection**, involving placement of the light source and detector to minimize specular reflectance; **transmission**, where the source and detector are on opposite sides of the sample; **interaction**, where the light source and detector are parallel, avoiding surface reflectance; **transflection**, where the source and detector are placed on the same side of the sample; and **diffuse reflection**, where the light source and detector can be placed at various angles, as the reflected light is scattered in many directions (Figure 2). Reflection and interaction modes prioritize diffuse reflectance, but inconsistent definitions in studies often cause confusion regarding these modes (Wei & Seng, 2021; Biswas & Chaudhari, 2024). The selection of NIR acquisition mode relies on the sample's shape, size, and condition. For solids, diffuse reflection is more commonly used than transmission, as it confines light penetration to obtain a high-quality spectrum. In contrast, transmission is more effective for liquids due to its ability to produce high signal-to-noise ratios with a fixed light path using a cuvette (S. Singh et al., 2021).

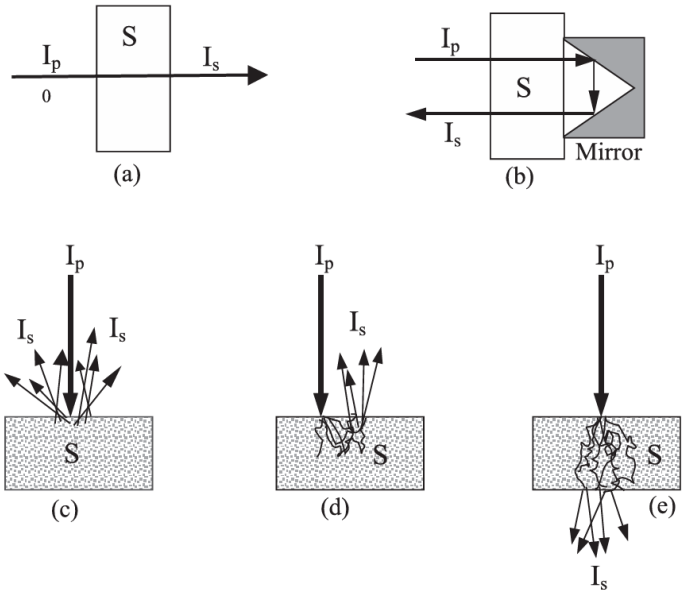

Figure 2. Modes of measurements of NIRS. (a) transmittance; (b) transflectance; (c) diffuse reflectance; (d) interactance, and (e) transmittance through scattering medium. From (Pasquini, 2017)

3.1.2. Advantages and limitations

- Advantages

NIR spectroscopy offers numerous advantages over other analytical techniques, making it a versatile and efficient tool in various applications. It is a rapid, user-friendly, and non-destructive technology that requires minimal chemical consumables, significantly reducing hazardous waste disposal costs, which are increasingly expensive for laboratories (Suksangpanomrung et al., 2024). With little to no sample preparation required, NIR spectroscopy is well-suited for analysing a wide range of sample types, including high-moisture liquids, slurries, and solids, while also enabling the simultaneous measurement of multiple constituents or properties (Manley & Baeten, 2018). Its instruments are highly adaptable, being rugged enough for use in both laboratory and field environments, and capable of supporting online and in-line measurements for continuous process monitoring (Yakubu et al., 2022). Recent advancements in portability have made handheld, backpack-mounted, and vehicle-mounted devices widely available, further enhancing real-time analysis capabilities (Manley & Baeten, 2018). Miniature spectrometers utilizing thin-film linear variable filter technology now provide high signal-to-noise ratios and enable field-based analysis of plants and fruits, such as determining the optimal harvesting time. These developments have also supported food quality control and authenticity verification, with applications tailored to these needs (Grabska et al., 2021).

One of the main benefits of NIR compared to other spectroscopic techniques is its capacity to employ longer pathlengths and utilize simpler optical components. NIR instruments often use quartz glass for windows, lenses, and sample cells, which are cost-effective and simpler to work with than the alkali salts required for MIR techniques. Additionally, NIR's deep light penetration allows it to generate more accurate representations of a sample's chemical properties, even from heterogeneous samples. By scanning larger areas and averaging properties, NIR can create pseudo-homogeneous spectra (Chaudhary et al., 2022; Pasquini, 2018).

Another benefit is the low absorptivity of NIR absorption bands, which makes it suitable with moderately concentrated samples and allows for longer pathlengths than MIR. This enables NIR to measure spectra through intact materials. For opaque biological samples, NIR can also perform diffuse reflectance analysis(Wei & Seng, 2021; Pellicer & Bravo, 2011). These combined advantages make NIR spectroscopy an excellent tool for real-time, online analyses and process control, as it is easy to use and provides quick, reliable results.

- Limitations

NIR spectroscopy faces several limitations that can impact its effectiveness in specific applications. The primary disadvantage is its low signal sensitivity, which restricts its ability to detect components present in low concentrations. This limitation arises because NIR absorptions are inherently weaker, simplifying the spectra and emphasizing the information on inherently strong chemical bonds, such as those between light atoms. While this can streamline the analysis, it limits the range of detectable chemical details. However, advanced chemometric techniques can extract valuable insights from the data, provided they are applied correctly by a skilled operator (Manley & Baeten, 2018; Suksangpanomrung et al., 2024).

Another significant challenge is the reliance of NIR spectroscopy on robust calibration models, which require large and diverse datasets to ensure accuracy and reliability. These datasets can be challenging and expensive to generate, as they depend on extensive sample collection, preparation, and analysis using reference methods (Agelet & Hurburgh, 2010). These reference methods are often time-intensive and costly, especially for complex or varied constituents, making calibration a resource-heavy process. Additionally, maintaining calibration sets over time is problematic due to sample instability, which complicates long-term calibration transfer and consistency (Qiao et al., 2023).

The initial cost of NIR instrumentation is also a barrier, particularly for routine use in quality control laboratories. While the upfront investment is significant, the reduced consumable costs and the potential long-term financial benefits of NIR compared to traditional chemical methods may

justify the expense. Effective use of NIR spectroscopy further requires skilled operators and sufficient training, especially when developing new calibrations or troubleshooting existing models. Despite these challenges, for qualitative analysis, where reference method costs are less relevant, and in applications with sufficient resources for robust calibration, NIR spectroscopy remains a powerful and efficient analytical tool (Wei & Seng, 2021).

3.1.3. Key applications in the food sector

The discovery of near-infrared (NIR) light by William Herschel in 1800 marked the beginning of its scientific exploration, though its analytical potential went largely unnoticed until the mid-20th century (Porep et al., 2015). Early food industry applications began as far back as 1938 with studies on gelatine (Manley & Baeten, 2018). The technique gained prominence in the 1960s and 1970s, led by K. H. Norris at the USDA Beltsville Laboratories. Norris pioneered methods for determining moisture content in grains, seeds, and oilseeds through indirect measurements, such as detecting water in methanol extracts (Porep et al., 2015). Concurrently, NIR spectroscopy was employed to assess fruit and vegetable quality, highlighting its potential in agricultural applications. McClure (2003) provided a thorough review of the early applications of NIRS in agriculture.

The 1980s marked a turning point, as advances in computing enabled sophisticated calibration techniques, broadening NIR's use in analysing key food components such as fats, sugars, proteins, and moisture across various matrices, including meat, milk, fruits, and vegetables (Teixeira Dos Santos et al., 2013). Comprehensive reviews by Grant (1987) and McClure (2003) documented these early breakthroughs, while Cen & He (2007) highlighted its role in modern food analysis. Reviews from the 1990s, including those by Williams & Stevensen (1990) and Martin (1992), expanded on NIR's applications for raw materials and processed foods, emphasizing its utility in quality control and compositional analysis. Osborne et al. (1993) and Wetzel (1998) further details its contributions to defect detection and sensory evaluations.

The extensive review by Woodcock et al. (2008) examines numerous reports on the use of NIR spectroscopy in the food and beverage industry from 1997 to 2008, showcasing how NIR spectroscopy, coupled with chemometric techniques, became indispensable for ensuring product integrity.

Today, NIR spectroscopy, bolstered by advanced chemometric analysis and computational power, is a cornerstone of modern agriculture and the food industry. It offers efficient, non-destructive solutions for composition analysis, quality control, and authenticity verification, solidifying its position as an essential tool in food science and safety (Yang & Berzaghi, 2024). Manley (2014),

Baeten et al. (2015), and Lohumi et al. (2015) have investigated the application of NIRS in tackling contemporary issues such as detecting food fraud, verifying geographical origin, and conducting non-destructive testing. Subsequent studies by Sørensen et al. (2016) and Escribano et al. (2017) emphasized its adaptability in identifying adulteration, evaluating authenticity, and maintaining quality standards. For instance, Shawky et al. (2024) conducted a comprehensive review on the use of NIRS for spice authentication. Most recently, Yang & Berzaghi (2024) reviewed the latest developments and applications of NIRS in predicting chemical composition and determining both adulteration and authenticity of various food products.

The advancement of portable NIR devices has significantly expanded the use of NIR technology, enabling real-time quality assessments directly in production environments. This advancement aligns with a broader trend of miniaturizing spectroscopic instruments across various applications (Grabska et al., 2021). Portable instruments have proven effective in food analysis, with early validation and comprehensive reviews provided by researchers such as Teixeira Dos Santos et al. (2013) and Alander et al. (2013). Furthermore, Ellis et al. (2015) have highlighted the potential of portable NIR instruments throughout the food supply chain. Despite their versatility, challenges persist due to the complex chemical and physical properties of food products, such as high moisture content, intricate matrices, and diverse surface textures. These factors, along with the demand for non-intrusive analysis through original packaging, underscore the ongoing efforts to refine and optimize their application (Grabska et al., 2021).

3.2.Significance of the chosen food matrices

3.2.1. Milk

Milk is a nutritionally rich and complex fluid, composed primarily of water (approximately 87%), which acts as a medium for dissolving various nutrients and contributes to its hydrating properties. The remaining composition includes essential macronutrients and micronutrients critical for Health and wellness. Lactose, the primary carbohydrate (4-5%), provides energy and enhances the flavor of dairy products, while proteins (around 3%) are categorised into caseins (80% of milk proteins) and whey proteins (20%). Caseins, insoluble and forming micelles, are rich in essential amino acids, while whey proteins are noted for their branched-chain amino acids, supporting muscle health and immune response. Milk's fat content comprises triglycerides, primarily saturated fatty acids, along with unsaturated and polyunsaturated fatty acids, including bioactive compounds such as conjugated linoleic acid, which may offer health benefits. Additionally, milk provides essential minerals like calcium and phosphorus that support bone health, along with vitamins A, D, E, and B-complex, which contribute to energy metabolism and overall well-being. Milk is secreted by nearly 4,500 mammalian species, with cows, buffaloes, goats, and sheep being

the primary sources for human consumption. Each species' milk is uniquely tailored to meet the developmental requirements of its offspring, varying in fat, protein, and lactose content. For instance, cow milk is characterized by balanced macronutrient levels, while sheep and buffalo milk tend to have higher fat and protein concentrations. Factors like breed, diet, and lactation stage influence its content at as well (Mohammadi et al., 2024; Patil et al., 2024; Porwal et al., 2024; Coppa et al., 2010).

Several processing techniques have been developed to prolong the shelf life of milk, including the production of milk powders via evaporation and drying methods. Among these, spray drying is the most widely employed method, which uses convection to remove water from finely dispersed milk particles by exposing them to a current of hot and dry air. This process results in the rapid creation of dry product particles averaging 50 microns in diameter. While both powdered and liquid milk provide similar nutritional benefits, their differing characteristics make them suitable for various applications (Forchetti & Poppi, 2017; Zouari et al., 2019).

Liquid milk, with its shorter shelf life and refrigeration requirement, is best suited for immediate consumption and is widely utilized in dairy-derived beverages and frozen desserts because of its creamy texture and rich flavor. In contrast, powdered milk, with its extended shelf life and lack of refrigeration needs, is ideal for long-term storage and diverse applications, including industrial processes, specialized diets, and emergency food reserves (Pugliese et al., 2017). It is especially valued for its capacity to be reconstituted, offering precise control over the moisture content of the final product. Powdered milk has become a key ingredient in several dairy and processed food products, such as ice cream, yogurts, chocolate, confectionery, bakery items, soups, and sauces, owing to its physical and functional attributes (Tirgarian et al., 2023; Zouari et al., 2020; Duncan & Webster, 2010). In recent years, camel and mare milk powders have garnered significant attention for their nutritional benefits, medical properties, and suitability in harsh climates where cows struggle to survive (Seifu, 2023). These milks are less likely to cause allergies, rendering them excellent substitutes for cow milk in certain food applications. Camel milk, rich in bioactive compounds and essential amino acids, closely resembles human milk, sparking interest in its potential use in hypoallergenic infant formulas (AlYammahi et al., 2023; Maryniak et al., 2018; Ehlayel et al., 2011). However, no such formulas are currently available in the EU due to limited camel milk production and the need for further research (Maryniak et al., 2022). Similarly, mare's milk has been suggested as an alternative to bovine milk in paediatric diets, owing to its highly digestible casein-to-whey protein ratio (Pieszka et al., 2016; Fantuz et al., 2016).

3.2.2. Fermented milk

Fermented foods have been essential to traditional diets worldwide, characterized by controlled

microbial growth and enzymatic activity to enhance food's sensory qualities, shelf life, and nutritional value. These foods, particularly fermented dairy products like yogurt, are valued for their health benefits, including regulating gut microbiota, boosting immunity, and improving nutrient profiles. Historically, fermentation practices, such as "back-slopping," involved reusing previous batches' cultures to produce consistent results (Yang et al., 2025). Advances in biotechnology have refined these processes, enabling the use of specific starter cultures, primarily lactic acid bacteria (LAB), to create standardized, high-quality products. LAB, like *Streptococcus thermophilus* and *Lactobacillus delbrueckii* subsp. *Bulgaricus* work symbiotically to enhance the quality, taste, and nutritional value of fermented milk products. LAB convert lactose into lactic acid and degrade proteins into peptides and amino acids, generating organic acids, esters, alcohols, and other flavour compounds (Praveen, 2025).

The milk matrix functions as a carrier, ensuring the vitality of LAB during gastrointestinal transit, where they contribute to host health. Encapsulation techniques further protect probiotics during storage and digestion, enabling their application in functional foods. Probiotics, such as *Lactobacillus* and *Bifidobacterium* spp. offer wide-ranging health benefits. They support gastrointestinal health, regulate metabolism, and may alleviate conditions like diabetes, obesity, and cardiovascular disorders. Emerging research also highlights the potential of probiotics to influence the gut-brain axis, improving mental health by modulating neurotransmitter production and reducing inflammation (Wasana et al., 2025; Sarita & Kovaleva, 2025; Yerlikaya, 2023). Fermented dairy products like yogurt, kefir, viili, and cultured buttermilk, among others, emphasize the versatility of products obtained through fermentation. Yogurt, popular for its taste, health benefits, and versatility, is made with thermophilic bacteria, while kefir combines lactic acid and alcoholic fermentation for unique textures and flavors (Bintsis & Papademas, 2022; Buttriss, 1997). Modern advancements allow precise control of variables like pH and temperature, enabling the large-scale production of diverse, health-conscious options such as low-fat and sugar-free varieties. The rich history and scientific innovations in fermentation continue to meet evolving dietary needs while promoting health (Yang et al., 2025).

3.2.3. Cheese

Cheese, one of the oldest fermented foods, has been around for about 8,000 years. It likely originated in the Fertile Crescent, near the Tigris and Euphrates rivers, but there's also evidence showing that people in Xinjiang, China, were making cheese as far back as 1450 BC. In its early days, cheesemaking was a practical way for communities to preserve extra milk, turning it into a nutrient-packed, long-lasting food using simple, artisanal methods. Fast forward to modern times, and cheesemaking has evolved dramatically, especially with industrialization in the 19th century

(Fox & McSweeney, 2017). Cheese now accounts for nearly 40% of the world's milk usage, with global production hitting around 26 million tonnes in 2019. The United States, Germany, and France dominate this market, contributing about half of the world's total cheese output (Veena, 2024).

Cheese quality depends on raw material composition, microbial activity, and environmental factors during ripening, all of which are interdependent. Raw milk composition, especially protein and fat level, significantly impacts cheese yield and texture. As a diverse and academically challenging dairy product, cheese is biologically and biochemically dynamic, making it inherently unstable compared to other dairy products. Its production involves a complex sequence of biochemical processes that, when well-balanced, create desirable flavors and aromas, but if disrupted, can cause off-flavors and odors (Veena, 2024; Hammam & Ahmed, 2019). However, cheese represents a dynamic fusion of tradition and science, offering a wide range of textures, flavors, and functional properties. Its enduring appeal lies not only in its gastronomic versatility but also in its ability to adapt to evolving consumer preferences and technological advancements, ensuring its relevance in modern diets and food systems (Falih et al., 2024; Rashidinejad et al., 2017).

3.2.4. Quality authentication of dairy products

Traceability is a key aspect of quality in agribusiness, defined by ISO 8402 as the capacity to track the history, application, or location of an entity through documented identifications. It includes (1) origin traceability: focusing on an animal's identity, breed, and geographical origin and (2) process traceability: covering production methods such as feeding, processing, and detecting adulteration (Manikas & Manos, 2009). In addition, guidelines like the Food Chemicals Codex (FCC) and Codex Alimentarius provide global standards for food quality, safety, and fraud detection, forming the basis for national legislation worldwide. Certification systems such as FSSC 22000 and ISO standards ensure high-quality food production and packaging practices (Martins et al., 2024).

Figure 3 provides a comprehensive overview of the processes involved in the quality authentication of dairy products.

- Fraud detection

Despite its nutritional benefits, milk is highly prone to adulteration and microbial contamination. Adulteration, driven by economic incentives and high global demand, involves adding substances such as water, melamine, urea, starch, or preservatives. These practices pose serious health risks, as seen in the 2008 melamine scandal in China, which led to the hospitalization of over 50,000 people and the death of six infants (Kamal & Karoui, 2015; Shawky et al., 2024a). Milk powder

is highly prone to contamination and frequently adulterated with non-milk proteins such as wheat, pea, and soy, or blended with whey powder or milk from other species for economic advantages. More hazardous adulterants include substances like detergents, urea, ammonium sulphate, formalin, boric acid, caustic soda, salicylic acid, benzoic acid, hydrogen peroxide, melamine, and sugars, many of which can lead to severe health issues (Patil et al., 2024; Chen et al., 2017). For these reasons, regulations have been implemented, such as the European Union's Regulation 2020/692, which outlines the rules for importing raw milk and milk products for human consumption, including their movement and handling after entry. Similarly, the FAO provides guidelines for export certificates in international dairy trade to ensure compliance with food safety and quality standards (Ferreira et al., 2024).

- Traceability:

One common form of fraud in the dairy industry involves misrepresenting the species of origin, where premium milks such as those from mare, goat, or buffalo are substituted with cow's milk to cut production costs and boost financial returns. This practice is often linked to seasonal fluctuations and the lower production yields of ovine, caprine, and bubaline species, as well as more exotic sources like camels or donkeys, which increases their economic value (Mafra et al., 2022; Kamal & Karoui, 2015). Identifying the animal species is especially critical for high-value traditional products, such as cheese that bear European Union (EU) labels like Protected Designation of Origin (PDO), Protected Geographical Indication (PGI), or Traditional Specialty Guaranteed (TSG) (Chaudhary et al., 2022).

Milk fat profoundly influences the nutritional, physical, and sensory qualities of dairy products. Key components like conjugated linoleic acid (CLA) and omega-3 polyunsaturated fatty acids (PUFAs), including ALA, EPA, and DHA, offer notable health advantages. While milk and dairy contribute 15% of total fat and 25% of SFAs in Western diets, beneficial fatty acids like EPA, DHA, and CLA remain present only in small amounts (Bodkowski et al., 2024; Butler et al., 2019). The fatty acid profile of milk is influenced by several factors, including the cow's breed, season, lactation stage, and diet, with diet playing a particularly significant role (Magan et al., 2021; Lerch et al., 2015; Gunun et al., 2024). Strategic feeding practices, such as enhancing diets with vegetable oils, oilseeds, marine lipids, and altering feed sources, can enhance the concentration of health-promoting fatty acids while optimizing the feed-to-concentrate ratio. Additionally, concerns about feed quality, such as mycotoxin contamination, and the influence of feeding on milk quality, remain priorities for milk producers (Yakubu et al., 2022). For instance, Tóth et al. (2019) reported that supplementing dairy feed with linseed and fish oil improved milk's fatty acid composition by increasing polyunsaturated fatty acids and favourably decreasing the n-6/n-3 ratio without

negatively affecting sensory properties or milk fat and protein content.

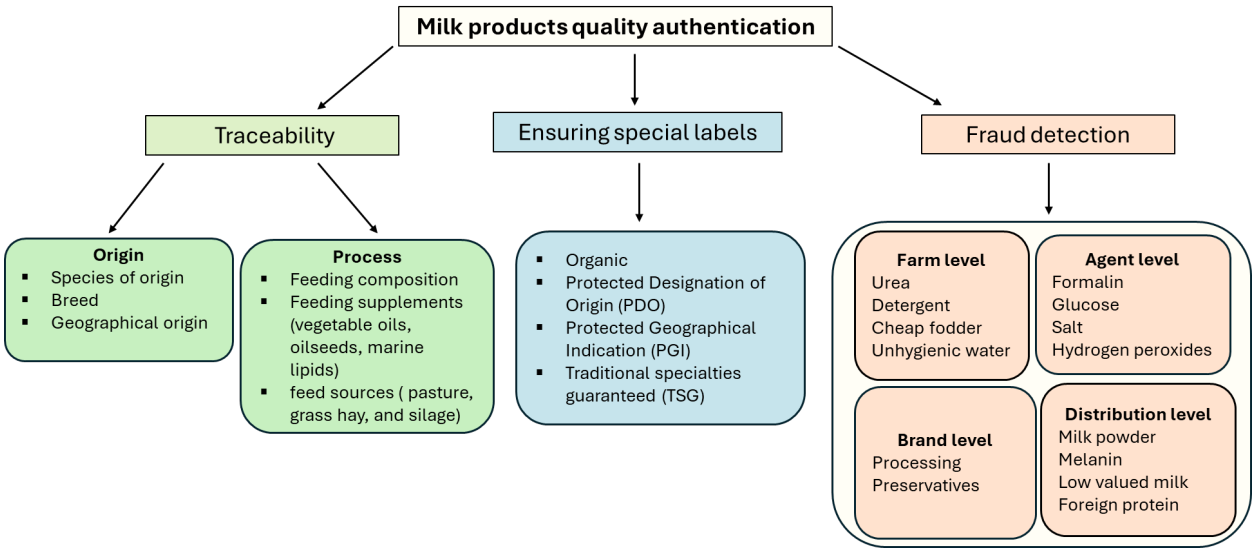

Figure 3. Quality Authentication of dairy products: Traceability and Fraud Detection Overview. Modified from (Patil et al., 2024)

3.3.Application of Near-Infrared Spectroscopy in the dairy industry

Near-infrared (NIR) spectroscopy, first applied in the dairy industry in the late 1970s, has emerged as a robust analytical technology, offering rapid, non-destructive, cost-effective, and environmentally friendly solutions. The International Organisation for Standardisation (ISO) and the International Dairy Federation (IDF) established guidelines for its use in 2006, focusing on off-line analysis of milk products. In 2019, the standard was significantly revised to encompass a wider variety of dairy samples in liquid, semi-solid, and solid states, reflecting its expanding utility in diverse dairy applications (Pu et al., 2020, Porep et al., 2015).

A recent review by Ferreira et al. (2024), reported that, dairy authentication studies show **41%** used spectroscopic methods for precision analysis, **27%** employed chromatographic techniques for their accuracy and versatility, and **23%** relied on biological techniques like DNA markers for selectivity. Electroanalytical methods made up only **4%** due to limited regulatory acceptance. Recent innovations have focused on combining spectroscopic, chromatographic, and biological methods to optimize analytical accuracy and efficiency. Techniques such as solid-phase extraction (SPE), dispersive SPE , and other advanced sample preparation methods improve the sensitivity and reliability of subsequent analyses (Ferreira et al., 2024). These advancements support the broader use of NIR spectroscopy in diverse food and dairy applications, including industrial-scale processes, pilot studies, and laboratory research, emphasizing its potential to ensure quality control, traceability, and consumer trust in the global food supply chain (Fodor et al., 2024).

NIRS is extensively employed throughout the dairy processing chain, from assessing raw milk quality at intake points to routine off-line quality checks in laboratories and real-time on-line or in-line monitoring along production lines. At-line systems are located near production lines but still rely on manual sampling. In contrast, on-line systems create a bypass for continuous sampling, while in-line systems are fully integrated into production lines, using immersion probes, flow cells, or optical windows to analyse materials as they are processed. On-line and in-line configurations eliminate manual sampling delays, enabling immediate, continuous monitoring under challenging high temperature and pressure conditions, providing significant advantages for real-time process control. (Pu et al., 2020; De Marchi et al., 2018). However, adapting NIRS to dynamic production environments poses challenges, particularly in managing variables such as temperature fluctuations, product flow, and compositional heterogeneity. These factors can affect spectral consistency and the accuracy of calibration models (Porep et al., 2015). As a result, calibration development must account for such variables to ensure robust predictive performance, highlighting the importance of ongoing research to optimize NIR applications in industrial settings. Pu et al. (2020) and Loudiyi et al. (2022) presented an in-depth reviews of the use of NIRS for real-time monitoring in dairy processing and storage. Similarly, Mohammadi et al. (2024) and Bittante et al. (2022) provided comprehensive insights into the application of NIRS for the prediction of milk and cheese composition.

Beyond dairy processing, NIRS has been fundamental in detecting food adulteration and ensuring product authenticity. Its application extends to milk powders, whey protein concentrates (WPCs), cheeses, and other dairy products. It has been used to monitor rennet coagulation in milk, analyse cheese and butter properties, and differentiate milk samples by feeding systems, production methods, and nutritional parameters (Capuano et al., 2015; Azad & Ahmed, 2016). For example, a recent study by Foschi et al. (2025) revealed that ATR-FTIR spectroscopy and chemometric analysis successfully classified ricotta whey cheese according to milk origin (sheep, cow, goat, and water buffalo) , achieving an accuracy of 97%. Valenti et al. (2013) employed NIRS with PLS-DA to classify milk based on different feeding systems (maize silage, pasture, hay). However, the method showed limitations in distinguishing samples based on altitudes or breeds, consistent with findings from earlier studies.

NIR has also been applied to detect milk adulteration, such as melamine, with high sensitivity using chemometric techniques. For instance, Balabin & Smirnov (2011) utilized NIR spectroscopy to scan infant formula, milk powder, and liquid milk samples within the 1110-1500 nm spectral range to detect melamine. By employing various chemometric tools, including PLS, polynomial-PLS, ANN, and support vector regression (SVR), they successfully identified melamine

concentrations as low as 0.76 ± 0.11 ppm. These results align with earlier findings by Chen et al. (2017), Lu et al. (2009) and Wu et al. (2016), who also detected melamine in adulterated milk using NIR. Table 1 highlights various studies exploring the applications of NIRS technology in dairy products.

Table 1. Overview of near infrared spectroscopy applications in dairy products

Sample	Compound evaluated or objective of analysis	Mode of measurement	Chemometric technique	Analytical parameters obtained	References
Thawed raw milk	Estimation of the concentration of caproic, caprylic, capric, lauric, myristic, myristoleic, palmitoleic and oleic acids	Transmittance (1600-1800 nm)	PLSR, leave-one-out validation	R^2 (calibration) from 0.61 to 0.79 R^2 (validation) from 0.62 to 0.76	(Muncan, Kovacs, et al., 2021)
Raw milk	Quantification of fat, protein and lactose	Transmittance (960-1690 nm)	PLSR, group-wise cross-validation	R^2 (validation) from 0.82 to 0.99	(Diaz-Olivares et al., 2020)
Milk powder, liquid milk, infant formula	Detection of melamine	Transmittance (1110-1500 nm)	PLS, polynomial-PLS, ANN, SVR	LOD = 0.76±0.11 ppm	(Balabin & Smirnov, 2011)
Milk powder	- Classification of brands - Quantification of protein	Diffuse-reflectance (4000-10,000 cm^{-1})	PLS-DA PLSR	100% accuracy R^2(validation)= 0.99	(Chen et al., 2018)
Milk powder	- Prediction of density, insolubility, moisture and surface free fat.	Diffuse-reflectance (350-2500 nm)	PLSR	R^2(prediction) from 0.72 to 0.88	(Wang et al., 2021)
Raw milk	Classification based on the feeding system, breed of cow and altitude of the farm	Reflectance (1100-2498 nm)	PLS-DA	Discrimination succeeded only for the feeding system	(Valenti et al., 2013)
Raw milk	Classification of feeding systems	Reflectance (400-2498 nm)	PLS-DA	91.5% to 95.5% accuracy	(Coppa et al., 2012)
Ricotta cheese	Classification of animal origin (sheep, cow, goat, and water buffalo)	Attenuated Total Reflectance Fourier-transform infrared (ATR- FTIR) (4000-500 cm^{-1})	SPORT-LDA	correct classification = 97 %	(Foschi et al., 2025)
Cheese	Classification of pasture and preserved-forage cheeses	Reflectance (400–2500 nm)	PLS-DA	Correct classification = 0.96% for pasture and for preserved forage samples	(Andueza et al., 2013)
Grated hard cheese	Detection and quantification potential adulterants (microcellulose, silicon dioxide, wheat flour, semolina, and sawdust)	Reflectance (4000-10,000 cm^{-1})	OC-PLS, DD-SIMCA, PLS	100% accuracy R^2(validation) from 0.79 to 0.97	(Visconti et al., 2024)
Cheese	Prediction several chemical and physical traits	Reflectance (1100 - 2498 nm)	Bayesian models	R^2(validation) from 0.04 to 0.83	(Stocco et al., 2019)
Cheese	Prediction of fatty acid composition	Transmittance (850- 1050 nm)	PLSR	R^2(validation) from 0.04 to 0.67 to 0.96	(Manuelian et al., 2017)
Yoghurt	Prediction of the evolution of pH during fermentation	Near infrared light backscatter sensor (Transmittance, 800 nm)	linear regressions	R^2 = 0.993	(Arango et al., 2020)

PLSR: Partial Least Squares Regression; **ANN:** Artificial Neural Networks; **SVR:** Support Vector Regression; **PLS-DA:** Partial Least Squares-Discriminant Analysis; **OC-PLS:** One-Class Partial Least Squares; **DD- SIMCA:** Data-Driven Soft Independent Modelling by Class Analogy; **PLS:** Partial Least Squares; **SPORT-LDA:** Sequential Preprocessing through ORThogonalization Linear Discriminant Analysis

3.4.Application of the electronic nose (e-nose) technique in the dairy industry

An electronic nose (e-nose) is an analytical device designed to mimic the human sense of smell. Officially defined in 1994, it consists of an array of chemical sensors with partial specificity and a pattern-recognition system to detect and classify complex odors. Rather than identifying individual volatile compounds, the E-nose generates a quantitative olfactory profile, creating a unique "fingerprint" of a sample's aroma. The system typically includes gas sensors, such as metal oxide semiconductors (MOS), conducting polymers (CP), quartz microbalances (QMB), and other sensor types, along with sample handling and data analysis software. Emerging technologies like nanotechnology and MEMS have enhanced sensor performance, while integration with multivariate statistical tools (e.g., PCA, LDA, PLSR, ANN) enables advanced analysis for applications in food quality, environmental monitoring, and medical diagnostics (P. Singh et al., 2025; M. Wang & Chen, 2024; Y. Yang & Wei, 2021).

The application of the e-nose technology in the dairy industry has revolutionized quality assessment by providing a rapid, precise, and non-destructive method for evaluating product aroma, detecting microbial contamination, and identifying adulteration. Traditional quality control methods, such as microbial culture and chemical analysis, are time-consuming and labor-intensive, which has led to the adoption of e-nose systems as a practical alternative. In milk production, for instance, (Eriksson et al., 2005) demonstrated the potential of e-nose devices equipped with MOSFET and CO_2 sensors to differentiate between milk obtained from healthy cows and those suffering from acute clinical mastitis. Their study achieved 100% classification accuracy under specific incubation conditions, highlighting the technology's reliability. (Balivo et al., 2024) applied e-nose technology to analyze milk from buffaloes fed with hydroponic barley forage instead of traditional maize silage. The study achieved 90% classification accuracy using linear discriminant analysis (LDA), showing that e-nose systems can track dietary influences on milk quality by detecting variations in volatile organic compounds (VOCs).

Beyond identifying contamination and dietary effects, e-nose technology has also been employed for monitoring the microbial quality of milk. (Y. Yang & Wei, 2021) research integrated e-nose technology with artificial neural networks (ANN) to predict total bacterial count (TBC) in milk samples. This approach achieved remarkable accuracy, with a strong correlation ($R^2 > 0.99$) between predicted and reference TBC values. Such findings underscore the potential of e-nose devices to replace traditional cultivation-based methods, which are time-consuming, with a rapid and cost-effective alternative. Similarly**,** (Tóth et al., 2019) used e-nose measurements to distinguish between ultra-high temperature (UHT) milk products with varying fat contents, demonstrating a strong connection between volatile profiles and product classification. These applications reveal how e-nose technology can play a pivotal role in ensuring the safety,

authenticity, and overall quality of milk in the dairy sector. Additionally, (Darvishi et al., 2025) study showed how e-nose systems equipped with metal oxide sensors could detect melamine adulteration in milk powder, achieving up to 99.5% precision when combined with chemometric techniques such as Principal Component Analysis (PCA) and Support Vector Machines (SVM). This highlights the technology's ability to safeguard consumers by rapidly identifying economically motivated adulteration.

In yogurt production, e-nose devices have been widely used to evaluate aroma and flavor, which are critical factors influencing consumer acceptance. (Tian et al., 2020) combined e-nose data with advanced chemometric models, including random forest (RF) and back-propagation neural network (BPNN) algorithms, to classify yogurt samples based on consumer sensory evaluations of satisfactory versus unsatisfactory flavors. While PCA alone could not effectively distinguish between the two groups, RF and BPNN achieved nearly 100% classification accuracy, with RF slightly outperforming BPNN. Similarly,(Demarigny et al., 2021) demonstrated the capability of a portable e-nose device, the NeOse Pro, to monitor yogurt fermentation in real-time. Their study successfully differentiated between pre-fermentation milk and post-fermentation yogurt, as well as between products fermented with different bacterial strains, such as *Lactobacillus delbrueckii* subsp. *bulgaricus* and *Streptococcus thermophilus*. This approach provided a clear separation in PCA plots and identified acetaldehyde as a key volatile compound in yogurt flavor development. Moreover**,** (Tian et al., 2017) investigated the influence of probiotic strains on yogurt flavor using a GC-MS coupled with an e-nose. Their findings revealed that certain probiotics, such as *Lactobacillus casei* and *Lactobacillus acidophilus*, significantly impacted minor volatile compounds, while others had little effect. These studies collectively highlight the role of e-nose systems in guiding yogurt production toward consistent and desirable sensory profiles.

E-nose technology has also found substantial application in cheese production, particularly for monitoring aroma changes and detecting adulteration. (Štefániková et al., 2019) utilized an ultra-fast gas chromatography-based e-nose to evaluate the quality of steamed cheese varieties over a 14-day storage period. Their analysis revealed distinct separations between smoked and unsmoked cheese samples based on volatile compound profiles, including acetaldehyde, propanoic acid, furfural, and ethyl hexanoate. Similarly**,** (Mendoza-martinez et al., 2022) used the Cyranose® 320 e-nose to differentiate fresh Mexican cheese prepared from different types of cow's milk, which is critical for product certification and quality assurance. Beyond flavor evaluation, e-nose devices have been instrumental in detecting adulteration in cheese and other dairy products. (Tian et al., 2022; Tian et al., 2023) conducted a series of studies using the Hercules II e-nose to identify adulterated raw milk samples containing substances like neutralizing agents (NaOH, NaSCN) or vegetable oils. These studies demonstrated that e-nose, when combined with machine learning

algorithms, could rapidly and accurately detect adulteration, providing a valuable tool for ensuring product authenticity and protecting consumer trust.

Overall, the integration of e-nose technology into the dairy industry represents a significant advancement in modern food quality control. From milk to yogurt and cheese, e-nose systems have proven their utility in monitoring fermentation processes, evaluating flavor profiles, detecting microbial contamination, and identifying adulteration. By offering rapid, reliable, and cost-effective analysis, e-nose technology addresses the increasing global demand for standardized and safe dairy products. As studies have shown, the continued development and application of e-nose devices are expected to play a central role in enhancing dairy production efficiency and ensuring the delivery of high-quality, authentic products to consumers worldwide. This technological innovation not only benefits producers by streamlining quality control processes but also strengthens consumer confidence in dairy products by safeguarding against fraud and contamination.

3.5.Chemometrics:

The analysis of NIRS data relies on chemometrics, which applies mathematics, statistics, and computational methods to chemical analysis. These tools are essential for handling challenges in NIR spectra, such as overlapping peaks, sensitivity to sample properties, and data redundancy (Agelet & Hurburgh, 2010). Chemometric methods are divided into classification (unsupervised and supervised) and regression (linear and non-linear) approaches, with their principles, advantages, and limitations summarized in Table 2 and Table 3, respectively.

Table 2. Summary of PCA and PCA-LDA: Principles, Advantages, and Limitations

Method	Principle	Advantages	Disadvantages	References
PCA (Principal Component Analysis**)**	**Unsupervised:** Transforms original correlated variables into a new set of uncorrelated variables (principal components) that capture maximum variance in descending order.	- Simplifies complex data for visualization. - Detects outliers and trends. - Reduces noise and redundancy. - Useful for preprocessing before classification or regression.	- Only captures linear relationships. - Components may be hard to interpret. - Sensitive to scaling and outliers.	(Michael et al., 2025; Brereton, 2022; Jollife & Cadima, 2016)
PCA-LDA (PCA-Linear Discriminant Analysis)	**Supervised:** PCA extracts the most informative features, then LDA finds linear combinations that maximize between-class variance while minimizing within-class variance.	- Reduces computational cost by lowering dimensions. - Improves class separability compared to PCA alone. - Works well with high dimensional spectral data.	- PCA step may discard useful class-related information. - Assumes normal distribution and equal covariance among classes. - Limited for non-linear class boundaries.	(de Almeida et al., 2021a; Lasalvia et al., 2022; Tominaga, 1999)

Table 3. Summary of PLSR and SVR: Principles, Advantages, and Limitations

Method	Principle	Advantages	Disadvantages	References
PLSR (Partial Least Squares Regression)	**Linear:** Finds latent variables that maximize covariance between predictor matrix XX and response vector YY, combining feature reduction and regression in one step	- Handles highly collinear and noisy data - Ideal for spectroscopic calibration - Provides interpretable loadings and variable importance scores - Reduces overfitting when validated correctly	- Requires careful selection of latent variables - Risk of overfitting with small datasets - Sensitive to outliers	(Ezenarro & Schorn-García, 2025; Zifarelli et al., 2020; Cheng & Sun, 2017)
SVR (Support Vector Regression)	**Non-Linear:** Uses kernel functions to map data into higher-dimensional space, then finds the optimal hyperplane within a tolerance margin	- Handles non-linear and complex data relationships well - Robust to overfitting with proper regularization - Works well in high dimensional spaces like spectra	- Choice of kernel and tuning parameters is critical - Less interpretable than linear methods -Computationally intensive for very large datasets	(Cheng & Sun, 2017; Ezenarro & Schorn-García, 2025; Balabin & Lomakina, 2011)

4. MATERIALS AND METHODS

This section is divided into three parts, outlining the process of sample preparation, the experimental setup, and the multivariate analysis techniques applied to the analysis of milk powder, fermented milk, and cheese.

4.1. Evaluation of the quality of reconstituted cow, camel and mare milk samples using NIRS and chemometric techniques

4.1.1. Experimental design

As the initial phase of the experimental design, we will characterize and compare milk powders by measuring the following properties: water activity, insolubility index, density, and amino acid profile. In the second phase, we will analyse the prepared reconstituted milk samples using NIRS to predict quality parameters such as pH, conductivity, amino acid profile, dry matter, viscosity, fat content, and color properties. These parameters were measured using appropriate reference methods. Figure 4 summarize the experimental design used during this experiment.

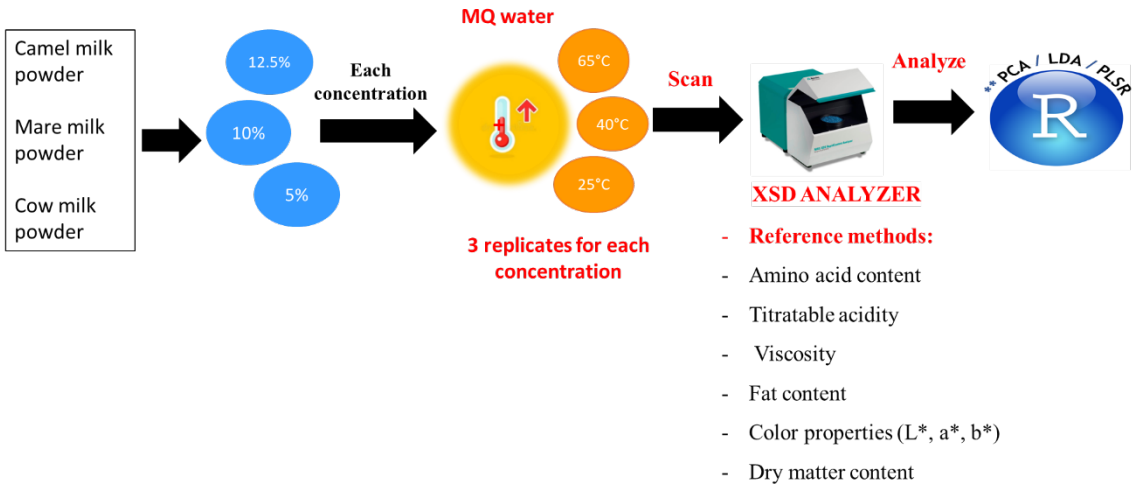

Figure 4. Experimental design of the NIRS analysis of reconstituted milk samples; PCA: Principle Component Analysis; LDA: Linear Discriminant Analysis; PLSR: Partial Least Squares Regression

4.1.2. Preparation of the reconstituted milk samples

- Analysed Milk Powders

This study used three commercially produced milk powders purchased from retail sources: skimmed cow milk powder produced by the Tutti brand in Budapest, Hungary, as well as whole camel and mare milk powders from the Saumal and Sydyk brands, respectively, sourced in Almaty, Kazakhstan.

- Preparation of Reconstituted Milk Samples

Due to the restricted market availability of milk powder samples, particularly for mare and camel milk, we aimed to include diverse variations during the milk powder reconstruction process to ensure that factors like concentration and temperature were adequately represented in our models. Samples of milk powder from cow, camel, and mare were reconstituted using Milli-Q water at three concentration levels (C1 = 5%, C2 = 10%, C3 = 12.5%). Each concentration was then dissolved at three different temperatures (T1 = 25 °C, T2 = 40 °C, and T3 = 65 °C), with three replicates performed for every concentration-temperature combination. The obtained samples were thoroughly mixed using a vortex mixer for 6 minutes to guarantee uniformity. This process yielded a total of 81 samples (3 milk types × 3 concentrations × 3 temperatures × 3 replicates). Once cooled, the prepared milk samples were promptly refrigerated and stored at 4 °C, till subsequent analysis.

4.1.3. Analysis of the Milk Powder Samples

The milk powder samples were analysed in triplicate for the following quality parameters:

- Water Activity

The milk powders' water activity (aw) was assessed at 25 °C with a Novasina LabMaster-aw neo device (Novasina AG, Switzerland) incorporating built-in temperature control (range: 0–60 °C). Approximately 1.5 ± 0.5 g of milk powder was weighed into the sample cup, which was then positioned in the measurement chamber and sealed tightly. After the system reached stability, the water activity values were recorded at 25 °C.

- Loose Bulk Density

The milk powders' density was evaluated as loose bulk density. This was determined by filling a 100 mL graduated cylinder with dried milk powder, ensuring it was precisely levelled without compressing, up to a predefined level. The loose bulk density was then calculated by applying the following formula:

$$\text{loose density } (kg.m^{-3}) = \text{powder weight } (kg)/\text{powder volume } (m^3).$$

- Insolubility Index

The insolubility index of the milk powders was determined following the method described by Pugliese et al., (2017). A 10 g sample of dried milk powder was carefully stirred into 100 mL of water at 25 °C for around 5 minutes. The resulting mixture was allowed to rest for 5–15 minutes, after which it was stirred with a spatula. A 50 mL portion of the suspension was then centrifuged for 5 minutes at 5× g. After removing the supernatant, the tube was refilled with water and

centrifuged again under the same conditions. The volume of the sediment was recorded. Additionally, the sediment underwent oven drying at 70 °C until consistent weight was achieved. The insolubility index was quantified both by the volume of the wet residue (mL), following the IDF method, and by the weight of the dried sediment (mg).

- Amino Acid Profile

Milk powder samples (80–120 mg) were hydrolysed in sealed vessels (KUTESZ, Budapest, Hungary) with 10 mL of 6 M HCl at 110 °C for 24 h in a block thermostat under a nitrogen atmosphere (FALC Instruments, Treviglio, Italy). The hydrolysates were neutralised with 10 mL of 4 M NaOH and filtered successively through standard paper and a 0.22 µm membrane (Nalgene, Rochester, NY, USA). Amino acids were quantified on an Automatic Amino Acid Analyzer AAA400 (Ingos Ltd., Prague, Czech Republic) equipped with an Ionex Ostion LCP5020 cation-exchange column (220 × 37 mm). After post-column derivatisation with ninhydrin, colorimetric detection was carried out at 570 nm and 440 nm. Separation was achieved in a strongly acidic medium using a step-gradient of lithium-citrate buffers of decreasing acidity (0.18 M, pH 2.80; 0.20 M, pH 3.05; 0.36 M, pH 3.35; 0.33 M, pH 4.05; and 1.20 M, pH 4.65). Chromatograms were processed with CHROMuLAN082 and compared with standard amino-acid mixtures.

4.1.4. Analysis of reconstituted Milk Samples

Triplicate measurements were performed for the quality evaluation of the reconstituted milk samples, as outlined below:

- NIRS Analysis

The NIR spectra of the reconstituted milk samples were acquired in transflectance mode using an XDS Rapid Content Analyzer (Metrohm, Denmark), spanning the spectral range of 400–2500 nm. Samples were scanned in a randomized sequence, with approximately 1.5 mL of each reconstituted milk sample introduced into a transflection vessel and sealed with a gold reflector plate, establishing a path length of 0.5 mm. Each sample underwent three consecutive scans at a spectral resolution of 0.5 nm. All spectral measurements were performed at ambient temperature (25 °C).

- Dry Matter Content

The dry matter content was calculated as the percentage by mass of material retained following a standardized drying procedure. Approximately 2 g of milk sample was subjected to oven drying at 105 °C until a constant weight was obtained (De Knegt & Van Den Brink, 1998).

- pH and Conductivity

The pH and electrical conductivity of the samples were assessed using a combined pH/conductivity meter (Mettler Toledo SevenMulti, Columbus, OH, USA). Calibration was performed at 25 °C to ensure accuracy.

- Acidity According to Soxhlet–Henkel (Titratable Acidity)

Titratable acidity was quantified in Soxhlet–Henkel degrees (SH°). This parameter was determined by titrating the milk samples with a 0.1 N NaOH solution, using phenolphthalein as the endpoint indicator (Fabro et al., 2006). The acidity of the milk was then calculated using the following formula:

$$°SH = \text{Added NaOH mL} \times \text{NaOH factor} \times 2.$$

- Viscosity

The flow curves were measured at a controlled temperature of 25 ± 0.2 °C using an MCR302 modular compact rheometer (Anton Paar, Austria) configured with coaxial cylindrical geometry (CC27). Data acquisition was managed through Rheo Compass software (version 3.63). During the initial measurement phase, the shear rate was progressively increased on a linear scale from 0.1 s^{-1} to 1000 s^{-1}. Thirty data points were collected at logarithmically decreasing time intervals, varying from 10 seconds to 2 seconds. In the subsequent phase, viscosity measurements were recorded at fixed intervals of three seconds, producing 30 data points at a constant shear rate of 1000 s^{-1}. From these data, the apparent viscosity at a shear rate of 750 s^{-1} during the ramp-up phase was determined, along with the mean dynamic viscosity at the steady maximum shear rate.

- Fat Content

The total fat content (v/v%) was measured using the Gerber (acido-butyrometric) method, in accordance with the ISO 2446 and IDF 105 standards. The procedure was performed as outlined by Trout & Lucas (1947) and Esen & Güzeler (2023).

- Color characteristics

The color characteristics of the samples were assessed using a ColorLite sph 850 spectrophotometer (ColorLite GmbH, Katlenburg-Lindau, Germany) across wavelengths from 400 to 700 nm, with a D65 light source and a 2° observer angle. The resulting colorimetric values were reported using the CIE (Commission Internationale de la Éclargie) L*, a*, and b* color components.

4.1.5. Data Analysis

Descriptive statistics and two-way analysis of variance (ANOVA) were performed on the collected data using IBM SPSS27 software (Armonk, NY, USA, 2020) for statistical evaluation Two-way ANOVA was used to assess differences between sample groups, considering the following factors: milk powder type, concentration, and temperature during reconstruction. The normality of residuals of all dependent variables was checked using the Kolmogorov–Smirnov (KS) test, and the homogeneity of variances was tested using the Levine's test. Upon obtaining statistically significant outcomes from the two-way ANOVA ($p < 0.05$), post hoc test was applied: Tukey's test for homogeneity of variance and the Games–Howell test for non-homogeneity of variance, to assess group differences.

Chemometric evaluation of the NIRS data was conducted using R-project software (version 4.3.1) with the package aquap2, employing principal component analysis (PCA) (Cowe & McNicol, 1985), PCA-based linear discriminant analysis (PCA-LDA) (Tominaga, 1999), partial least square regression (PLSR) (Li et al., 2002) and support vector regression (SVR) (Soares & Anzanello, 2018) techniques. The analysis focused on the wavelength range of 1100–1850, given that the wavelengths most pertinent to the performance of classification and regression models were concentrated within the longer spectral region. Wavelengths beyond 1850 nm were excluded due to absorbance exceeding the detector's linear response range.

A preliminary check for atypical or outlying data points within the spectral dataset was conducted using PCA. PCA-LDA was utilized to develop classification models to differentiate between the types of reconstituted milk, temperature and concentration levels. Three PCA-LDA models were created for each temperature level to distinguish between milk types and concentrations, and for each type of milk, three classification models were developed for each concentration level to differentiate between the temperatures used during the preparation. The PLSR method was employed to develop prediction models for the quality parameters of the reconstituted milk samples, namely the pH, conductivity, amino acid profile, dry matter, viscosity, fat content, and color properties.

Model validation for the PCA-LDA classification was carried out using a leave-one-repeat-out cross-validation strategy. In this approach, data corresponding to one repeat were systematically excluded from the training dataset and reserved as the validation set, while the remaining two repeats, comprising roughly two-thirds of the total data, were used to train the model. This process was repeated three times, ensuring each repeat (one-third of the data) served once as the validation set. Similarly, Partial Least Squares Regression (PLSR) models underwent validation through the

same leave-one-repeat-out cross-validation method, treating three consecutive spectral scans as a single repeat unit.

To prevent overfitting, especially given the limited number of samples, a rigorous data partitioning method was adopted for creating training and test subsets. Specifically, two-thirds of the data were allocated for model training, with the remaining one-third reserved for independent prediction testing. This data split was carefully balanced by accounting for critical factors including sample concentration, reconstruction temperature, replicate number, and the sequence of consecutive scans.

To ensure the integrity and fairness of the validation process, two key principles were strictly applied: (1) all consecutive scans belonging to the same sample were assigned entirely to either the training set or the test set and (2) the proportion of training to test samples was maintained consistently across all groups defined by temperature and concentration categories.

For comparative purposes, a similar validation method was applied to SVR. Dimensionality reduction was achieved via PCA by selecting principal components (PCs) that accounted for 95% of the total variance, which were then used as input variables for SVR modelling. Hyperparameters were selected by tuning the error weight (C: 0.1–10) and maximum error value (ε: 0.01–0.5) parameters, and testing various kernel functions (linear, polynomial, and radial). The cost function was optimized to reduce coefficients and prediction errors, resulting in the best-performing model for each parameter.

Before model construction, raw spectral data underwent various pretreatment processes aimed at reducing noise by employing smoothing methods and enhancing the chemical information signals through techniques such as derivation, normalization, and differentiation. The range of pretreatments applied comprised multiplicative scatter correction (MSC) (Dhanoa et al., 2024), standard normal variate (SNV), the Savitzky–Golay second derivative with a 21-point window (Sgolay 2-21-0), de-trending (deTr) (Barnes et al., 1989; Savitzky & Golay, 1964), alongside combinations of these methods. From these, only the spectral pretreatment that produced the most accurate and reliable model results was chosen for reporting.

4.2.Identifying key factors that distinguish fermented milk based on feeding type and probiotic potential with e-nose and NIRS techniques

4.2.1. Experimental design

In the initial phase of the experimental design, the fatty acid profiles of the experimental raw milk samples were analysed and compared to those of the control samples. During the second phase, the fermented milk samples was examined using NIRS and e-nose techniques to assess differences in chemical composition and aromatic compounds between the experimental and control fermented milk samples, as well as across different probiotic types. Figure 5 summarize the experimental design used during this experiment.

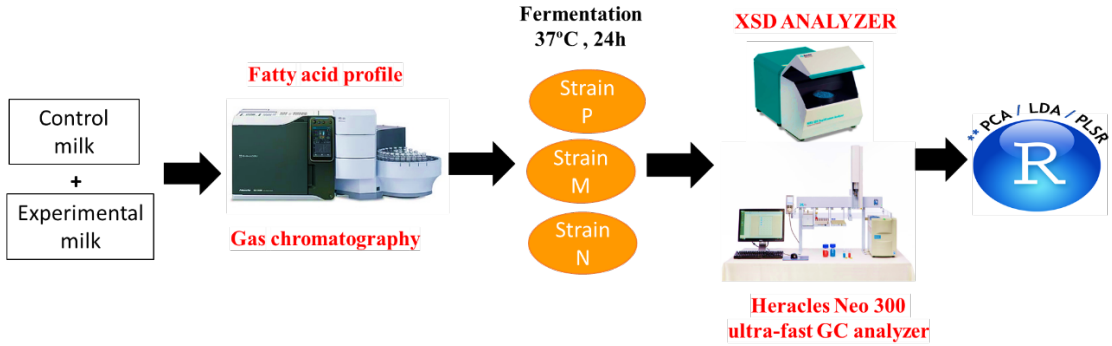

Figure 5. Experimental design of the NIRS and e-nose analysis of fermented milk samples PCA: Principle Component Analysis; LDA: Linear Discriminant Analysis; PLSR: Partial Least Squares Regression

4.2.2. Preparation of fermented milk samples

- Raw milk samples

Three separate 6-week trials were carried out to evaluate the impact of Total Mixed Ration (TMR) diets supplemented with fat sources rich in polyunsaturated fatty acids (PUFAs) in comparison to control diets primarily composed of saturated fatty acids (SFAs). Each trial included 70 Holstein cows, which were evenly divided into experimental and control groups. To minimize variability and ensure comparability between groups, cows were paired based on key factors including the number of lactations, days in milk (DIM), milk yield recorded during the previous 305-day lactation period, milk composition parameters (specifically protein and fat content), and somatic cell count (SCC). These paired cows were then randomly assigned to either the experimental or control feeding groups.

The feeding regimens for the control and experimental groups were implemented concurrently in

each trial, thereby controlling seasonal and environmental variations that could influence the results. Comprehensive details regarding the nutritional composition of the feeds used in the trials are provided in Table 4.

Table 4. Description of the experimental design of the feeding trials

Date range	Trial number	Control feed	Experimental feed	Season	Number of cows
29.06.2022-21.07.2022	Trial 1	TMR + hydrogenated palm oil	TMR + whole linseed + linseed oil	Summer	70
02.11.2023-19.12.2023	Trial 2	TMR + hydrogenated palm oil	TMR + whole linseed + algae extract	Autumn	70
02.05.2024-20.05.2024	Trial 3	TMR + hydrogenated palm oil	TMR + whole linseed + algae extract + fish oil + linseed oil	Spring	70

All the trials were performed at the dairy farm operated by Pálhalmai Agrospeciál Kft. in Dunaújváros, Hungary. The specialized feed supplements for the experimental groups were provided by ADEXGO Kft., located in Balatonfüred, Hungary. Throughout the entirety of each 6-week trial period, bulk milk samples were collected on a weekly schedule to systematically monitor compositional changes over time. For fermentation studies, bulk milk samples, each consisting of approximately 101 units, were specifically collected during the final two weeks of each trial. This sampling protocol yielded a total of twelve distinct milk samples, calculated as two weeks multiplied by three separate trials and two dietary treatments (control and experimental). Immediately following collection, all samples were promptly refrigerated and maintained at a controlled temperature of 4 °C to prevent compositional degradation, thereby ensuring sample integrity for all subsequent analytical assessments and fermentation processes.

- Fermented milk samples

Preparation of bacterial strain suspensions

Three distinct strains of *Lactobacillus bulgaricus* bacteria were obtained in freeze-dried form from the Department of Biomeasurement Technology Laboratory, Graduate School of Agriculture Science, Kobe University, Japan. The strains, *L. bulgaricus* S06, *L. bulgaricus* S04, and *L.*

bulgaricus S09, were individually used to ferment milk samples based on their probiotic potential. Their classification was determined by evaluating their growth rate, optical density, biomass production, minimal inhibitory concentration of bile salts, and their ability to recover after three hours of exposure to low pH conditions in the presence of pepsin. Accordingly, the strains were classified as follows: probiotic (P): *L. bulgaricus* S06; moderate (M): *L. bulgaricus* S09; and non-probiotic (N): *L. bulgaricus* S04.

Before fermentation, the *L. bulgaricus* strains were activated through the following process: 100 mg of each freeze-dried strain was aseptically transferred into a 100 mL flask containing reconstituted skim milk. The prepared bacterial suspensions were then incubated at 37°C for 24 hours to promote bacterial activation.

Preparation of fermented milk samples

All collected milk samples underwent pasteurization at 63°C for 30 minutes using an ultrasonic bath to ensure microbial safety. After pasteurization, 200 mL aliquots of milk were aseptically dispensed into sterile jars and inoculated with 0.2 mL of the prepared bacterial suspensions. Each feeding trial was performed independently to maintain experimental integrity. Samples were systematically labelled as follows: CTRF (non-fermented control milk), EXPF (non-fermented experimental milk), CTR (control fermented milk), EXP (experimental fermented milk), CN (control milk inoculated with the non-probiotic strain), CM (control milk inoculated with the moderate strain), CP (control milk inoculated with the probiotic strain), TN (experimental milk inoculated with the non-probiotic strain), TM (experimental milk inoculated with the moderate strain), and TP (experimental milk inoculated with the probiotic strain). For each condition, triplicate preparations (R1, R2, R3) were made, resulting in a total of 144 samples, comprising 108 fermented and 36 fresh milk samples. The inoculated samples were incubated at 37°C for 13 hours to facilitate fermentation, while the fresh milk samples were promptly refrigerated at 4°C to preserve their integrity for subsequent fatty acid profile analyses. This rigorous approach ensured reproducibility and reliability across all experimental conditions.

4.2.3. Fatty acid profile analysis

The fatty acid analysis of the milk samples was conducted using previously frozen samples that were thawed prior to the analysis, as described by Varga-Visi et al. (2022). In brief, the samples were homogenized (IKA T25 Ultra Turrax, IKA, Staufen, Germany) with chloroform:methanol (2:1 vol:vol), containing 100 mg/L butylated hydroxytoluene (BHT) as an antioxidant and internal fatty acid standard (C19:0, Sigma, cat. no. 72332, Supelco, Bellefonte, PA, USA). Total lipid extraction was performed based on the method of Folch et al. (1957). Fatty acid methyl esters were

prepared using 1% H_2SO_4 in methanol, as described by Christie (2003).

Fatty acid composition was analysed using gas chromatography (Shimadzu Nexis 2030, Kyoto, Japan) equipped with flame ionization detector (FID), after separation in a Zebron ZB-WaxPlus capillary column (30 m × 0.25 mm × 0.25 micrometer film, Phenomenex Inc., Torrance, CA, USA). Operating conditions included an injector temperature of 220°C, a detector temperature of 250°C, and a helium flow rate of 28 cm/s. The oven temperature program was set as follows: an initial hold at 60°C for 2 minutes, followed by a gradual increase to 150°C, then from 150°C to 180°C at 2°C/min with a 10-minute hold at 180°C, and finally from 180°C to 220°C at 2°C/min with a 16-minute hold at 220°C. Nitrogen was used as the make-up gas. Chromatographic evaluation was performed using LabSolutions 5.93 software (Shimadzu, Kyoto, Japan) with the Post Run module and manual peak integration. Fatty acid composition was expressed as a percentage of total FAMEs. Fatty acids were identified based on retention times compared to a certified reference material (CRM) external standard (Supelco 37 Component FAME Mix, Merck-Sigma Aldrich, CRM47885, Steinheim, Germany).

4.2.4. NIRS analysis

The NIR spectra of the fermented milk samples were acquired using the XDS Rapid Content Analyzer (Metrohm, Herisau, Switzerland) operating in transflectance mode, spanning a wavelength range of 400–2500 nm. For each analysis, 1.5 mL of sample was placed into a transflection vessel and covered with a gold reflector plate to achieve a 0.5 mm path length. Samples were scanned in a randomized sequence to minimize bias. Each sample underwent three consecutive scans at a spectral resolution of 0.5 nm, with spectral data collected at room temperature (25°C).

4.2.5. E-nose analysis

E-nose measurements were performed using a Heracles Neo 300 ultra-fast GC analyser (Alpha MOS, Toulouse, France). The autosampler and analyser were controlled with AlphaSoft version 16 software (Alpha MOS, Toulouse, France). The measurement and data acquisition followed the protocol detailed by (Yakubu et al., 2023). Briefly, samples were stored at 4 °C prior to analysis. For each measurement, 1 mL of sample was placed into a 20 mL glass vial sealed with a silicon-PTFE septum, then kept on a cooled tray at 4 °C until analysed. To generate a saturated headspace, samples were incubated at 50 °C for 3 minutes, after which 5 mL of headspace gas was injected into the analyser. Ultra-high purity hydrogen served as the carrier gas, with controlled temperature and flow parameters maintained throughout. Odor compounds were first trapped in a cold trap at 30 °C, then flushed, heated, and passed through two chromatographic columns (MXT-5 and MXT-

1701; Restek, Bellefonte, PA, USA) operating from 50 °C to 250 °C. Separation of volatile compounds was achieved on the columns and detected by dual flame ionization detectors (FID). Each sample analysis lasted 2 minutes. The resulting chromatograms recorded compound retention times, which were converted into Kovats retention indices. Odor fingerprints were generated from the chromatograms, where each peak corresponded to a virtual sensor and the Odor intensity was quantified by the peak area.

4.2.6. Data analysis

For each feeding trial, a one-way analysis of variance (ANOVA) was conducted to assess the levels of saturated (SFA), monounsaturated (MUFA), and polyunsaturated fatty acids (PUFA) in raw milk samples. The analyses were carried out using IBM SPSS Statistics 27 (Armonk, NY, USA, 2020), evaluating variations in fatty acid content across groups defined by feeding type. To verify the normality of residuals for all dependent variables, the Anderson-Darling test was employed due to its robustness in detecting deviations. Additionally, the Shapiro-Wilk test was used to confirm the ANOVA's normality assumption, and its results supported this assumption. Statistically significant differences were considered at $p < 0.05$. Groups with significant differences ($p \leq 0.05$) were labelled with distinct letters (a–f) and identical letters indicated no significant difference between control and experimental groups.

Chemometric analysis of the NIRS and e-nose datasets, including spectral preprocessing, was performed using R (version 4.3.1). The aquap2 package was utilized for both principal component analysis (PCA) (Cowe & McNicol, 1985) and PCA-based linear discriminant analysis (PCA-LDA) (Tominaga, 1999). For NIRS data, analysis focused on the 1100–1850 nm spectral range, where the most informative wavelengths for classification were located. Wavelengths above 1850 nm were excluded because absorbance values over 2 exceed the detector's linear range (Shen et al., 2010). Spectral pretreatments were applied to minimize noise and enhance chemical signal clarity. These included multiplicative scatter correction (MSC) (Dhanoa et al., 2024), standard normal variate (SNV), Savitzky-Golay second derivative with a 21-point window (SGolay 2-21-0), de-trending (deTr) (Barnes et al., 1989; Savitzky & Golay, 1964), and their combinations. Only the preprocessing method yielding the best model performance was reported.

The NIRS and e-nose datasets were analysed separately. An initial PCA was performed on each dataset to detect outliers and reveal underlying patterns. PCA score plots were generated in various dimensional combinations, with the clearest and most variance-explaining plot chosen for further interpretation. Ellipses in the PCA score plots were computed using the mean and covariance of

the data points, where the axes corresponded to the principal components and their sizes represented the data spread along these components, reflecting a 95% confidence interval.

Next, PCA-LDA was used to develop classification models distinguishing fermented milk samples by feeding type and bacterial strain. Six classification models were developed, three for each dataset (NIRS and e-nose) corresponding to the three feeding trials. PCA-LDA, a two-step supervised classification technique, first reduced dimensionality using PCA to extract uncorrelated components, then applied LDA to enhance group separation. PCA transformed the high-dimensional data into orthogonal principal components retaining most of the variance, while LDA projected these onto a subspace that maximized between-class variance relative to within-class variance (de Almeida et al., 2021b). The PCA-LDA models were validated using a threefold cross-validation technique. In this method, one-third of the dataset was set aside as a validation set, while the remaining two-thirds were used to train the model. This process was repeated three times, each time with a different third of the data designated for validation.

To identify the most contributing wavelengths for classification, the weighted sum of PCA-LDA loadings was analyzed. In the NIRS dataset, this approach assigned a contribution coefficient to each wavelength, with key wavelengths identified by the highest peaks in the contribution graph (Hair et al., 2013). Likewise, in the e-nose dataset, the most influential virtual sensors were identified, with those exhibiting the highest contribution coefficients being highlighted. The volatile compounds linked to these sensors were determined using the Closest Sensors (C-S) feature in the AroChemBase v8 database, accessed via AlphaSoft version 16 software (Alpha MOS, Toulouse, France). By matching sensor IDs with their corresponding C-S numbers, the related volatile compounds and their sensory attributes were identified, offering a clearer understanding of the chemical foundations underlying the classification models.

4.3.Evaluation of the impact of cattle feed on cheese ripening process by NIRS

4.3.1. Experimental design

Initially, fresh cheese samples were analysed and scanned using the MicroNIR 1700 EC spectrometer. The following key quality parameters were measured and analysed with appropriate reference methods: dry matter content, crude fat content, crude protein content, and ash content. In the second phase of the study, the aged cheese samples were examined using the NIRS XDS analyser. This evaluation aimed to identify differences between stored samples from the experimental group and those from the control group to provide a comprehensive assessment of the effects of storage conditions on the cheese samples. Figure 6 presents the detailed protocol of the experiment.

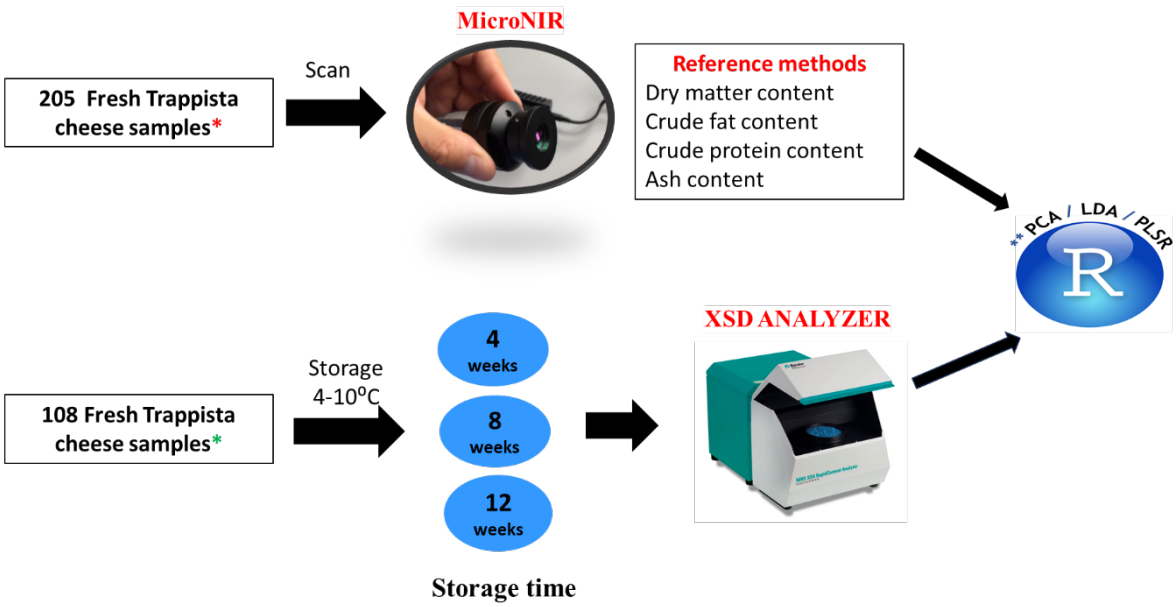

Figure 6. Experimental design of the NIRS and E-nose analysis of experimental and control cheese samples PCA: Principle Component Analysis; LDA: Linear Discriminant Analysis ; PLSR: Partial Least Squares Regression

4.3.2. Preparation of the cheese samples

Control and experimental Trappista cheese samples were sourced from ADEXGO Kft. The control Trappista cheese was produced using milk obtained from control feeding trials (Trials 1, 2, and 3), while the experimental cheese was made from milk derived from experimental feeding trials (Trials 1, 2, and 3). The detailed experimental design and feeding trial protocols are outlined in Table *4*.

A total of 205 fresh cheese samples were vacuum sealed to ensure optimal preservation and stored at a stable temperature of 4 °C in a refrigerator until further analysis. These samples were produced as part of three feeding trials: Trial 1 included 37 control and 40 experimental samples, Trial 2 consisted of 36 control and 40 experimental samples, and Trial 3 comprised 27 control and 25 experimental samples.

Additionally, 108 cheese samples, including replicates obtained from Feeding Trial 2, were stored at 4 °C - 10 °C. These samples were monitored at four predefined storage intervals: 0, 4, 8, and 12 weeks, to evaluate changes over time. To enhance the reliability and reproducibility of the results, the entire experiment was performed twice.

4.3.3. Analysis of fresh cheese samples

- Crude fat content

The crude fat content of the cheese samples was analysed by using a 3 g dried sample, which was processed through a Soxhlet apparatus for 2-3 hours with petroleum ether as the solvent, following the AOAC (2000) method No. 30-10.

Crude fat (%) = Weight of fat ∗ 100 / Weight of cheese sample

- Crude protein content

The crude protein content of the cheese was determined using the Kjeldahl method, as outlined in AOAC (1920) method No. 87. Approximately, 2 g of the cheese sample was weighed and placed into a digestion tube. 20 ml of concentrated sulfuric acid (98%) and two digestion mixture tablets (acting as catalysts) were added. The sample was digested for 3-4 hours until the contents became transparent in color. After digestion, the mixture was cooled to room temperature and diluted to a final volume of 50 mL. The ammonia trapped in sulfuric acid was released by adding 40% sodium hydroxide during distillation and collected in a flask containing 4% boric acid solution with a methyl indicator. The mixture was then titrated with a standard 0.1N sulfuric acid solution.

The conversion factor of 6.38 was used to calculate the crude protein content from the percentage of nitrogen in the cheese.

$$\textbf{Total Nitrogen} = (14.007 \times (T - B) \times N \times 100) / W$$

Where: **T**: Volume (in mL) of the standard sulfuric acid solution used in the titration for the test material; **B**: Volume (in mL) of the standard sulfuric acid solution used in the titration for the blank determination; **N**: Normality of the standard sulfuric acid solution; **W**: Weight (in grams) of the test material.

- Ash content

The total ash content of the cheese was measured by weighing a 3g of the sample in a pre-weighed crucible. The sample was charred over a flame until it turned black, then placed in a muffle furnace at 550°C for 5 hours or until a grey ash color was achieved. The procedure followed AOAC (2000) method No. 08-01. The ash content was calculated using the formula provided below:

Ash (%) = Weight of ash ∗ 100/ weight of sample

- Dry matter content

The dry matter of the cheese was determined following AOAC (2000) method No. 44-15A. A. 5g

of the sample was dried in a conventional drying oven at 105 ± 5°C until a constant weight was achieved. The moisture content was then calculated using the formula provided below:

Moisture (%) = (weight of original sample − weight of dried sample) ∗ 100 / weight of original sample

4.3.4. NIRS analysis of stored cheese samples

Before conducting the NIRS measurements, the cheese was carefully prepared by cutting it into circular slices with a uniform thickness of 1 cm. To ensure precision and consistency across all samples, a 3D-printed model was utilized during the cutting process to achieve the exact 1 cm thickness. Once the cheese was cut into standard layers, the slices were further shaped into circles specifically designed to fit the NIRS circular glass cuvette. Figure 7 illustrates the process of cheese preparation for NIRS analysis.

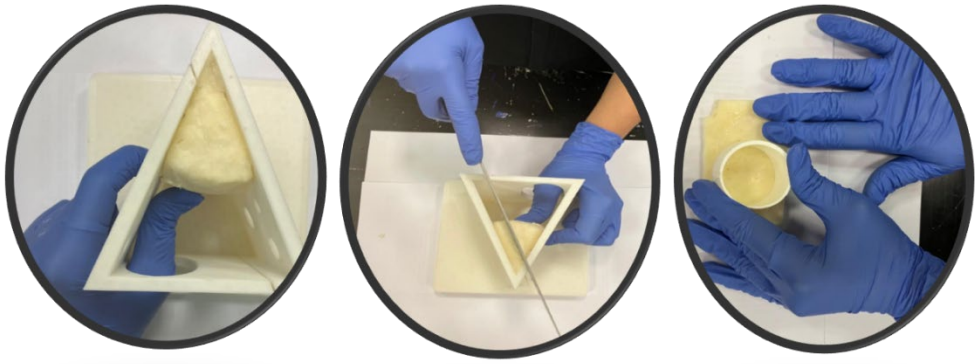

Figure 7. Cheese sample preparation procedure for the NIRS analysis

The NIR spectra of fresh cheese samples were acquired using a MicroNIR 1700 EC spectrometer (Viavi Solutions Inc., Chandler, AR, USA). This device incorporates a multielement InGaAs array detector integrated with a linear variable filter (LVF). The measurements were performed in diffuse reflectance mode, covering a wavelength range of 908–1676 nm with a spectral resolution of 6.2 nm. For the aged cheese samples, spectral data were collected using the XDS Rapid Content Analyzer (Metrohm, Herisau, Switzerland) in transflectance mode, which covers a broader wavelength range of 400–2500 nm.

All cheese samples were scanned in random order to avoid bias. Each sample underwent three consecutive scans with the XDS analyser, whereas the MicroNIR analysis involved 3 to 6 scans per sample. Throughout the process, the sample temperature was carefully maintained between 20 and 24 °C. This precise temperature control was essential due to the high moisture content of the cheese, as significant temperature variations could distort the water spectrum. Such distortions

would complicate spectral interpretation and potentially reduce the accuracy of the analysis.

4.3.5. Data analysis

For each feeding trial, one-way analysis of variance (ANOVA) was conducted to evaluate the levels of dry matter, crude fat, crude protein, and ash in the fresh cheese samples. The analysis was performed using IBM SPSS Statistics 27 software (Armonk, NY, USA, 2020) to examine compositional differences among sample groups based on feeding type. The normality of residuals for all dependent variables was verified using the Kolmogorov-Smirnov (KS) test. Statistically significant differences between groups were determined when the ANOVA p-value was below 0.05.

Chemometric analysis of the NIRS data was performed using R-project software (v4.3.1) with the aquap2 package, utilizing principal component analysis (PCA) (Cowe & McNicol, 1985) and linear discriminant analysis (LDA) (Liu, 2013) methods. For the NIRS analysis of fresh cheese samples, the wavelength range of 908–1676 nm was selected, while the aged cheese samples were analyzed in the spectral range of 1100–1850 nm. Several spectral pretreatments were applied to the raw spectra, including multiplicative scatter correction (MSC) (Dhanoa et al., 2024), Savitzky-Golay second derivative with a 21-point window (SGolay 2-21-0), de-trending (deTr) (Barnes et al., 1989; Savitzky & Golay, 1964), and their combinations.

The PCA-LDA technique was employed to create classification models for distinguishing cheese samples based on feeding type and ripening period. A PCA-LDA classification model was developed to classify fresh cheese samples according to feeding type. Additionally, three PCA-LDA models were constructed for each ripening period (4, 8, and 12 weeks) to classify samples by feeding type. Two PCA-LDA models were developed for each feeding type (control and experimental) to classify samples based on ripening period.

The PCA-LDA models were validated using a threefold cross-validation method, where one-third of the data was excluded from the training set and used for validation, while the remaining two-thirds were used for model development. This process was repeated three times, with a different one-third of the data used as the validation set in each iteration. Furthermore, the wavelengths that significantly contributed to the classification models were identified.

5. RESULTS AND DISCUSSION

5.1. Evaluation of the quality of reconstituted cow, camel and mare milk samples using NIRS and chemometric techniques

5.1.1. Characterization of cow, camel and mare milk powder samples and reconstituted milk samples

During storage, maintaining water activity at a specific level is crucial to prevent the irreversible crystallization of amorphous lactose, which can cause lump formation in milk powder (Pugliese et al., 2017). As shown in Table 5, the mean of the water activity values for cow, camel, and mare milk powders were 0.24, 0.28, and 0.22, respectively. This reflects low moisture levels that help ensure microbial stability and long shelf life, particularly important in powdered dairy products (Zou et al., 2022). These findings align with those of Pugliese et al. (2017), who reported water activity levels in milk powders ranging from 0.24 to 0.33.

The insolubility index of the analysed powders ranged from 0.1 to 1.37, with skimmed cow milk powder exhibiting the lowest index and whole mare milk powder the highest. Pugliese et al. (2017) also observed similar trends, reporting insolubility indices for whole milk powders between 0.1 and 0.8 mL, and for skimmed milk powders from <0.1 to 0.1 mL. Wang et al. (2021) further confirmed these results, noting insolubility indices for various milk powders ranging from 0.14 mL to 7.54 mL, with skimmed milk powders consistently showing the lowest values. According to the International Dairy Federation (IDF) standard, the insolubility index measures the volume of sediment formed after rehydration, mixing, and centrifugation (Schuck, 2011). The solubility of milk powders is significantly influenced by the behavior of milk proteins. During rehydration, protein denaturation, caused by changes in temperature or pH, leads to aggregation and sediment formation, thereby increasing the insolubility index (Schuck, 2011; Augustin et al., 2003). In whole milk powders, coagulated proteins, along with entrapped milk fat globules may float to the surface (Kalyankar et al., 2015). A high insolubility index during storage is also associated with the Maillard reaction (Wang et al., 2021).

Bulk density is another critical factor affecting the commercial, economic, and functional value of milk powders (Sharma et al., 2012). Powders with higher bulk density are preferred due to reduced packaging, storage, and transportation costs (Schuck, 2011). The bulk density of the analysed milk powders varied between 393.65 and 678.9 kg/m³. This reflects how concentrated or “packed” the powder is, a higher bulk density typically indicates a denser powder which reduces packaging, storage, and transportation costs and improves flow and handling. Lower bulk density, by contrast,

often results from more porous or agglomerated powders that may dissolve more quickly but occupy more volume and can incur higher logistics cost (Ding et al., 2020; Pugliese et al. 2017)

Water activity, insolubility index, and bulk density are key quality indicators for milk powders. ANOVA results revealed that the type of dried milk was the most significant parameter, showing notable differences in water activity, bulk density, and insolubility index among the tested powders. Variations in processing plants, processing parameters, and external factors such as animal type, genetics, and breed can influence the physical properties of milk powders. Wang et al. (2021) also demonstrated that the type of dried milk was the primary factor leading to significant differences between milk powders.

Table 5. Mean ± SD of water activity, insolubility index and bulk density for each type of milk powder (cow, camel and mare)

Measured parameters	**Cow milk powder**	**Camel milk powder**	**Mare milk powder**
Water activity	0.24± 0.006^{a}	0.28± 0.002^{b}	0.22± 0.08^{c}
Insolubility index (mL)	0.1± 0.005^{a}	0.75± 0.03^{b}	1.37± 0.02^{c}
Bulk density (Kg m^{-3})	678.9± 14.1^{a}	393.65± 34.75^{b}	549.76± 16.21^{c}

Different letters (a-c, read vertically) assigned for significantly different groups ($p < 0.05$)

The two-way ANOVA results summarizing the main quality parameters of the reconstituted milk samples revealed significant differences based on the concentration or temperature levels used for reconstitution, as shown in Table 6.

The interaction between milk type and temperature significantly affected the conductivity, pH, and a* values of the milk samples. However, the type of powdered milk had a greater influence on pH and a* compared to temperature. Reconstituted camel milk exhibited the lowest pH values (~6.5), consistent with findings reported by Swelum et al. (2021).

Additionally, the interaction between milk type and concentration significantly influenced viscosity, titratable acidity, dry matter (%), L*, and b* values. Concentration appeared to have a stronger impact on dry matter content and viscosity than the type of powdered milk. The viscosity of the reconstituted milk increased with higher concentration and dry matter content, with cow and camel milk showing the highest viscosity. In contrast, titratable acidity was more affected by the type of powdered milk rather than concentration, with reconstituted camel milk recording the highest values.

In conclusion, most of the significant differences observed among cow, mare, and camel milk samples reconstituted to varying concentrations and temperatures were primarily attributed to the type of powdered milk used.

Table 6. Mean ± SD of the apparent viscosity, conductivity, pH, titratable acidity, dry matter and color parameters (L*,a*,b*) of cow, camel and mare milk samples reconstituted from milk powders at different concentrations (C1(5%), C2(10%), C3(12.5%)) and temperature levels (T1(25°C), T2(40°C), T3(65°C))

Reconstituted milk powder				
Measured parameters	**Experiment group**	**Cow milk**	**Camel milk**	**Mare milk**
Apparent viscosity (mPa s^{-1})	C1	3.88± 0.05^{Aa}	3.96± 0.05^{Ba}	3.63± 0.06^{Ca}
	C2	4.20± 0.06 ^{Ab}	4.25± 0.08^{Ab}	3.82± 0.05^{Bb}
	C3	4.53± 0.07^{Ac}	4.64± 0.13^{Ac}	4.00± 0.04^{Bc}
Conductivity (mS cm^{-1})	T1	6.41± 0.03^{Aa}	5.17± 0.12^{Ba}	2.25± 0.02^{Ca}
	T2	7.36± 0.11^{Ab}	5.93± 0.04^{Bb}	2.55± 0.09^{Cb}
	T3	8.32± 0.06^{Ac}	6.45± 0.06^{Bc}	2.71± 0.03^{Cc}
pH	T1	6.73± 0.06^{Aa}	6.57± 0.05^{Ba}	7.19± 0.04^{Ca}
	T2	6.71± 0.06^{Aa}	6.53± 0.08^{Ba}	7.12± 0.07^{Cb}
	T3	6.72± 0.05^{Aa}	6.51± 0.06^{Ba}	7.23± 0.04^{Ca}
Titratable acidity (°SH)	C1	6.36± 0.7^{Aa}	6.32± 0.44^{Aa}	2.00± 0.15^{Ca}
	C2	6.35± 0.29^{Aa}	6.90± 0.22^{Bb}	2.38± 0.19^{Cb}
	C3	6.95± 0.12^{Ab}	7.32± 0.23^{Bc}	2.56± 0.21^{Cb}
Dry matter (%)	C1	9.08± 0.31^{Aa}	8.75± 0.30^{Ba}	8.93± 0.14^{ABa}
	C2	11.18± 0.23^{Ab}	10.80± 0.14^{Bb}	10.82± 0.16^{Bb}
	C3	13.5± 0.46^{Ac}	12.57± 0.13^{Bc}	12.77± 0.68^{Bc}
L*	C1	68.56± 0.72^{Aa}	61.01± 0.85^{Ba}	57.51± 0.77^{Ca}
	C2	69.90± 0.63^{Ab}	62.69± 0.50^{Bb}	59.97± 0.68^{Cb}
	C3	70.75± 0.47^{Ac}	63.84± 0.60^{Bc}	61.67± 0.47^{Cc}
a*	T1	-0.74± 0.05^{Aa}	-3.01± 0.06^{Ba}	-0.92± 0.04^{Ca}
	T2	-0.77± 0.07^{Aa}	-3.20± 0.03^{Bb}	-1.00± 0.05^{Cb}
	T3	-0.74± 0.05^{Aa}	-3.33± 0.07^{Bc}	-1.02± 0.04^{Cb}
b*	C1	-2.57± 0.13^{Aa}	-5.73± 0.30^{Ba}	-5.18± 0.12^{Ca}
	C2	-1.91± 0.12^{Ab}	-4.69± 0.23^{Bb}	-4.45± 0.12^{Cb}
	C3	-1.36± 0.10^{Ac}	-3.97± 0.26^{Bc}	-3.94± 0.08^{Bc}

Distinct letters (a–c or A–C) were used to denote groups with significant differences. Lowercase letters correspond to comparisons within a single type of milk powder (read vertically), while uppercase letters refer to comparisons across the three types of milk powder (read horizontally). Only parameters that showed significant effects are reported.

5.1.2. NIRS results

- Visual analysis of the spectra and the PCA model

Figure 8 displays the raw near-infrared spectra of reconstituted cow, camel, and mare milk samples across the spectral range of 400–2500 nm. Two prominent peaks were observed around 1440 nm and 1950 nm, associated with the OH symmetric/asymmetric stretching and bending vibrations of water (Kasemsumran et al., 2007). Notable differences are evident in the raw spectra of the reconstituted milk samples, primarily attributed to variations in their chemical composition.

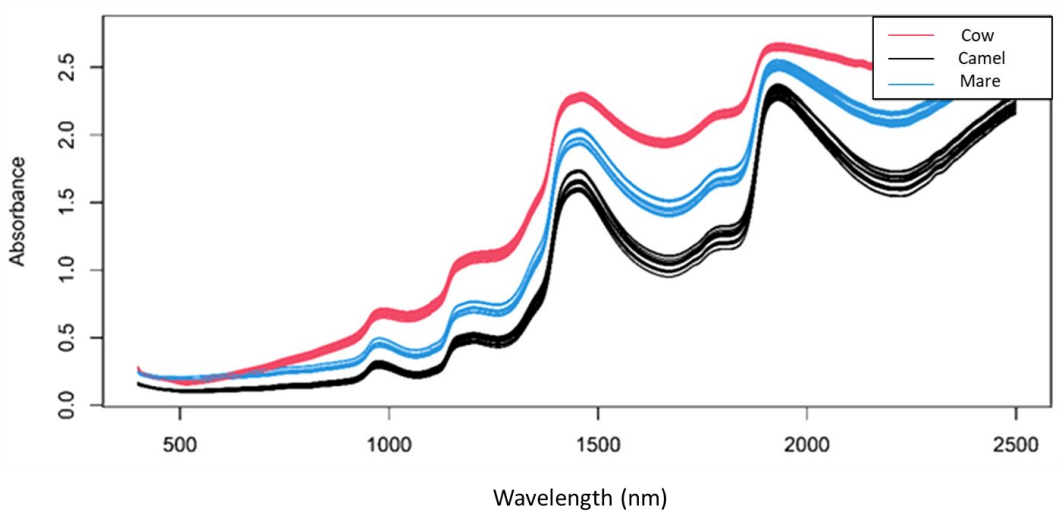

Figure 8. Raw spectra of reconstituted milk samples colored by the type of milk powder (400-2500nm); N= 243

Figure 9 (a) depicts the PCA score plot for reconstituted cow, camel, and mare milk at three concentration levels. The first two principal components, together explaining 99.14 % of the total variance, clearly segregate the three milk types. This clustering supports the ANOVA results, which showed that milk-powder type is a significant source of variation. Along the PC2 axis, an additional gradient differentiates samples by concentration. This trend is evident for camel and mare milk, whereas cow-milk samples cluster tightly, showing little concentration-dependent separation.

The wavelengths contributing most to the separation of cow milk from the other types are 1358 nm, 1450 nm, and 1664 nm (Figure 9 (b), PC1). In contrast, the wavelengths responsible for distinguishing camel and mare milk, as well as their different concentrations, are 1119 nm, 1280 nm, 1390 nm, 1554 nm, 1727 nm, and 1764 nm (Figure 9 (b), PC2). The 1280 nm wavelength is associated with the first overtone bands of bonded OH-H, while 1119 nm is linked to the C-H stretch overtone (H. Yu et al., 2020). Wavelengths at 1727 nm and 1764 nm are attributed to fat and fatty acid absorption, corresponding to the first overtone of CH stretching vibrations (Aernouts et al., 2011; Tsenkova et al., 2000). Additionally, 1390 nm is related to lactose absorption due to O-H stretch/O-H bend combination vibrations (Tsenkova et al., 2006), and 1450 nm is associated with the first overtone of OH stretching vibrations of water. The band at 1554 nm is attributed to

the first overtone of N-H bond stretching vibrations in amino groups (Ejeahalaka & On, 2020; Kuzmenko et al., 2019), while 1664 nm corresponds to the first overtone of aromatic absorptions (C-H groups) (Skeie et al., 2006). These relevant wavelengths and their associated functional groups provide critical insights into the compositional differences among the milk samples based on type. As such, they are considered reliable for constructing accurate predictive models.

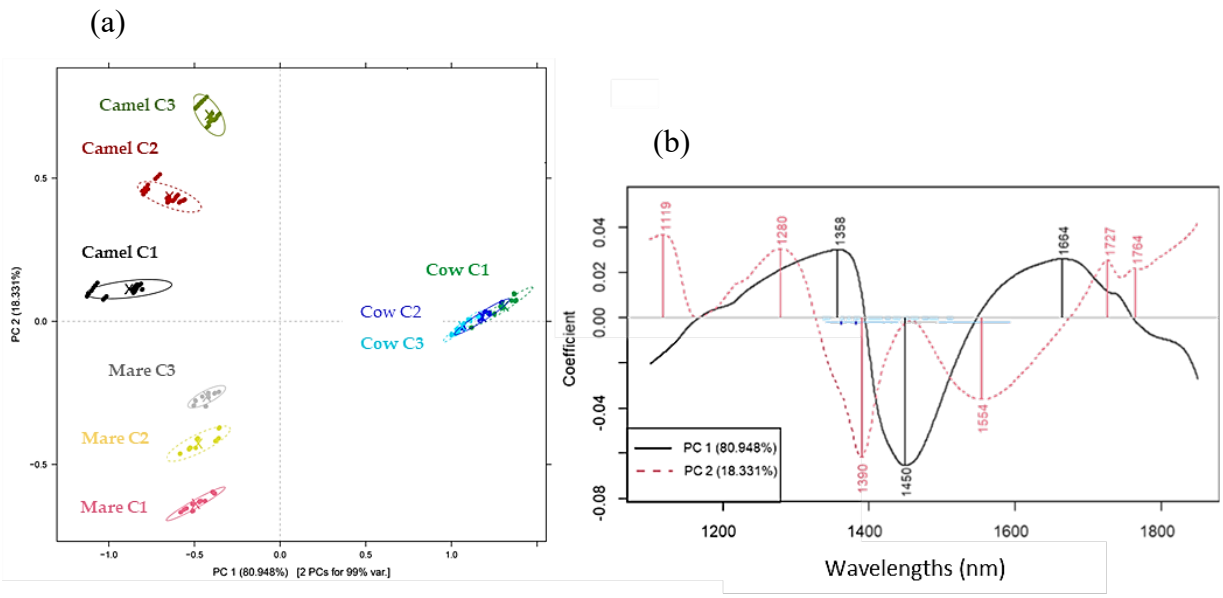

Figure 9. PCA score (a) and loadings (b) plot of reconstituted milk powders of cow, camel and mare colored by their concentration (smoothed and deTr-treated spectra); C1(5%), C2(10%), C3(12.5%)

- Classification models according to the reconstruction conditions

Three PCA-LDA models were created for each temperature level (25°C, 40°C, and 65°C) used to reconstitute the milk, aiming to differentiate between the type of milk and the applied concentration. Independent of the applied temperature, all the PCA-LDA models exhibited notable performance in distinguishing sample groups based on milk type and concentration, achieving an average recognition and prediction accuracy of 100%. For example, Figure 10 presents the PCA-LDA score plot for the classification of milk types and concentrations for samples prepared at 65°C. Similarly, Chen et al. (2018) reported 100% correct classification of milk powders from different brands using near-infrared spectroscopy (NIRS) combined with partial least squares-discriminant analysis (PLS-DA). Furthermore, Wang et al. (2021) achieved effective separation of milk powders by source (bovine, goat, and soy-based) using NIRS and PCA, highlighting the robustness of these methods for milk classification.

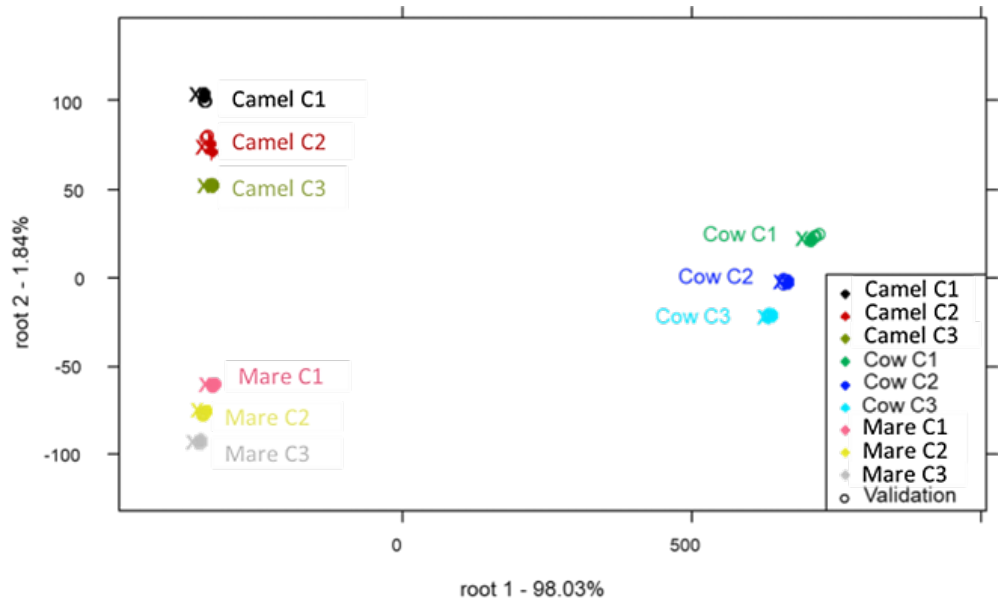

Figure 10. PCA-LDA of reconstituted milk samples at 65°C (T3) according to the concentration level on an MSC-treated spectra; C1(5%), C2(10%), C3(12.5%)

Figure 11 presents the PCA-LDA models developed to classify reconstituted milk samples at a 5% concentration based on their preparation temperature. A separate classification model was created for each type of milk. Overall, the models demonstrated effective discrimination between sample groups representing different preparation temperatures.

For cow milk samples (Figure 11 (a)), the classification model achieved an average recognition accuracy of 100% and a prediction accuracy of 81.5%. However, after cross-validation, 33.3% and 22.2% of the samples prepared at temperature level T2 were misclassified to the temperature levels T1 and T3, respectively.

In the case of camel milk samples (Figure 11 (b)), the model achieved both recognition and prediction accuracies of 100%, with all samples correctly classified according to their preparation temperature.

For mare milk samples (Figure 11 (c)), the model showed an average recognition accuracy of 100% and a prediction accuracy of 66.7%. After cross-validation, 33.3% of the samples prepared at T2 were incorrectly predicted as belonging to T3.

These results highlight the varying performance of the models across different milk types, with camel milk showing the highest classification accuracy and mare milk exhibiting some challenges in temperature-based discrimination.

The classification models exhibited strong performance in distinguishing samples based on type and concentration. Moreover, the accuracy in differentiating between type and concentration was higher compared to the discrimination of reconstruction temperature.

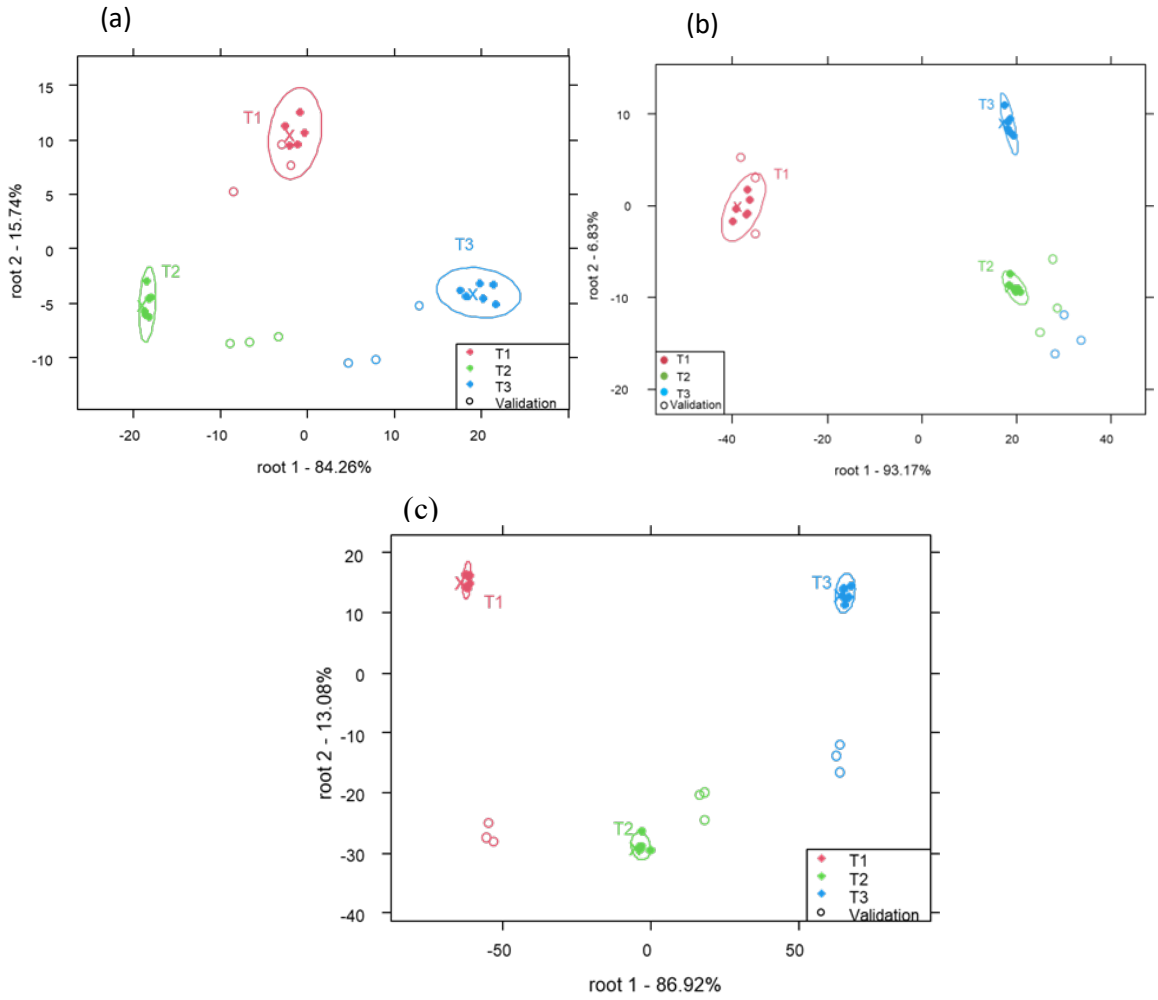

Figure 11. PCA-LDA score plot for the classification of reconstituted cow (a), camel (b) and mare (c) milk samples at a concentration of 5% according to the temperature of preparation (smoothed spectra (a), smoothed and SNV- treated spectra (b) and smoothed and MSC-treated spectra (c)); T1(25°C), T2(40°C), T3(65°C)

- PLSR and SVR models

Table 7, Table 8, Table 9 and Table 10 present the optimal pretreatment methods and key parameters of the PLSR models developed to predict the primary quality attributes of reconstituted milk samples. The best spectral pretreatment and model selection were based on minimizing the root mean square errors of cross-validation (RMSECV) and prediction (RMSEP), while maximizing the coefficients of determination for cross-validation (R^2CV) and prediction (R^2pr). The optimal number of latent variables was identified by locating the "knee" point in the RMSECV scree plot. Additionally, the optimized SVR models are summarized in Table 8 and Table 10. All

models utilized the first two principal components (PC1 and PC2) as input features, with a cost parameter set to 10 and a radial basis kernel function.

All measured physicochemical parameters (Table 7, Table 8) were predicted with high accuracy and low error. For PLSR, R^2CV and R^2pr ranged from 0.8058 to 0.9936 and 0.7081 to 0.9884, respectively. SVR models generally achieved better results, with R^2CV and R^2pr values ranging from 0.9144 to 0.9980 and 0.8052 to 0.9783, respectively. The PLSR model for fat content prediction, developed using the the Savitzky–Golay second derivative with a 21-point window gap pretreatment (sgol@2−21−0) and 4 latent variables, performed well with R^2CV and R^2pr values of 0.8058 and 0.7081, and RMSECV and RMSEP values of 0.4535% and 0.5153%, respectively. However, this model was not the best compared to others, likely due to the impact of freezing and thawing on the milk samples' water structure and homogenization (Muncan, Kovacs, et al., 2021). In contrast, the radial kernel-based SVR model achieved R^2CV and R^2pr values of 0.9347 and 0.8052, and RMSECV and RMSEP values of 0.2535% and 0.4175%, respectively, for fat content prediction. While these metrics are superior, certain considerations must be noted. For SVR models, the type of cross-validation used can influence results; removing too many samples may alter support vectors, while removing too few (non-SV samples) may not affect the model (Balabin & Lomakina, 2011). Applying a leave-three-consecutives-out CV (as used for PLSR) often resulted in nearly identical calibration and cross-validation outcomes, potentially leading to overly optimistic predictions. This was further evidenced by the significant gap between CV and independent prediction results, with notable standard deviations (± 0.1024 and ± 0.1383% for R^2pr and RMSEP, respectively). To maintain consistency between the two modeling approaches, the cross-validation method was kept unchanged.

In a study by D. Wu et al. (2008), a PLSR model for fat content prediction in infant milk powder using short-wave NIRS (800–1050 nm) achieved a higher R^2C of 0.945. Similarly, Aernouts et al., (2011) reported better results in predicting fat content in raw cow milk using NIRS in reflectance mode (1000–1700 nm), with an R^2CV of 0.996.

Table 7. Summary table of the PLSR models for the prediction of the viscosity (mPa s^{-1}), conductivity (mS cm^{-1}), pH, titratable acidity (°SH), dry matter (%), fat content (%) and color measurement (l*, a* and b*) of cow, camel and mare reconstituted milk samples, N= 243

Measured parameters	LV	Pretreatment	R^2C	RMSEC*	R^2CV	RMSECV*	R^2pr	RMSEP*
Viscosity	5	sgol@2−21−0	0.9198	0.0914	0.9121	0.0956	0.9004	0.0996
Conductivity	5	sgol@2−21−0	0.9861	0.248	0.9848	0.2592	0.9819	0.2836
pH	5	sgol@2−21−0	0.9801	0.0398	0.9785	0.0413	0.9652	0.0528
Titratable acidity	4	sgol@2−21−0	0.9543	0.4314	0.9506	0.4484	0.9299	0.5816
Dry matter	4	sgol@2−21−0	0.9174	0.4814	0.9122	0.4964	0.8662	0.6021
Fat content	4	sgol@2−21−0	0.9267	0.2797	0.8058	0.4535	0.7081	0.5153
L*	4	sgol@2−21−0	0.9747	0.7068	0.9726	0.7353	0.9558	0.9421
a*	4	sgol@2−21−0	0.9938	0.0862	0.9936	0.0862	0.9884	0.1203
b*	4	sgol@2−21−0	0.9795	0.2042	0.9778	0.2124	0.9701	0.2438

*RMSEC, RMSECV and RMSEP [viscosity] unit = mPa s^{-1}
RMSEC, RMSECV and RMSEP [conductivity] unit = mS cm^{-1}
RMSEC, RMSECV and RMSEP [titratable acidity] unit = °SH
RMSEC, RMSECV and RMSEP [dry matter, fat content] unit = %

Table 8. Summary table of the SVR models for the prediction of the apparent viscosity (mPa s-1), conductivity (mS cm-1), pH, titratable acidity (°SH), dry matter (%), fat content (%) and color measurement (L*, a* and b*) of cow, camel and mare reconstituted milk samples. N= 243; Number of PCs = 2; C parameter = 10; radial kernel in all cases

Measured parameters	ε	Pretreatment	R2C	RMSEC*	R2CV	RMSECV*	R2pr	RMSEP*
Viscosity	0.01	sgol@2−21−0	0.9604	0.0640	0.9604	0.0640	0.9404	0.0784
Conductivity	0.01	sgol@2−21−0	0.9980	0.0945	0.9980	0.0945	0.9974	0.1063
pH	0.1	sgol@2−21−0	0.9821	0.0380	0.9821	0.0380	0.9783	0.0417
Titratable acidity	0.01	sgol@2−21−0	0.9774	0.3108	0.9774	0.3107	0.9638	0.3877
Dry matter	0.1	sgol@2−21−0	0.9144	0.4874	0.9144	0.4874	0.8976	0.5293
Fat content	0.1	sgol@2−21−0	0.9348	0.2536	0.9347	0.2535	0.8052	0.4175
L*	0.1	sgol@2−21−0	0.9878	0.4939	0.9877	0.4938	0.9837	0.5631
a*	0.01	sgol@2−21−0	0.9979	0.0497	0.9979	0.0497	0.9957	0.0708
b*	0.01	sgol@2−21−0	0.9966	0.0825	0.9966	0.0825	0.9952	0.0961

*RMSEC, RMSECV and RMSEP [viscosity] unit = mPa s^{-1}
RMSEC, RMSECV and RMSEP [conductivity] unit = mS cm^{-1}
RMSEC, RMSECV and RMSEP [titratable acidity] unit = °SH
RMSEC, RMSECV and RMSEP [dry matter, fat content] unit = %

Table 9. Summary table of the PLSR models for the prediction of the amino acids content (%) of cow, camel and mare reconstituted milk samples, N= 243

Measured amino acids	LV	Pretreatment	R^2C	RMSEC (%)	R^2CV	RMSECV (%)	R^2pr	RMSEP (%)
Alanine	4	sgol@2−21−0, msc	0.9757	0.0042	0.9739	0.0044	0.8783	0.011
Arginine	4	sgol@2−21−0, msc	0.9849	0.0049	0.9837	0.005	0.9399	0.0095
Asparagine	4	sgol@2−21−0, msc	0.9837	0.0082	0.9825	0.0086	0.9518	0.0158
Cysteine	4	sgol@2−21−0	0.9478	0.005	0.9434	0.0052	0.789	0.0089
Glutamic acid	4	sgol@2−21−0, msc	0.9742	0.0304	0.9722	0.0315	0.9456	0.0519
Glycine	4	sgol@2−21−0, msc	0.9272	0.0064	0.9204	0.0067	0.9165	0.006
Histidine	4	sgol@2−21−0	0.9463	0.0041	0.939	0.0044	0.931	0.0053
Isoleucine	4	sgol@2−21−0	0.9442	0.0038	0.937	0.004	0.9061	0.0056
Leucine	4	sgol@2−21−0, msc	0.9804	0.0104	0.9789	0.0107	0.9526	0.0178
Lysine	4	sgol@2−21−0, msc	0.979	0.009	0.9774	0.0093	0.9609	0.0132
Methionine	4	sgol@2−21−0	0.9303	0.0047	0.9202	0.005	0.8863	0.0075
Phenylalanine	4	sgol@2−21−0	0.9684	0.0063	0.9651	0.0066	0.9251	0.0105
Proline	4	sgol@2−21−0, msc	0.9656	0.0119	0.9631	0.0124	0.9348	0.0175
Serine	4	sgol@2−21−0, msc	0.9822	0.006	0.9809	0.0062	0.9368	0.0129
Threonine	4	sgol@2−21−0	0.9419	0.007	0.934	0.0075	0.9015	0.0095
Tyrosine	4	sgol@2−21−0	0.9603	0.0083	0.9566	0.0087	0.9119	0.0118
Valine	4	sgol@2−21−0, msc	0.9759	0.005	0.9738	0.0053	0.8355	0.0139

Table 10. Summary table of the SVR models for the prediction of the amino acids content (%) of cow, camel and mare reconstituted milk samples. N= 243; Number of PCs = 2; C parameter = 10; radial kernel in all cases

Measured amino acids	ε	Pretreatment	R2C	RMSEC (%)	R2CV	RMSECV (%)	R2pr	RMSEP (%)
Alanine	0.1	sgol@2−21−0, msc	0.9712	0.0047	0.9711	0.0047	0.9305	0.0070
Arginine	0.1	sgol@2−21−0, msc	0.9835	0.0050	0.9835	0.0050	0.9634	0.0074
Asparagine	0.1	sgol@2−21−0, msc	0.9853	0.0081	0.9853	0.0081	0.9728	0.0109
Cysteine	0.5	sgol@2−21−0	0.9419	0.0049	0.9419	0.0049	0.8453	0.0078
Glutamic acid	0.1	sgol@2−21−0, msc	0.9751	0.0316	0.9751	0.0316	0.9539	0.0423
Glycine	0.1	sgol@2−21−0, msc	0.9509	0.0049	0.9509	0.0049	0.8988	0.0071
Histidine	0.1	sgol@2−21−0	0.9674	0.0033	0.9673	0.0033	0.9289	0.0049
Isoleucine	0.1	sgol@2−21−0	0.9586	0.0034	0.9586	0.0034	0.9073	0.0051
Leucine	0.1	sgol@2−21−0, msc	0.9835	0.0099	0.9835	0.0099	0.9721	0.0127
Lysine	0.1	sgol@2−21−0, msc	0.9870	0.0073	0.9870	0.0073	0.9808	0.0088
Methionine	0.1	sgol@2−21−0	0.9428	0.0046	0.9428	0.0046	0.8765	0.0066
Phenylalanine	0.1	sgol@2−21−0	0.9810	0.0050	0.9810	0.0050	0.9636	0.0066
Proline	0.1	sgol@2−21−0, msc	0.9659	0.0119	0.9659	0.0119	0.9313	0.0164
Serine	0.1	sgol@2−21−0, msc	0.9804	0.0066	0.9804	0.0066	0.9586	0.0095
Threonine	0.1	sgol@2−21−0	0.9529	0.0064	0.9528	0.0064	0.8943	0.0094
Tyrosine	0.1	sgol@2−21−0	0.9846	0.0051	0.9845	0.0051	0.9717	0.0068
Valine	0.1	sgol@2−21−0, msc	0.9537	0.0069	0.9537	0.0069	0.8949	0.0103

Predicting the amino acid composition of milk powders plays a vital role in evaluating their appropriateness for manufacturing high-value nutritional products, including infant formulas and foods targeted at malnourished or vulnerable groups. The PLSR models developed for individual amino acids exhibited excellent predictive capability, with cross-validation coefficients of determination (R^2CV) ranging from 0.9202 to 0.9837 and prediction coefficients (R^2pr) between 0.789 and 0.9202. Notably, the essential amino acids lysine, leucine, and phenylalanine, recognized for their significant nutritional value, were predicted with high accuracy. Glutamic acid, the most prevalent amino acid in milk, was also predicted with high accuracy, yielding R^2CV and R^2pr values of 0.9722 and 0.9456, respectively. These results considerably outperform those reported by McDermott et al. (2016) , who achieved only moderate predictive accuracy for free amino acids in bovine milk using NIRS, with cross-validation correlation coefficients spanning 0.51 to 0.75. When SVR was used as a calibration tool for predicting amino acid content, it

generally outperformed PLSR in most cases. Notably, the prediction accuracies for key amino acids like leucine, phenylalanine, and glutamic acid reached values between 0.9539 and 0.9721, with average prediction errors below 0.05%. The superior performance of SVR models can be attributed to their ability to capture complex nonlinearities often present in multicomponent natural systems like milk powders (Lu et al., 2009). In contrast, PLSR assumes a linear relationship between spectral data and properties, an assumption that is rarely fully met in biological samples with strong intermolecular and intramolecular interactions (Balabin & Lomakina, 2011). Several studies have reported better performance for nonlinear SVR models compared to linear PLSR when analysing milk samples using NIRS (Balabin & Smirnov, 2011; Lu et al., 2009; Liu et al., 2023). The lysine prediction model achieved the highest accuracy among all measured amino acids. The corresponding PLSR and SVR models are illustrated in Figure 12. The wavelengths most influential for lysine prediction using PLSR are shown in Figure 12 (c, b). Peaks observed between 1330–1600 nm were associated with the first overtone of O-H and N-H bonds in amino groups (Skeie et al., 2006).

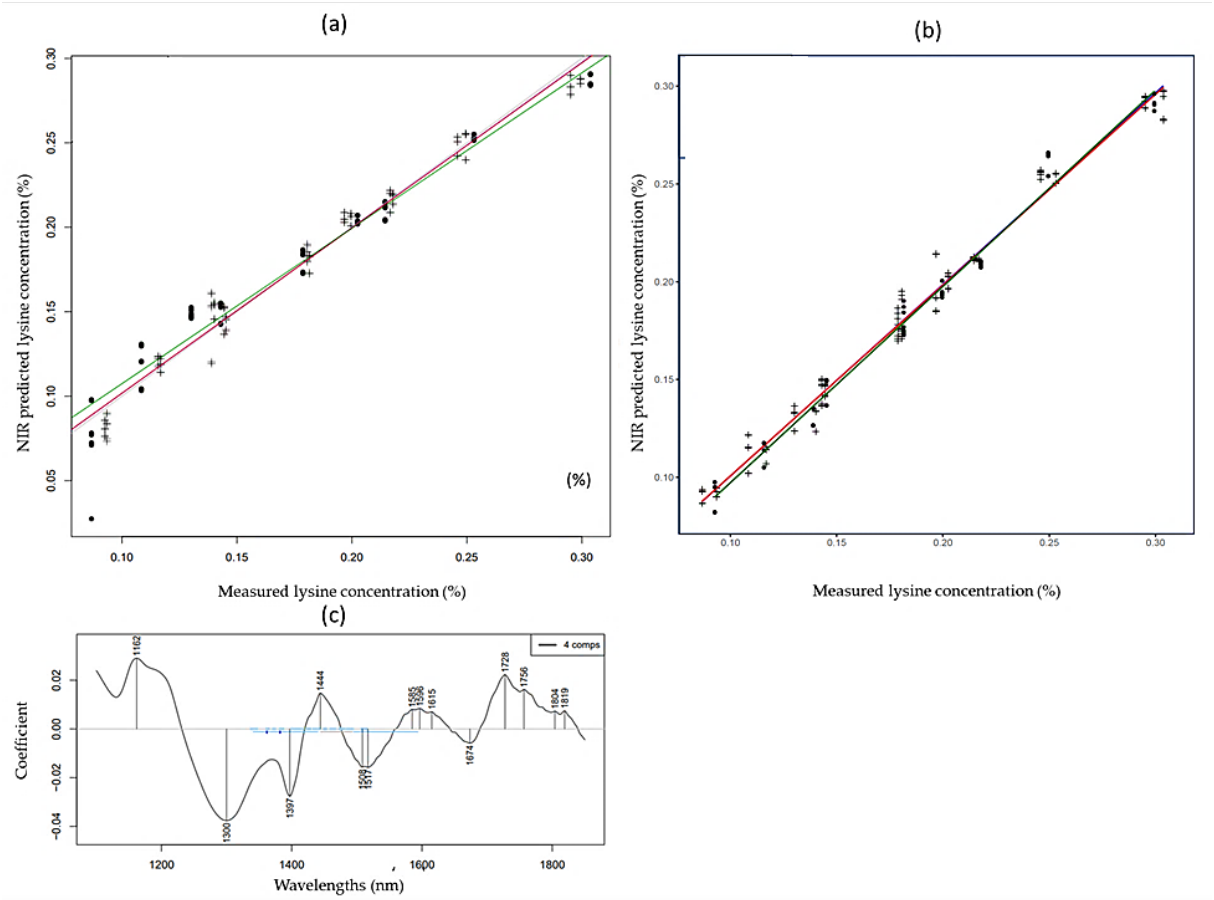

Figure 12. PLSR Y fit (a), SVR Y fit (b) and PLSR regression vector (c) for the prediction of lysine concentration of cow, mare and camel reconstituted milk samples (at different concentrations and temperature (smoothed and MSC-treated spectra)

The significance of these findings lies in their practical and nutritional implications. Accurate classification and prediction of milk powder quality and composition can inform industrial quality control, optimize reconstitution procedures, and ensure nutritional adequacy in high-value products such as infant formulas. Economically, powders with controlled bulk density and solubility reduce storage and transport costs, while health-wise, precise amino acid prediction supports formulation for vulnerable populations. Compared to prior studies, this work confirms and extends the utility of NIRS and chemometric approaches for multi-species milk analysis, offering a reliable method for industry adoption and enhancing consumer safety and product consistency. Furthermore, the observed trends in water activity, insolubility index, and bulk density align closely with previous reports (Pugliese et al., 2017;Wang et al., 2021), which identified these parameters as critical indicators of milk powder stability and processing quality. While Wang et al. (2021) focused primarily on predicting physical traits such as density and moisture content using PLSR models, our study expands this scope by incorporating amino acid profiling and advanced machine learning techniques like SVR, yielding higher predictive accuracy. This integration of physicochemical and compositional data strengthens the overall analytical framework, demonstrating that combining traditional quality metrics with modern chemometric modelling provides a comprehensive tool for ensuring milk powder quality across diverse species and processing conditions.

5.2. Identifying key factors that distinguish fermented milk based on feeding type and probiotic potential with e-nose and NIRS techniques

5.2.1. Comparison of the fatty acid profiles of experimental vs. control milk

To begin the analysis, we compared the compositions of saturated fatty acids (SFA), monounsaturated fatty acids (MUFA), and polyunsaturated fatty acids (PUFA) in raw milk from both control and experimental groups. Table 11 summarizes the fatty acid profiles of milk samples collected during trials 1, 2, and 3. To ensure accurate and unbiased comparisons, separate ANOVA tests were performed for each feeding trial, allowing assessment of statistical differences between the two milk types across each fatty acid category. This approach provides a clear insight into how dietary supplementation influences the fatty acid composition of raw milk. Figure 13 illustrates the mean total percentages of SFA, MUFA, and PUFA in control and experimental milk across all three trials.

The ANOVA results for trials 1 and 2 revealed significant differences in the PUFA content between the control and experimental groups, though no significant differences were observed in the SFA or MUFA levels. This outcome is likely related to the experimental feeds, which were

supplemented with whole linseed and algae extract, both known to be rich in PUFAs, particularly omega-3 fatty acids (Lerch et al., 2012), and are naturally protected from ruminal biohydrogenation, by the seed hull, and by the algal cell wall (Costa et al., 2022), to efficiently overcome bacterial modifications. The increase in PUFA levels can be linked to the direct incorporation/transfer of these dietary fatty acids into the milk fat, facilitated by the metabolic pathways in dairy cows that favor transfer of dietary PUFAs into milk fat (Lock & Bauman, 2004). However, SFAs are naturally more abundant in milk and less influenced by dietary variations, especially when the supplementation is aimed at increasing PUFA intake. This is due to the biohydrogenation process in the rumen, where unsaturated fatty acids are often converted to saturated ones, making it challenging to reduce SFA levels through dietary interventions alone. Likewise, MUFA levels appear to be regulated more by metabolic processes in dairy cows than by dietary fat composition (Glasser et al., 2008; Yakubu et al., 2023). Moreover, *de novo* fatty acid synthesis in the mammary gland is primarily producing saturated fatty acids (Lanier & Corl, 2015), thus their presence is always determinant.

In trial 3, the ANOVA analysis demonstrated significant alterations in the levels of saturated (SFA), monounsaturated (MUFA), and polyunsaturated fatty acids (PUFA) between the control and experimental groups. The experimental diet, enriched with a blend of linseed, linseed oil, algae extract, and fish oil, exerted a substantial influence on the fatty acid composition of the milk. This shift can be attributed primarily to the elevated content of PUFAs and MUFAs introduced by linseed oil and fish oil, both well-known sources of beneficial unsaturated fats. These dietary unsaturated fatty acids were effectively incorporated into the milk fat, resulting in a marked decrease in SFA levels alongside increased MUFA and PUFA concentrations in the experimental samples.

The inclusion of linseed oil and fish oil likely improved the availability of these unsaturated fats and facilitated their transfer into the mammary gland for secretion into milk. Additionally, the higher unsaturated fat content in the diet may have inhibited ruminal biohydrogenation. Thereby preserving more unsaturated fatty acids for absorption and subsequent incorporation into milk fat. This inhibition of biohydrogenation not only reduced SFA formation but also favored the accumulation of MUFAs and PUFAs.

These findings highlight the intricate and dynamic relationship between dietary inputs, rumen microbial metabolism, and the cow's endogenous metabolic pathways responsible for fatty acid synthesis. Understanding this interplay is crucial for developing nutritional strategies that optimize milk fatty acid profiles, enhancing their nutritional quality for human consumption.

Table 11. The fatty acid profile of control and experimental milk samples from trial 1,2 and 3

Fatty acid composition (%)		Trial 1		Trial 2		Trial 3	
		CTR 1	EXP 1	CTR 2	EXP 2	CTR 3	EXP 3
SFA	Butyric acid (C4:0)	ND	ND	0.14	0.08	2.04	2.22
	Caproic acid (C6:0)	0.47	0.62	0.91	0.77	1.68	1.64
	Octanoic acid (C8:0)	1.05	1.02	1.00	1.02	1.37	1.28
	Capric acid (C10:0)	3.94	3.91	0.74	0.70	3.45	3.42
	Undecylic acid (C11:0)	0.11	0.10	0.06	0.06	0.40	0.34
	Lauric acid (C12:0)	5.25	5.26	3.54	3.76	3.71	3.66
	Tridecylic acid (C13:0)	ND	ND	0.11	0.12	0.23	0.18
	Myristic acid (C14:0)	15.14	15.52	11.48	12.01	12.06	11.33
	Pentadecanoic acid (C15:0)	1.39	1.40	1.07	1.14	1.06	0.97
	Palmitic acid (C16:0)	32.92	31.23	32.20	30.70	33.67	31.01
	Margaric acid (C17:0)	0.45	0.46	0.57	0.56	0.55	0.59
	Stearic acid (C18:0)	12.76	13.66	12.18	11.57	9.94	9.47
	Arachidic acid (C20:0)	0.17	0.16	0.19	0.19	0.26	0.22
	Heneicosanoic Acid (C21:0)	0.01	0.01	0.04	0.05	ND	0.01
	Behenic acid (C22:0)	0.04	0.04	0.06	0.08	0.05	0.06
	Tricosanoic acid (C23:0)	0.01	0.01	0.02	0.02	ND	ND
	Lignoceric acid (C24:0)	0.02	0.02	0.03	0.04	ND	ND
	Total	**73.75± 0.78**	**73.43± 0.92**	**64.33± 2**	**62.88± 2.1**	**70.45± 1.58**	**66.42± 1.7**
MUFA	Myristoleic acid (C14:1)	1.19	1.16	0.98	1.08	0.92	0.94
	Pentadecanoic acid (C15:1)	ND	ND	ND	ND	0.01	0.01
	Heptadecenoic Acid (C17:1)	ND	ND	0.17	0.17	0.14	0.14
	Palmitoleic Acid (C16:1 n-7)	0.13	0.13	1.44	1.42	1.58	1.71
	Elaidic acid (C18:1 n-9t)	NA	NA	0.52	0.82	0.85	3.34
	oleic acid (C18:1 n-9c)	20.06	19.83	24.73	24.56	18.63	18.39
	Vaccenic acid (C18:1 n-7)	1.11	1.16	0.33	0.59	0.36	0.53
	Eicosenoic acid (C20:1 n-9)	0.03	0.03	0.07	0.08	0.11	0.17
	Erucic acid (C22:1 n-9)	0.004	0.004	ND	ND	0.02	0.03
	Nervonic Acid (C24:1 n-9)	0.003	0.002	ND	ND	ND	ND
	Total	**22.46± 0.77**	**22.44± 0.62**	**28.23± 1.56**	**28.72± 1.64**	**22.62± 1.4**	**25.26± 1.3**
PUFA	Docosapentaenoic Acid (C22:5 n-3)	0.03	0.04	0.05	0.05	0.06	0.07
	Adrenic Acid (C22:4 n-6)	ND	ND	ND	ND	0.043	0.027
	Docosahexaenoic Acid (C22:6 n-3)	ND	ND	0.02	0.11	ND	ND
	Eicosapentaenoic Acid (C20:5 n-3)	0.02	0.03	0.03	0.03	0.03	0.04
	Eicosatetraenoic Acid (C20:4 n-3)	0.02	0.02	ND	ND	ND	ND
	Eicosatrienoic acid (C20:3 n-3)	0.004	0.01	NA	NA	0.01	0.05
	Arachidonic Acid (C20:4 n-6)	0.16	0.15	0.16	0.15	0.18	0.13
	Cis-11,14-Eicosadienoic Acid (C20:2 n-6)	0.01	0.01	ND	ND	0.04	0.05
	Dihomogammalinolenate (C20:3 n-6)	0.12	0.10	0.14	0.12	0.13	0.10
	Linolelaidic acid (C18:2 n-6t)	ND	ND	0.37	0.60	0.03	0.06
	Linoleic acid (C18:2 n-6)	2.72	2.85	3.45	3.58	3.29	3.43
	Gamma-Linolenic Acid (C18:3 n-6)	ND	ND	0.03	0.03	0.03	0.02
	Alpha-Linolenic Acid (C18:3 n-3)	0.36	0.54	0.48	0.57	0.50	0.70
	c9, t11-Conjugated linoleic acid	0.33	0.37	0.61	0.83	0.31	0.77
	Total	**3.78± 0.07**	**4.11± 0.08**	**5.34± 0.37**	**6.08± 0.27**	**4.65± 0.14**	**5.45± 0.15**

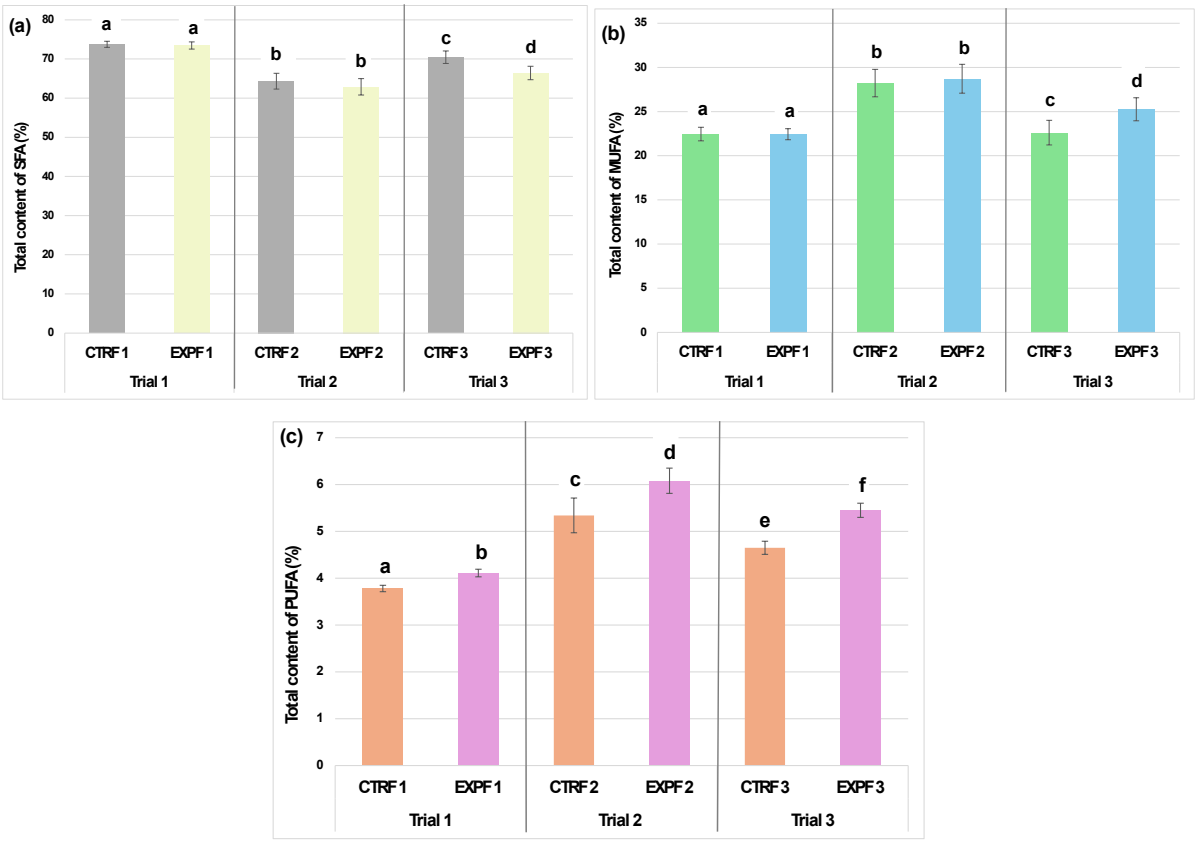

Figure 13. Mean total content (%) ±STD of (a) saturated fatty acids (SFA), (b) monounsaturated fatty acids (MUFA) and (c) polyunsaturated fatty acids (PUFA) of control milk and experimental milk from trial 1, 2 and 3. Letter (a–f) represent significantly different groups ($p \leq 0.05$), based on ANOVA ; CTRF (non-fermented control milk), EXPF (non-fermented experimental milk)

5.2.2. NIRS and e-nose analysis

- Visual analysis of the spectra and PCA models

The raw NIR spectra of the experimental and control fermented milk samples from trials 1, 2, and 3 in the spectral range of 400–2500 nm, are shown in Figure 14. Two prominent peaks are evident around 1440 nm and 1950 nm, associated with the OH symmetric/asymmetric stretching and bending vibrations of water (Kasemsumran et al., 2007). The dominance of water peaks in the spectra made it challenging to detect the characteristic absorption peaks of fat and other milk components (Tsenkova et al., 2000). Additionally, a noticeable baseline shift was observed, likely caused by light scattering associated with the increased size of casein micelles during the fermentation process,(Muncan, Tei, et al., 2021). To address this, the second derivative was applied to the raw spectra within the 1100–2400 nm range. This approach allowed the separation of overlapping peaks and corrected baseline variations. The second derivative spectra are displayed in Figure 15, revealing distinct spectral features beyond water absorption. Notable absorption bands at 1160, 1210, 1726, 2308, and 2354 nm were identified, which can be attributed to the C-H bond absorption.

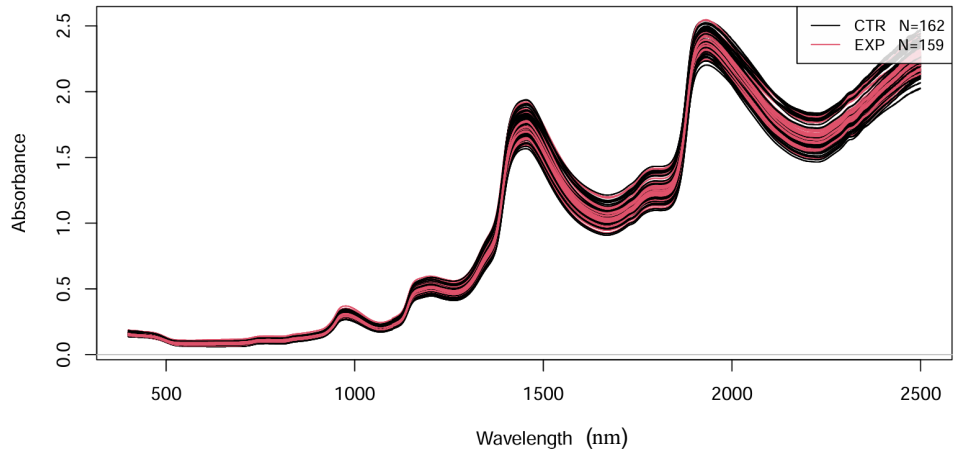

Figure 14. NIR raw spectra of experimental and control fermented milk samples from trial 1, 2 and 3 in the full range of 400-2500 nm: Control group (N= 162) and experimental group (N= 159) after outlier elimination (3 scans); CTR (control fermented milk), EXP (experimental fermented milk)

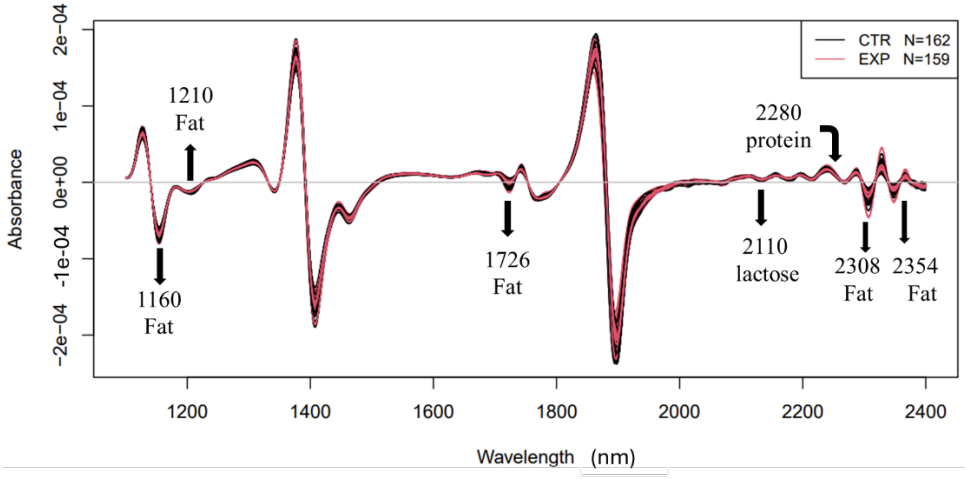

Figure 15. Second derivative spectra of experimental and control fermented milk samples from trial 1, 2 and 3 in the range of 400-2500 nm: Control group (N= 162) and experimental group (N= 159) after outlier elimination (3 scans); CTR (control fermented milk), EXP (experimental fermented milk)

Next, we conducted a detailed examination of the visual representations of the e-nose and NIRS data by analysing their respective PCA models. This analysis attempted to identify patterns or trends within the data that could reveal underlying similarities or differences between the fermented milk samples. By means of these models, we aim to get insights into the relationships among the data points, highlighting potential groupings or variations within the datasets. To ensure a fair comparison between the control and experimental samples, a PCA score plot was generated for each trial.

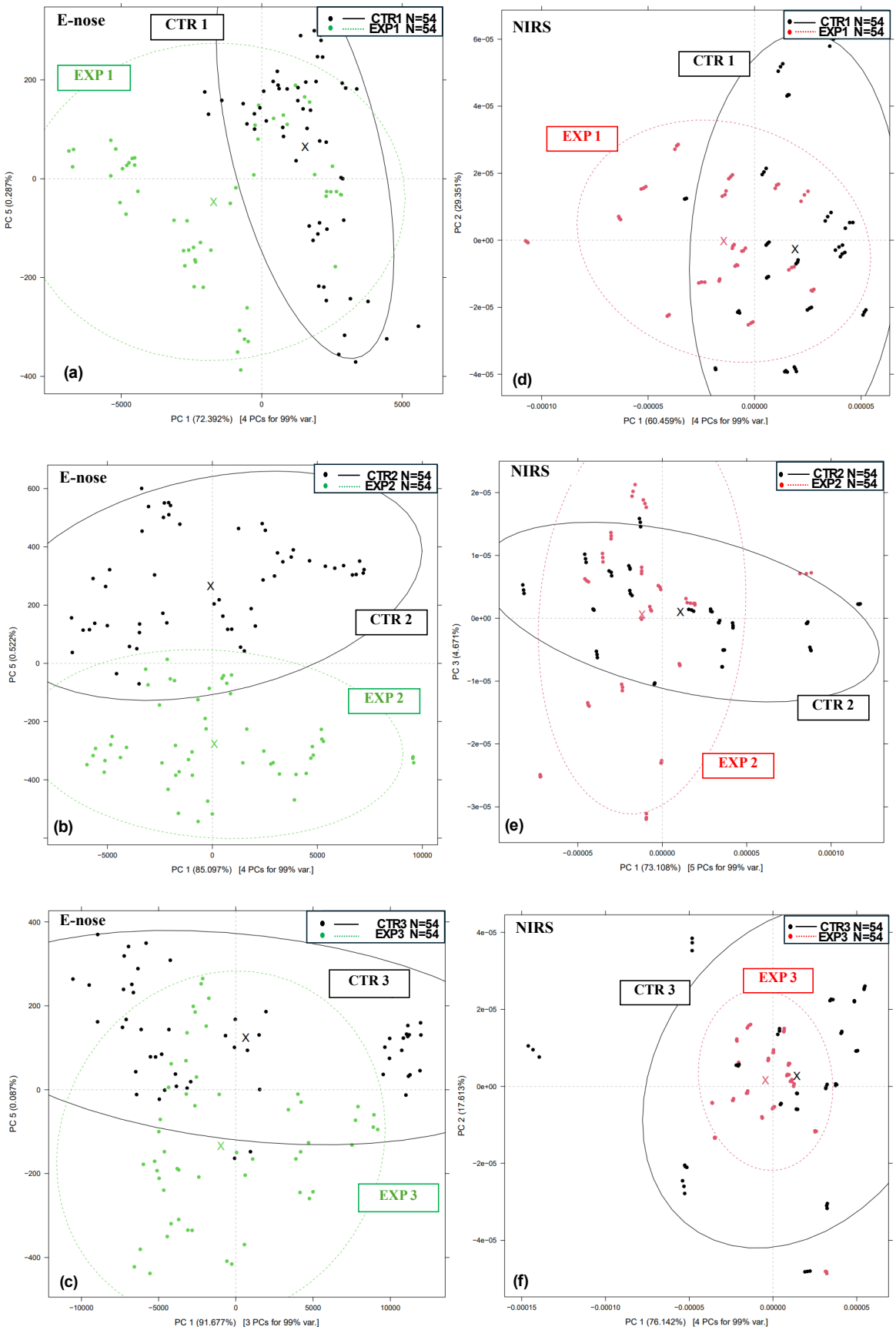

Figure 16. PCA score plots for experimental and control fermented milk samples across three different feeding trials, with trial 1 (a), trial 2 (b) and trial 3 (c) in the case of data points derived from the e-nose dataset and trial 1 (d), trial 2 (e) and trial 3 (f) in the case of data points derived from the NIRS dataset; CTR (control fermented milk), EXP (experimental fermented milk)

Figure 16 (a, b, c) illustrates the PCA score plots derived from e-nose data, comparing experimental and control fermented milk samples across the three feeding trials (trials 1, 2, and 3, respectively). Each plot represents the data along the first principal component (PC1) and the fifth principal component (PC5), which together account for the majority of variance captured in the datasets. Specifically, PC1 and PC5 explain 72.68% of the total variance in trial 1, increasing to 85.62% in trial 2, and reaching 91.76% in trial 3. This progressive increase suggests a stronger pattern of variation detected by the e-nose in later trials.

Similarly, Figure 16 (d, e, f) displays PCA score plots generated from NIRS data for the same experimental and control fermented milk samples across the three trials. The principal components vary between trials but consistently capture a high proportion of variance: PC1 and PC2 explain 89.81% in trial 1; PC1 and PC3 account for 77.78% in trial 2; and PC1 and PC2 together represent 93.75% in trial 3. These high values indicate that the first few principal components effectively summarize the spectral variability within each trial's samples.

The observed differences in variance explained and the patterns across trials likely arise from inherent biological variability among the samples. Variations in key chemical constituents such as fat, protein, and moisture content influence both the volatile compound profiles detected by the e-nose and the spectral characteristics measured by NIRS. Consequently, these compositional differences drive the sample separation and clustering patterns seen in the PCA plots, highlighting the complex interplay between milk composition and analytical response in these feeding trials.

The e-nose analysis score plots indicated a subtle trend toward differentiation between the experimental and control groups, with the clearest separation observed during trial 2. This separation was primarily along the PC1 and PC5 dimensions, where PC5 captured a slight yet discernible separation pattern between the two groups in trial 2. In contrast, trials 1 and 3 showed considerable overlap between the experimental and control samples, lacking any distinct clustering. This overlap suggests that the volatile compound profiles of the two groups were largely similar in these trials, indicating limited discriminatory power of the e-nose under those conditions. Similarly, the NIRS data failed to reveal any definitive separation between experimental and control fermented milk samples across all three trials. The PCA plots based on spectral data showed no evident grouping or pattern that could distinguish between the two sample types.

- Discrimination models of the fermented milk samples based on feeding type and probiotic potential

In the subsequent step, a detailed analysis was conducted by employing the PCA-LDA technique to uncover distinct groupings within the NIRS and e-nose datasets. This method is utilized to classify the fermented milk samples and assess the model's capability to precisely distinguish them based on two critical factors: the type of feeding and the existence of probiotic potential. The NIRS and e-nose datasets encompass essential information that reflects the chemical composition and sensory profiles of the fermented milk samples, which vary according to the feeding type and probiotic properties. The objective is to determine whether these variations in feeding type and probiotic content result in unique, identifiable patterns within the data that can be used to accurately classify the samples.

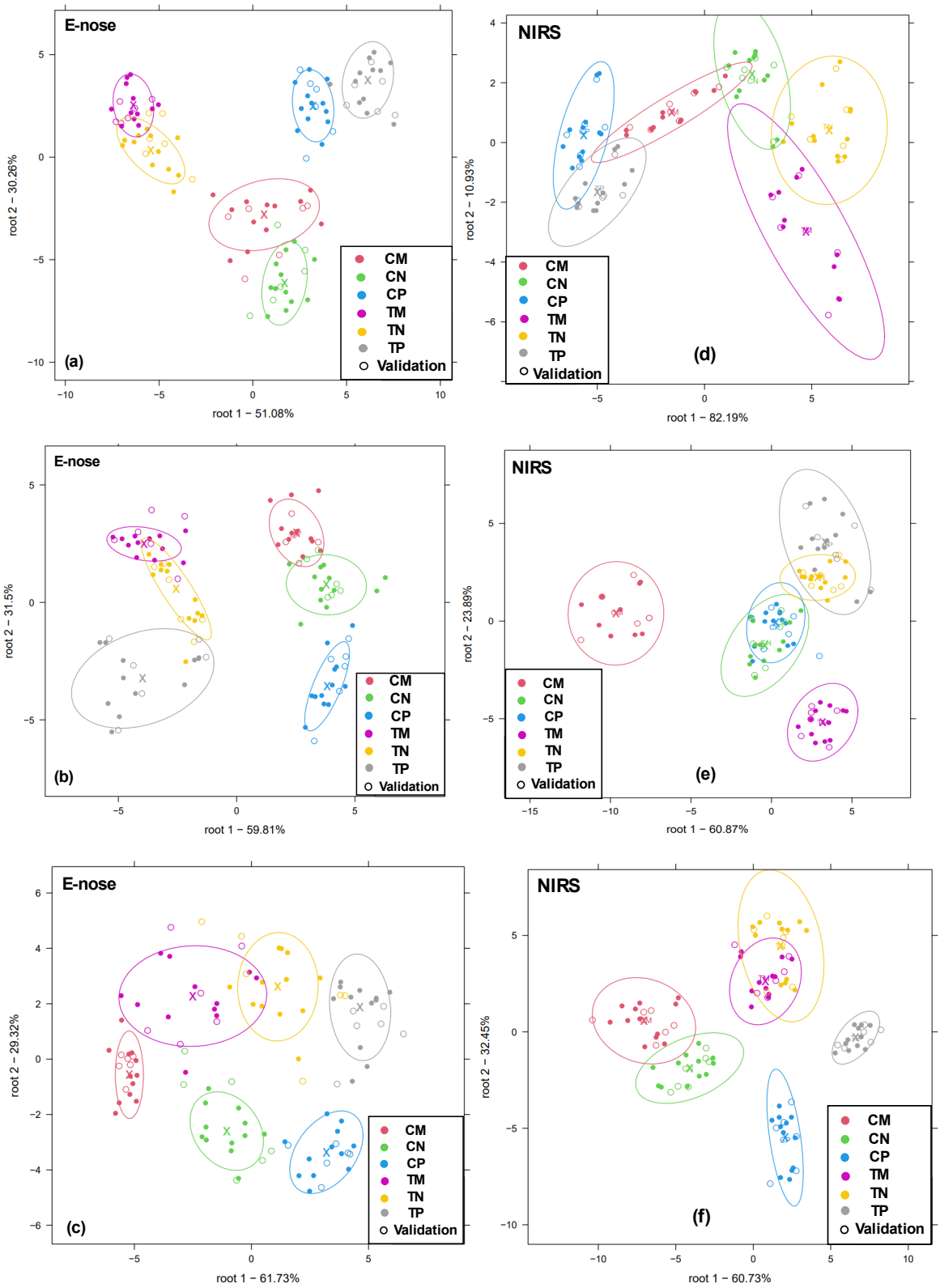

Figure 17. PCA-LDA models for experimental and control fermented milk samples across three different feeding trials, with trial 1 (a), trial 2 (b) and trial 3 (c) in the case of data points derived from the e-nose dataset and trial 1 (d), trial 2 (e) and trial 3 (f) in the case of data points derived from the NIRS dataset; CN (control milk inoculated with the non-probiotic strain), CM (control milk inoculated with the moderate strain), CP (control milk inoculated with the probiotic strain), TN (experimental milk inoculated with the non-probiotic strain), TM (experimental milk inoculated with the moderate strain), TP (experimental milk inoculated with the probiotic strain)

Table 12. Confusion table of the PCA-LDA models for experimental and control fermented milk samples across three different feeding trials, with trial 1, trial 2 and trial 3 in the case of data points derived from the e-nose and NIRS datasets; CN (control milk inoculated with the non-probiotic strain), CM (control milk inoculated with the moderate strain), CP (control milk inoculated with the probiotic strain), TN (experimental milk inoculated with the non-probiotic strain), TM (experimental milk inoculated with the moderate strain), TP (experimental milk inoculated with the probiotic strain)

			NIRS						E-nose					
			CM	CN	CP	TM	TN	TP	CM	CN	CP	TM	TN	TP
Trial 1	training	CM	94.5	0	0	0	0	0	100	2.75	0	0	0	0
		CN	5.50	100	0	0	0	0	0	97.25	0	0	0	0
		CP	0	0	94.5	0	0	0	0	0	100	0	0	0
		TM	0	0	0	100	0	0	0	0	0	97.25	5.58	0
		TN	0	0	0	0	100	0	0	0	0	2.75	94.42	0
		TP	0	0	5.5	0	0	100	0	0	0	0	0	100
		Average recognition: 98.2%							**Average recognition: 98.2%**					
	Cross-validation	CM	94.42	0	0	0	0	0	100	5.50	0	0	0	0
		CN	5.58	100	0	0	0	0	0	94.5	0	0	0	0
		CP	0	0	91.67	0	0	0	0	0	100	0	0	0
		TM	0	0	0	100	0	0	0	0	0	94.5	5.50	0
		TN	0	0	0	0	100	0	0	0	0	5.50	94.5	0
		TP	0	0	8.33	0	0	100	0	0	0	0	0	100
		Average prediction: 97.6%							**Average prediction: 97.3%**					
Trial 2	training	CM	100	0	0	0	0	0	100	0	0	0	0	0
		CN	0	100	0	0	0	0	0	100	0	0	0	0
		CP	0	0	100	0	0	0	0	0	100	0	0	0
		TM	0	0	0	100	0	0	0	0	0	97.25	0	0
		TN	0	0	0	0	94.42	0	0	0	0	2.75	94.42	0
		TP	0	0	0	0	5.58	100	0	0	0	0	5.58	100
		Average recognition: 99%								**Average recognition: 99%**				
	Cross-validation	CM	100	0	0	0	0	0	100	0	0	0	0	0
		CN	0	100	0	0	0	0	0	100	0	0	0	0
		CP	0	0	100	0	0	0	0	0	100	0	0	0
		TM	0	0	0	100	0	0	0	0	0	90.5	0	0
		TN	0	0	0	0	94.5	5.50	0	0	0	9.5	94.5	0
		TP	0	0	0	0	5.50	94.5	0	0	0	0	5.50	100
		Average prediction: 98%							**Average prediction: 97.5%**					
Trial 3	training	CM	100	0	0	0	0	0	100	0	0	0	0	0
		CN	0	100	0	0	0	0	0	100	0	0	0	0
		CP	0	0	100	0	0	0	0	0	100	0	0	0
		TM	0	0	0	100	5.58	0	0	0	0	96.8	0	0
		TN	0	0	0	0	94.42	0	0	0	0	3.20	100	0
		TP	0	0	0	0	0	100	0	0	0	0	0	100
		Average recognition: 99%							**Average recognition: 99.5%**					
	Cross-validation	CM	100	0	0	0	0	0	100	0	0	0	0	0
		CN	0	100	0	0	0	0	0	100	0	0	0	0
		CP	0	0	100	0	0	0	0	0	100	0	0	0
		TM	0	0	0	100	6.50	0	0	0	0	93.8	4.50	0
		TN	0	0	0	0	93.5	0	0	0	0	6.2	95.5	0
		TP	0	0	0	0	0	100	0	0	0	0	0	100
		Average prediction: 98.2%							**Average prediction: 98.2%**					

Figure 17 showcases the PCA-LDA classification models generated using both e-nose and NIRS data to differentiate between experimental and control fermented milk samples across three distinct feeding trials. Panels (a), (b), and (c) present the classification results derived from the e-nose data for trials 1, 2, and 3, respectively. Correspondingly, panels (d), (e), and (f) display the PCA-LDA classification models based on the NIRS data for the same sets of samples and trials.

The outcomes of the PCA-LDA models, including the recognition and prediction percentage of accuracy, are summarized in Table 12. Across all trials, the models exhibited strong performance, with recognition accuracies ranging from 98% to 99.5% and prediction accuracies between 97% and 98%. These findings suggest that both the e-nose and NIRS methods were effective in distinguishing between the experimental and control fermented milk samples. However, some inconsistencies were observed between the e-nose and NIRS models regarding misclassified groups. For instance, the e-nose models for trials 1, 2, and 3 successfully distinguished between the two groups. In contrast, the NIRS PCA-LDA model for feeding trial 1 showed a slight misclassification rate, with 8.33% of control fermented milk samples containing strain P (CP) being incorrectly classified as experimental fermented milk samples with strain P (TP). This discrepancy reveals a subtle difference in performance between the two sensor technologies. While NIRS excels at capturing the overall molecular composition of milk, it may be less sensitive than the E-nose to minor variations between control and experimental samples. This could be attributed to NIRS focusing on broader chemical properties such as water, fat, and protein content, whereas the e-nose is more responsive to volatile compounds that may undergo more pronounced changes during fermentation.

When examining the discrimination of fermented milk samples based on their probiotic potential, most samples fermented with the probiotic strain P were correctly classified. This suggests that strain P probably caused unique changes in volatile compounds or molecular profiles during fermentation, setting these samples apart from those fermented with other strains. These distinct alterations in milk composition appeared consistent across all feeding trials, indicating that the metabolic activity of strain P played a key role in defining the final properties of the fermented milk. However, misclassifications were more common for samples fermented with the moderate probiotic strain M and the non-probiotic strain N. While samples fermented with strain P were generally well-differentiated due to the distinct biochemical changes it produced, samples fermented with strains M and N showed considerable overlap in their fermentation profiles, resulting in a higher rate of misclassification. This underscores the differing levels of distinctiveness among probiotic and non-probiotic strains, with strain P standing out as the most readily identifiable.

In the next phase of our analysis, we will focus on identifying the most contributing virtual sensors and wavelengths that significantly improved the performance of the classification models. By using this approach, we aim to achieve a more detailed understanding of two key aspects: (1) the variations in volatile profiles and chemical composition between control and experimental fermented milk samples, irrespective of the strain used during fermentation. This will enable us to explore how fermentation impacts milk composition independently of the probiotic strain. (2) The strain-specific differences in chemical and volatile profiles between control and experimental samples. This will allow us to investigate how each probiotic strain uniquely shapes the molecular changes and volatile compounds in fermented milk. Through this focused analysis, we can gain a clearer understanding of the underlying factors/casual chemical bonds that enhance the classification model's ability to differentiate between various fermented milk samples.

- Contributing wavelengths

Table 13 offers a comprehensive overview of the key wavelengths that played a significant role in distinguishing between the experimental and control fermented milk samples. Figure 18 displays the results highlighting the wavelengths that contributed to the discrimination of fermented milk samples based on the type of feeding. Additionally, Figure 19 and Figure 20 illustrate the wavelengths contributing to the differentiation of the experimental and control fermented milk samples, respectively, according to the strain type.

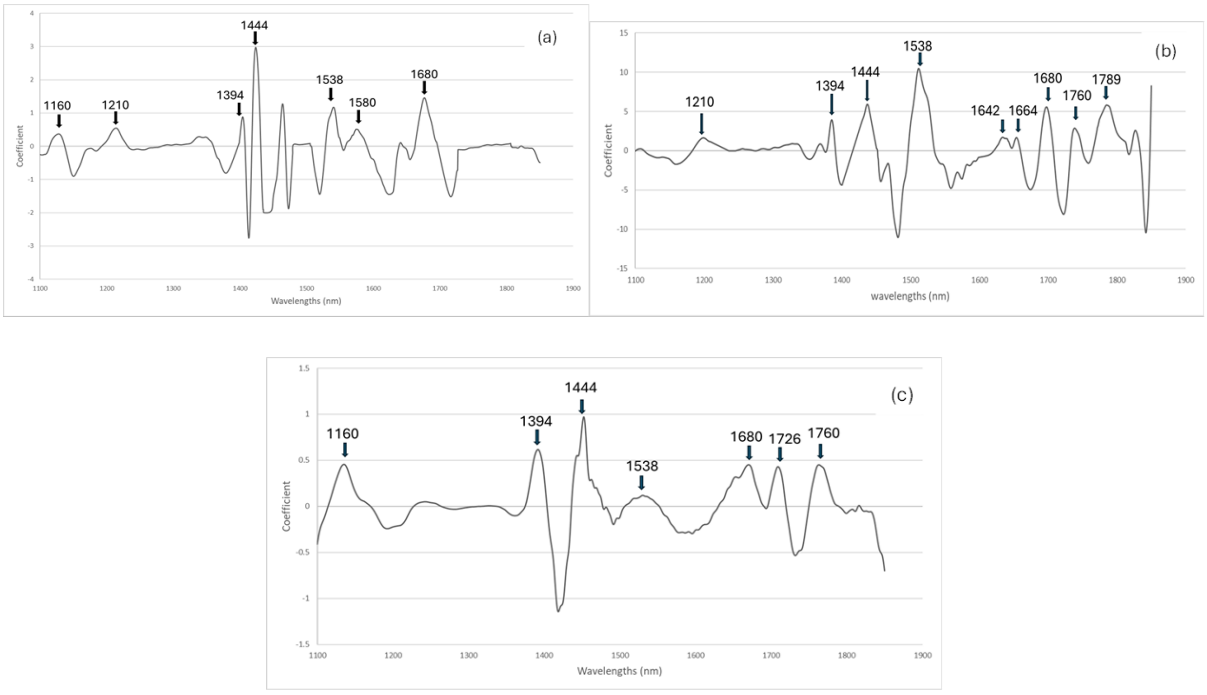

Figure 18. Contributing wavelengths to the discrimination of fermented milk samples from trial 1 (a), trial 2 (b) and trial 3 (c), based on the type of feeding

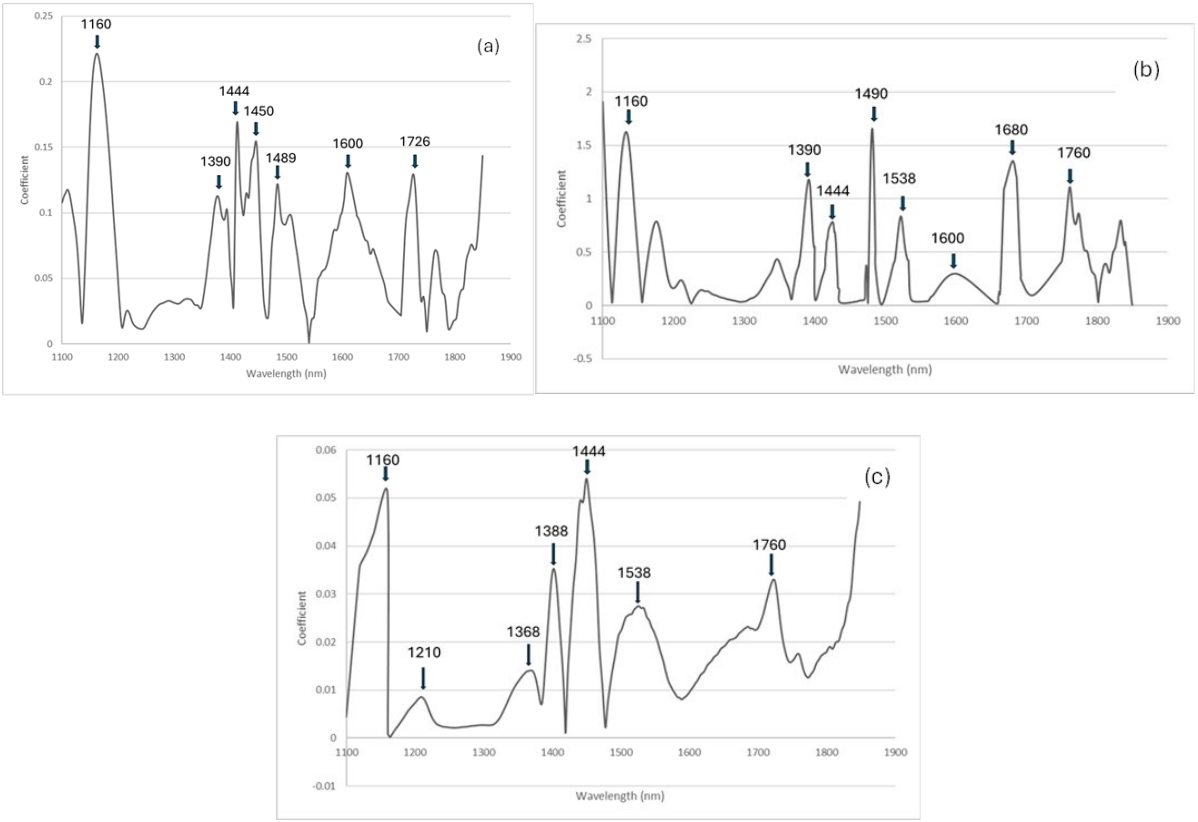

Figure 19. Contributing wavelengths to the discrimination of experimental fermented milk samples from trial 1 (a), trial 2 (b) and trial 3 (c), based on the type of strain

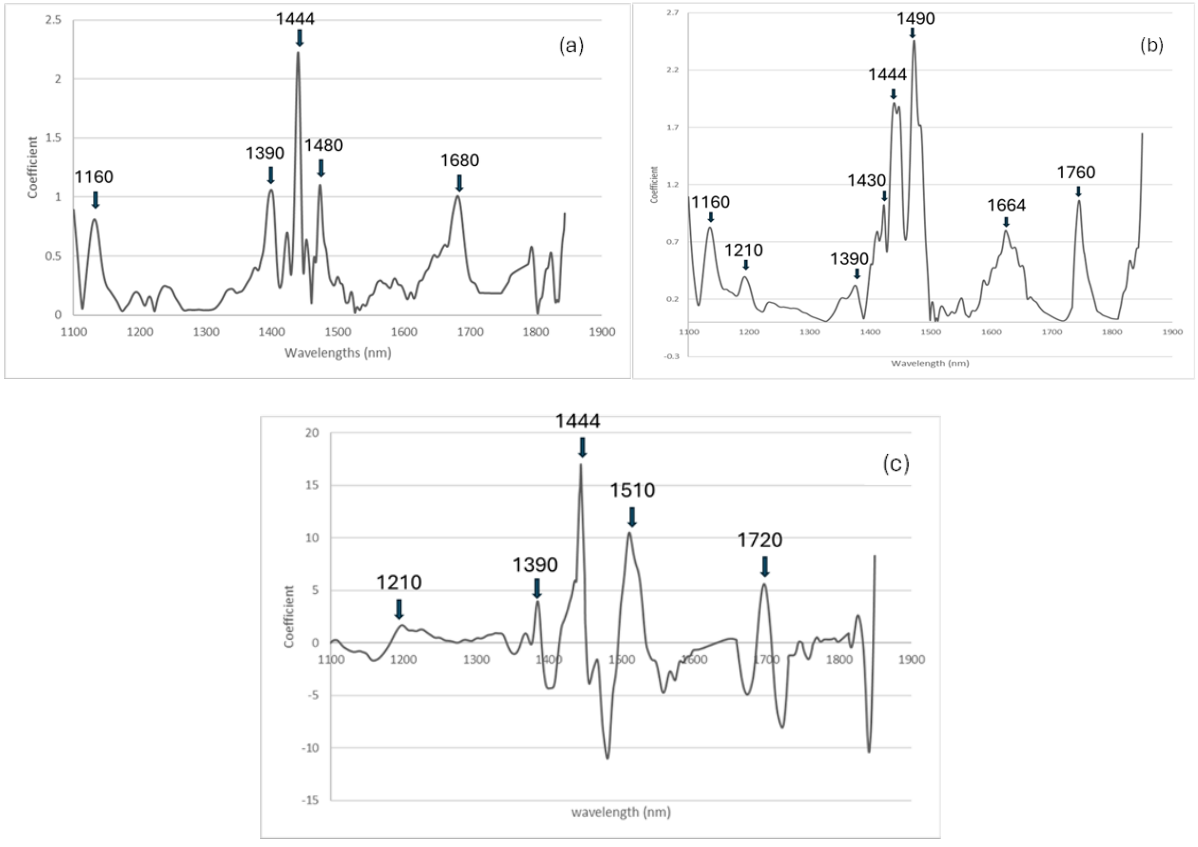

Figure 20. Contributing wavelengths to the discrimination of control fermented milk samples from trial 1 (a), trial 2 (b) and trial 3 (c), based on the type of strain

Table 13. Summary of contributing wavelengths to the classification of fermented milk samples according to the type of feeding and the probiotic potential, along with their corresponding band assignments

wavelength (nm)	Band assignment	References
1300-1400	Overtones and combination of O-H stretching vibrations	(Muncan, Kovacs, et al., 2021)
1440	First overtone of the OH stretching vibrations of water	(Czaja et al., 2023; Muncan, Tei, et al., 2021)
1164	Second overtone of C-H stretching vibration of various chemical groups (–CH2, –CH3,–CH=CH–) and fat related C-O stretching	(Suksangpanomrung et al., 2024; Hernández-Jiménez et al., 2024; Tsenkova et al., 2000; Ejeahalaka & On, 2020; Hourant et al., 2000)
1210	Second overtone of C-H stretching vibrations specifically in CH2 and CH3 groups	(Tsenkova et al., 2000; Suksangpanomrung et al., 2024; Núñez-Sánchez et al., 2016; C. Wang et al., 2021)
1538-1580	Overtones and combination bands of O-H, C-H and N-H bonds in carbohydrates (lactose, glucose, fructose), lactic acid, proteins, lipids and fatty acids	(Sharma et al., 2023; Ejeahalaka & On, 2020; Suksangpanomrung et al., 2024)
1664-1680	First overtone of the C-H stretching vibration of methyl (–CH3) and Ethenyl (–CH=CH–) groups, associated to lipids and fatty acids, lactic acid and proteins	(Hernández-Jiménez et al., 2024; Grabska et al., 2018; Muncan, Tei, et al., 2021; Hourant et al., 2000)
1712-1760	First overtone of the C-H stretching vibration of methyl (–CH3), methylene (–CH2) and ethenyl groups (–CH=CH–)	(Muncan, Tei, et al., 2021; Grabska et al., 2018; González-Martín et al., 2020; Hourant et al., 2000)
1789	Stretching vibrations of C=O bonds associated to acids and esters	(González-Martín et al., 2020)

The wavelengths of 1164 nm and 1210 nm are linked to the absorption properties of fats and fatty acids, arising from the second overtone of C-H stretching vibrations and the absorption of water due to O-H groups (Hourant et al., 2000; Suksangpanomrung et al., 2024). The spectral region around 1164 nm is particularly noteworthy as it is associated with the presence of unsaturated fatty acids (–HC=CH–) in the aliphatic chains of fats, such as oleic acid (C18:1), which exhibit a strong absorption peak in this range (da Silva Medeiros et al., 2024). This specific wavelength played a key role in the strain-specific discrimination of experimental fermented milk, likely due to the higher content of unsaturated fatty acids in the experimental samples compared to the controls. Hourant et al. (2000) reported similar findings, noting that oils rich in polyunsaturated fatty acids show greater absorption near 1164 nm than those with saturated fatty acids. Additionally, the wavelengths of 1538 nm and 1580 nm are indicative of water, lactose, carbohydrates, and lactic acid absorption, providing valuable insights into the fermentation process and the metabolic activity of microorganisms (Sharma et al., 2023; Muncan, Tei, et al., 2021). The spectral region between 1300-1400 nm is typically attributed to the first overtone of O-H stretching vibrations (Muncan, Kovacs, et al., 2021). Notably, the 1300-1600 nm range contributed significantly to strain-specific classifications. The O-H stretching overtone in this region is sensitive to subtle changes in water structure or interactions with other components, such as proteins or carbohydrates. Different fermentation strains can alter water structure or its interactions with proteins and fats, leading to variations in absorption characteristics within this spectral range (Muncan, Tei, et al., 2021).

The 1600-1800 nm range is primarily associated with the first overtone of C-H stretching vibrations and C=O (carbonyl) vibrations (Hourant et al., 2000). Interestingly, a significant number of contributing wavelengths are concentrated in this region. Grabska et al. (2018) conducted a detailed analysis of NIR bands related to fatty acids, identifying numerous overtone and combination bands of CH, OH, and C=O vibrations within this spectral range. Key markers include 1680 nm and 1642 nm, which indicate the presence of double bonds in unsaturated fatty acids like oleic acid (C18:1), known for its strong absorption due to its cis double bond configuration (González-Martín et al., 2020). Similarly, the wavelengths of 1726 nm and 1712 nm reflect the presence of unsaturated fatty acids such as oleic, linoleic, and linolenic acids, highlighting their abundance in the samples (Grabska et al., 2018) , while 1760 nm corresponds to saturated components (Núñez-Sánchez et al., 2016).

This correlation reinforces the hypothesis that the fatty acid profile and content, particularly the presence of unsaturated and polyunsaturated fatty acids with their characteristic double bonds, is a critical factor in distinguishing different types of fermented milk. The consistency of spectral

patterns in this region, regardless of the microbial strains used, makes them reliable markers for differentiation. Additionally, the 1300-1600 nm range, dominated by water absorption, was particularly significant for strain-specific differentiation, as variations in water structure and interactions influenced by different strains resulted in distinct absorption characteristics.

- Contributing virtual sensors

Table 14 offers a detailed summary of the key sensors that effectively distinguished the experimental fermented milk samples from the control samples, emphasizing the specific volatile compounds responsible for these distinctions. During milk fermentation, a diverse array of volatile compounds is generated, influenced by factors such as milk composition, fermentation conditions, and microbial activity. These compounds play a crucial role in shaping the aroma and flavor of fermented milk, with lactic acid bacteria (LAB) being particularly important in producing ketones, aldehydes, esters, and alcohols (Yu et al., 2024).

Table 14. Summary of contributing virtual sensors to the classification of fermented milk samples according to the type of feeding and probiotic potential, along with their corresponding volatile compounds

Discrimination tendency	C-S*	Volatile Compounds	Sensory Description
Experimental VS control Control (strain based) Experimental (strain based)	488	propanal	etheral, plastic, pungent, solvent
Experimental VS control	612	Ethyl acetate	acidic, butter, caramelized, etheral, fruity, orange, pineapple, pungent, solvent
Experimental VS control Control (strain based) Experimental (strain based)	690	2,3-pentanedione	butter, caramelized, creamy, fresh, fruity, sweet
		pentanal	almond, green, herbaceous, malty, pungent, rubber
		pentan-2-one	acetone, etheral, fruity,thinner
Experimental VS control Experimental (strain based)	775	1-hexen-3-one	cooked vegetable, leafy, linseed oil, metallic
		1-hexen-3-ol	Green
Experimental VS control Control (strain based) Experimental (strain based)	584	butan-2,3-dione	butter, caramelized, creamy, fruity, pineapple, spirit
Experimental VS control Control (strain based) Experimental (strain based)	710	ethyl propanoate	Acetone, fruity, solvent
		propyl acetate	caramelized, fermented, fruity, ketonic, solvent, sweet
		Acetoin	butter, coffee, creamy
Experimental VS control Control (strain based) Experimental (strain based)	598	butan-2-one	butter, cheese, chemical, chocolate, etheral, gaseous
Experimental VS control Experimental (strain based)	518	dimethyl sulfide	cabbage, fruity, gaseous, gasoline, moldy, sulfurous, vegetable soup
Control (strain based)	1097	Ethyl heptanoate	Fruity
Experimental (strain based)	802	Hexanal	Acorn, fatty, fishy, fruity, grassy, green, herbaceous, leafy, tallowy
Experimental (strain based)	1402	phenylpropanol, alpha-methyl, acetate	Fruity
Experimental VS control Experimental (strain based)	437	ethanol	Sweet, bitter, drying
Experimental VS control Experimental (strain based)	894	Ethyl pentanoate	fruity, grassy, green, minty, orange, yeasty
		(Z)-4-heptenal	biscuit, boiled potato, creamy, dairy, sweet
Experimental VS control Control (strain based)	562	butanal	chocolate, green, malty, pungent

*C-S = Closest sensors from AroChemBase v8 database

Esters such as ethyl propanoate, propyl acetate, and ethyl pentanoate were linked to contributing sensors. These esters, commonly found in fermented milk, are primarily formed during fermentation through esterification, a process where alcohols react with carboxylic acids or amino acids (Li et al., 2024). Known for imparting fruity, floral, and pleasant aromas, esters are a direct result of LAB activity, which synthesize organic acids during fermentation (Wang et al., 2024).

Diketones like 2,3-pentanedione, butan-2,3-dione, and acetoin are secondary metabolites produced by LAB during fermentation. These compounds arise from the breakdown of specific amino acids and lipids in milk, contributing sensory notes such as buttery and creamy flavors that enhance the aroma of fermented milk (Yu et al., 2024; Tang et al., 2024). However, high concentrations can lead to undesirable off-flavors. The type and concentration of diketones produced depend on the microbial culture and milk composition, highlighting the influence of LAB strain selection on the intensity and balance of these flavors (Li et al., 2024).

Contributing sensors were also associated with aldehydes such as butanal, pentanal, propanal, and (Z)-4-heptenal. Aldehydes are primarily generated from the metabolism of lipids, proteins, or carbohydrates during fermentation. LAB activity accelerates lipid breakdown, resulting in short-chain aldehydes with distinctive aromas. Of particular interest are (Z)-4-heptenal and pentanal, which are derived from the oxidation of unsaturated fatty acids (Li et al., 2024). (Z)-4-heptenal, originating from the breakdown of omega-6 fatty acids like linoleic acid, contributes a grassy, green, and fatty aroma (Li et al., 2024; Sghaier et al., 2015; He et al., 2022), adding a fresh, vegetative character to fermented milk products.

Ketones such as pentan-2-one, 1-hexen-3-one, and butan-2-one also played a role in differentiating the samples. These compounds are mainly formed through the oxidative degradation of n-6 and n-3 polyunsaturated fatty acids (notably linoleic and linolenic acids) and the metabolism of amino acids by LAB (Peinado et al., 2016; Chi et al., 2024). For instance, 1-hexen-3-one contributes a leafy and fresh aroma, while pentan-2-one adds fruity and ethereal notes with a faint solvent-like or sweet character.

Among alcohols, 1-hexen-3-ol was identified as a contributor, originating from the oxidation of n-6 type polyunsaturated fatty acids such as linoleic acid (Coleman et al., 2023). This compound imparts a green, herbal, and slightly fruity scent, enhancing the freshness and complexity of fermented milk.

Notably, specific volatile compounds derived from the breakdown of unsaturated fatty acids, such as 1-hexen-3-one, 1-hexen-3-ol, hexanal, and (Z)-4-heptenal, were found at relatively high levels in the experimental group. These compounds played a significant role in differentiating

experimental fermented milk samples based on the strain used. This indicates that the choice of bacterial strain in fermentation is a key factor in the production of these compounds, more so than in the control milk. The E-nose sensors effectively detected distinct volatile compounds, particularly those associated with the oxidative breakdown of unsaturated fatty acids. These fatty acid derivatives, identified by specific sensors, serve as reliable markers for aroma and flavor differences, underscoring the importance of unsaturated fatty acids in distinguishing fermented milk products.

These findings demonstrate that targeted dietary interventions can effectively enhance the nutritional and sensory quality of milk, with clear benefits for human health, including improved intake of beneficial unsaturated fatty acids. The use of NIRS and e-nose technologies provides rapid, non-destructive tools to monitor milk composition and fermentation, supporting precision feeding and probiotic strategies. Specific wavelengths and virtual sensors, such as 1164–1210 nm for unsaturated fatty acids and sensors detecting key volatiles like 1-hexen-3-one, 1-hexen-3-ol, and (Z)-4-heptenal, were critical in distinguishing experimental from control samples. These markers highlight the direct impact of dietary supplementation and microbial activity on milk's chemical and sensory profiles. For the dairy industry, this enables production of functional and differentiated products with higher market value, while also informing economic decisions on feed formulation. Compared to prior studies, these results extend current knowledge by demonstrating that NIRS and e-nose can simultaneously assess both nutritional and sensory attributes of milk with high accuracy. Previous research has largely focused on using NIRS for quantifying major milk components such as fat, protein, and lactose (Diaz-Olivares et al., 2020) or detecting adulterants and quality parameters like density and moisture in milk powders (Wang et al., 2021;Chen et al., 2018). Similarly, studies such as Valenti et al. (2013) and Coppa et al. (2012) applied NIRS to classify milk by production systems or cow breeds, while Foschi et al. (2025) used ATR-FTIR to determine the animal origin of dairy products. Our work builds upon these approaches by integrating spectral and volatile data to capture both biochemical and aromatic changes resulting from dietary supplementation and fermentation. This combined analytical framework provides a more comprehensive tool for precision monitoring of milk quality, linking nutritional improvements with sensory differentiation in a way that previous single-method studies could not achieve.

5.3.Evaluation of the impact of cattle feed on cheese ripening process

5.3.1. Analysis of fresh cheese samples

- Compositional analysis

Table 15 presents the mean total content (%) ± standard deviation (STD) of dry matter, crude fat, crude protein, and ash for control and experimental fresh cheese samples across trials 1, 2, and 3, along with the corresponding results of ANOVA statistical analysis. The primary objective of the ANOVA tests was to evaluate the influence of feed supplementation with polyunsaturated fatty acid (PUFA)-rich sources on the compositional attributes of the cheese samples, specifically targeting parameters essential for nutritional quality and functionality. The ANOVA results revealed significant differences in dry matter content between control and experimental cheese samples in trials 1 and 3, while no significant differences were observed in trial 2. This variability suggests that the effect of PUFA-rich feed on moisture content in cheese may depend on trial-specific conditions, such as environmental factors, feed composition, or animal physiological responses during milk production. The observed differences in dry matter indicate alterations in the cheese's water-binding properties, potentially affecting texture and shelf life.

Across all three trials, crude fat content showed significant differences between the control and experimental groups. This consistent trend highlights the strong influence of PUFA supplementation on the fat profile of the cheese, potentially altering the lipid composition to favor unsaturated fatty acid content. Such changes could have important implications for the health-related properties of the cheese, as increased PUFA levels are associated with better cardiovascular health benefits.

Protein content displayed significant differences between the control and experimental groups in trials 1 and 3 but not in trial 2. These findings suggest that PUFA supplementation can influence the protein structure or content in cheese, possibly due to changes in milk protein composition or proteolytic activity during cheese production. The variability across trials might possibly reflect interactions between feed components and the metabolic pathways regulating milk protein synthesis.

The ANOVA results indicated significant differences in ash content between control and experimental cheese samples in trials 1 and 2, while no significant differences were observed in trial 3. Changes in ash content may be associated with variations in milk mineral levels, such as calcium and phosphorus, which could influence both the quality and nutritional value of the cheese.

The results from this study clearly demonstrate that feed supplementation with PUFA-rich sources significantly influenced the compositional attributes of fresh cheese. Consistent changes in crude fat content across all trials, along with significant differences in dry matter, protein, and ash content

in specific trials, highlight the robust and dynamic effects of the experimental feeding strategy. Variations in ash content observed only in trials 1 and 2 further emphasize the potential influence of trial-specific conditions on the mineral profile of the cheese.

Table 15. Mean total content (%) ±STD of dry matter, crude fat, crude protein and ash of control and experimental fresh cheese from trial 1, 2 and 3. Letter (a–b) represent significantly different groups ($p \leq 0.05$), based on ANOVA

		Dry matter (%)	Crude fat (%)	Crude protein (%)	Ash (%)
Trial 1	CTR 1	56.14 ± 2^{a}	28.69 ± 2^{a}	21.55 ± 1.3^{a}	4 ± 0.1^{a}
	EXP 1	54.73 ± 1.1^{b}	26 ± 1.8^{b}	21.87 ± 0.4^{b}	5 ± 0.7^{b}
Trial 2	CTR 2	65.74 ± 3.8^{a}	30.7 ± 3.3^{a}	28.74 ± 2^{a}	5.4 ± 0.8^{a}
	EXP 2	65.86 ± 3.5^{a}	32.98 ± 3.5^{b}	28.38 ± 1.8^{a}	5.16 ± 0.7^{b}
Trial 3	CTR 3	63.32 ± 1.5^{a}	30.37 ± 1.33^{a}	24.13 ± 0.44^{a}	3.55 ± 0.5^{a}
	EXP 3	60 ± 1.9^{b}	34.9 ± 1.5^{b}	24.86 ± 1^{b}	3.52 ± 0.4^{a}

- NIRS analysis

The raw NIR spectra of experimental and control cheese samples from trial 1 (a), trial 2 (c), and trial 3 (e), covering the spectral range of 908–1676 nm is shown in Figure 21. Distinguishing between control and experimental cheese samples through visual inspection is challenging. The spectra of both types of cheese displayed similar peaks, reflecting the chemical composition characteristic of cheese. These peaks are primarily associated with the presence of lipids, proteins, and water, which are the key components of cheese. Two prominent peaks are evident around 1210 nm and 1450 nm. The peak at 1210 nm corresponds to the second overtone of C-H stretching vibrations, specifically in CH_2 and CH_3 groups, which are associated with lipids (Tsenkova et al., 2000; Suksangpanomrung et al., 2024; Núñez-Sánchez et al., 2016; C. Wang et al., 2021). The peak at 1450 nm is attributed to the combination of OH symmetric and asymmetric stretching modes of water (Kasemsumran et al., 2007). Despite the considerations mentioned above, the spectra exhibited unwanted variability, including baseline shifts, scattering effects and the dominance of water absorption peaks. Therefore, it was necessary to apply pre-processing methods to minimize these issues and extract meaningful information effectively (Tsenkova et al., 2000).

To address this, the application of the second derivative to the raw spectra enhanced the resolution of overlapping peaks and minimized baseline fluctuations. The second derivative spectra, displayed in Figure 21 for trial 1 (b), trial 2 (d), and trial 3 (f), revealed distinct spectral features beyond water absorption. Notably, the absorption bands at 1160 nm and 1210 nm are assigned to the C-H bond of lipids and the peak at 1338 nm is attributed to overtones and combination of O-H stretching vibrations in water and proteins (Muncan, Kovacs, et al., 2021)

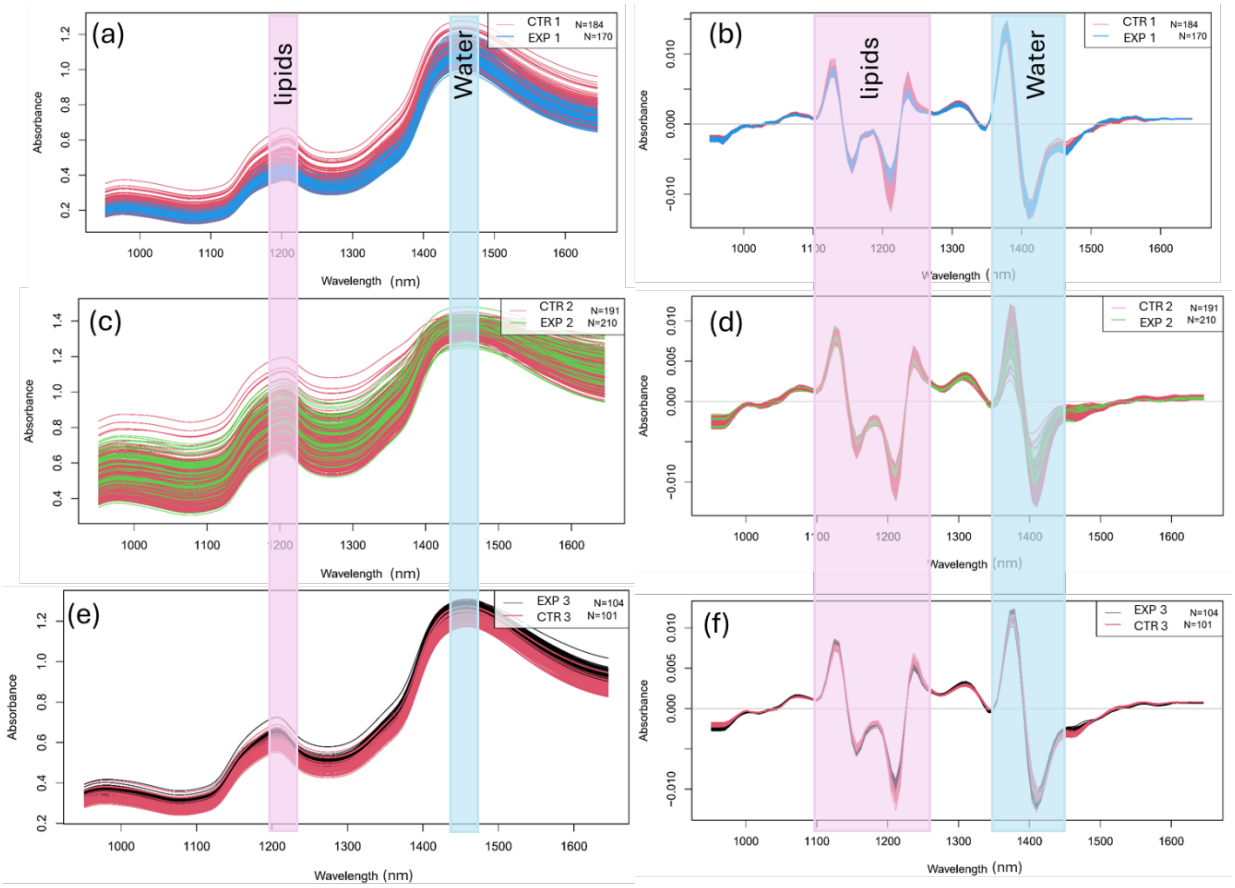

Figure 21. NIR raw spectra of experimental (EXP) and control (CTR) fresh cheese samples from trial 1 (a), trial 2 (c), and trial 3 (e) in the range 908–1676 nm, and second derivative spectra of experimental and control fresh cheese samples from trial 1 (b), trial 2 (d), and trial 3 (f) in the same range.

- Classification models of the fresh cheese samples based on feeding type

In this phase of analysis, a more detailed investigation was conducted using the Linear Discriminant Analysis (LDA) technique to identify distinct groups within the NIRS datasets. This method was applied to classify the cheese samples and assess the model's ability to effectively differentiate them based on the type of feeding. The NIRS datasets contain critical information about the chemical composition of the cheese samples, which vary according to the feeding type. The primary objective was to determine whether these feeding-induced variations result in distinguishable patterns in the data, probably enabling accurate classification of the samples. Figure 22 shows the classification models developed NIRS data for the experimental and control fresh cheese samples across three distinct feeding trials. The results of these classification models, which summarize both the recognition accuracies and the prediction accuracies, are compiled in Table 16.

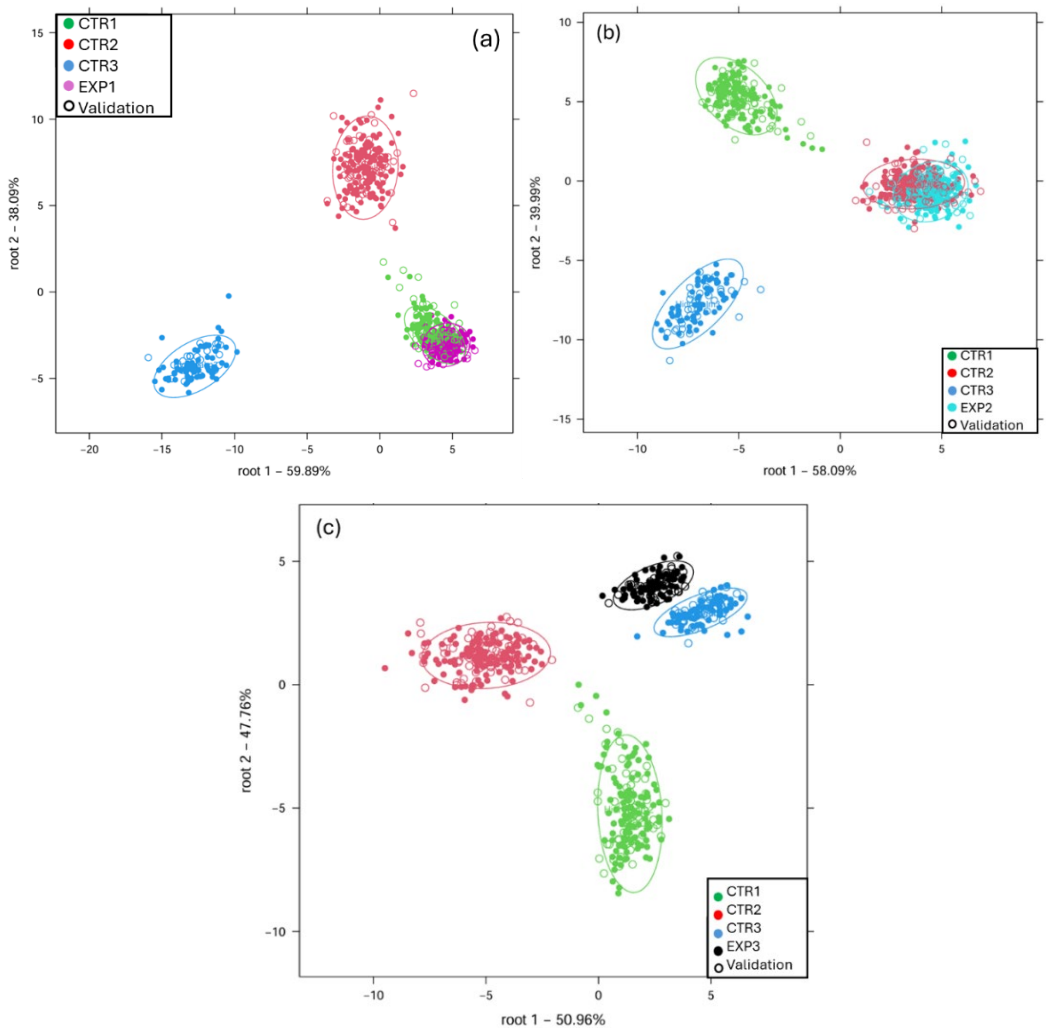

Figure 22. LDA models for the classification of experimental and control fresh cheese samples across three different feeding trials, with trial 1 (a), trial 2 (b) and trial 3 (c); Control fresh cheese samples (CTR), Experimental fresh cheese samples (EXP)

Table 16. Confusion table of the PCA-LDA models for experimental and control fresh cheese samples across three different feeding trials

		Training				Cross-Validation			
		CTR1	CTR2	CTR3	EXP1	CTR1	CTR2	CTR3	EXP1
Trial 1	CTR1	96.74	0	0	3.82	96.2	0	0	4.71
	CTR2	0	100	0	0	0	100	0	0
	CTR3	0	0	100	0	0	0	100	0
	EXP1	3.26	0	0	96.18	3.8	0	0	95.29
	Average recognition = 98.23%					**Average prediction = 97.87%**			
Trial 2		CTR1	CTR2	CTR3	EXP2	CTR1	CTR2	CTR3	EXP2
	CTR1	99.73	0	0	0	99.46	0	0	0
	CTR2	0.27	83.77	0	10.95	0.54	84.81	0	13.33
	CTR3	0	0	100	0	0	0	100	0
	EXP2	0	16.23	0	89.05	0	15.19	0	86.67
	Average recognition = 93.13%					**Average prediction = 92.73**			
Trial 3		CTR1	CTR2	CTR3	EXP3	CTR1	CTR2	CTR3	EXP3
	CTR1	100	0	1.08	0	100	0	1.63	0
	CTR2	0	100	0	0	0	100	0	0
	CTR3	0	0	98.92	0	0	0	98.73	0
	EXP3	0	0	0	100	0	0	0	100
	Average recognition = 99.73%					**Average prediction = 99.5%**			

Across all trials, the classification models consistently demonstrated high performance, with recognition accuracies ranging from 93% to 99% and prediction accuracies between 92% and 99%. Notably, the model for trial 3, which involved feeding with a supplement rich in fish oil, whole linseed, linseed oil and algae extract, achieved perfect classification. The model accurately distinguished between the control and experimental fermented milk samples with 100% accuracy. This suggests that the supplement induced a distinct set of molecular changes during cheese production, allowing clear differentiation between the two sample groups.

However, trials 1 and 2 exhibited some misclassifications. For trial 1, misclassifications occurred between control and experimental samples from the same trial. In the training set, 3.82% of experimental samples were misclassified as control samples, while 3.26% of control samples were misclassified as experimental samples. These misclassification rates increased slightly in cross-validation, with 4.81% of experimental samples misclassified as controls and 3.8% of control

samples misclassified as experimental. Trial 2 exhibited even higher misclassification rates, with 10.95% of experimental samples misclassified as control samples and 16.23% of control samples misclassified as experimental in the training set. In cross-validation, these misclassification rates were 13.33% for experimental samples misclassified as controls and 15.19% for control samples misclassified as experimental.

Additionally, minor misclassifications were observed between control cheese samples, indicating subtle variations in their chemical profiles. These misclassifications highlight the inherent similarity in the chemical composition of the control cheese samples, which were produced from milk harvested in different seasons and from different animals, contributing to natural variability in their chemical characteristics.

The varying degrees of distinctiveness in the chemical profiles of the cheeses from different feeding trials are noteworthy, with the supplement of feeding trial 3 standing out as the most easily classifiable due to its rich composition of polyunsaturated fatty acids, which likely contributed to more noticeable biochemical changes. This underscores the potential of feed supplements, to induce distinct molecular signatures in cheese, which can be captured by classification models, allowing for more accurate differentiation between supplemented and non-supplemented cheese samples.

- Contributing wavelengths

As the next step in our analysis, we focus on identifying the key wavelengths that most significantly enhance the performance of the classification models. By pinpointing these wavelengths, we aim to gain deeper insights into the chemical composition differences between control and experimental cheese samples from the same trial, ensuring a fair comparison since the trials were conducted in different seasons. This approach will help us better understand how feed supplementation influences the cheese's chemical composition. Through this targeted analysis, we can uncover the specific factors driving the classification model's ability to effectively differentiate between the various cheese samples.

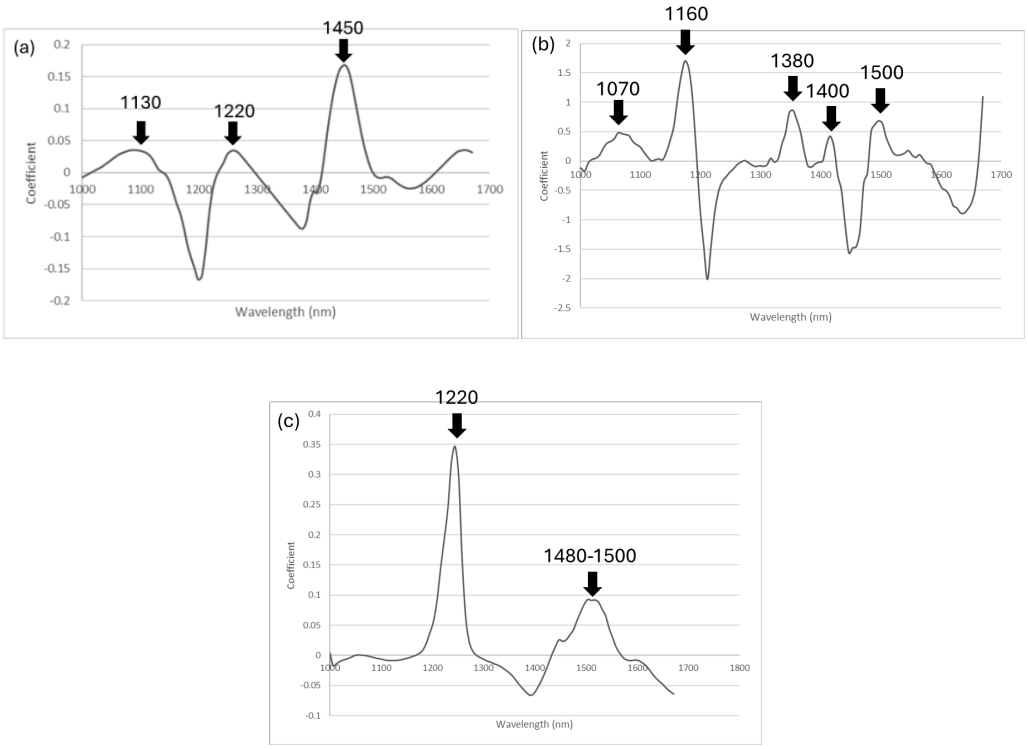

Figure 23. Contributing wavelengths to the discrimination of fresh cheese samples from trial 1 (a), trial 2 (b) and trial 3 (c), based on the type of feeding

Figure 23 shows Contributing wavelengths to the classification of fresh cheese samples from trial 1 (a), trial 2 (b) and trial 3 (c), based on the type of feeding. In Feeding Trial 1, the most significant wavelength contributing to the analysis was observed at 1450 nm, which corresponds to the first overtone of O-H stretching vibrations in water (Czaja et al., 2023; Muncan, Tei, et al., 2021). This peak indicates the strong role of water absorption in distinguishing between control and experimental samples. Additionally, smaller peaks were noted at 1130 nm and 1220 nm. The 1130 nm peak is attributed to the second overtone of C-H stretching vibrations in various chemical groups (–CH_2, –CH_3, –CH=CH–) and fat-related C-O stretching vibrations (Suksangpanomrung et al., 2024; Hernández-Jiménez et al., 2024; Tsenkova et al., 2000; Ejeahalaka & On, 2020; Hourant et al., 2000), while the 1220 nm peak specifically corresponds to the second overtone of C-H stretching vibrations in CH_2 and CH_3 groups (Tsenkova et al., 2000; Suksangpanomrung et al., 2024; Núñez-Sánchez et al., 2016; C. Wang et al., 2021). Overall, water absorption emerged as the dominant marker for differentiating control and experimental samples, with minor contributions of fat related compounds' absorption.

In Feeding Trial 2, the highest contributing wavelength was observed at 1160 nm. This wavelength is associated with the presence of fat and integrated fatty acids (with ester bonds), particularly unsaturated fatty acids (Hourant et al., 2000). Additional peaks were identified at 1380 nm, 1400–

1409 nm, and 1500 nm. The 1400–1409 nm region is linked to the combination of stretching and bending vibrations in CH_2, indicative of fat content. The 1500 nm peak corresponds to the first overtone of N-H stretching vibrations, related to proteins (Downey et al., 2005; Sharma et al., 2023), while the 1380 nm peak is assigned to overtones and combinations of O-H stretching vibrations, indicative of water absorption (Muncan, Kovacs, et al., 2021). For this trial, fat and fatty acids absorption were the key markers for distinguishing experimental and control samples, with minor contributions from fat and proteins.

In Feeding Trial 3, the primary contributing wavelength was observed at 1220 nm, attributed to the second overtone of C-H stretching vibrations in CH_2 and CH_3 groups, indicative of fat and fatty acids content. Additional contributions were observed in the 1480–1500 nm range, which corresponds to the first overtone of N-H stretching vibrations, related to proteins (Downey et al., 2005). Fat and fatty acid absorption were the most critical markers for differentiating control from experimental cheese samples in this trial, with protein absorption providing secondary contributions.

Across the three feeding trials, specific but trial-dependently different wavelength regions emerged as key markers for distinguishing between control and experimental samples. Water absorption (1450 nm) was the primary marker in Trial 1, while fat and fatty acid absorption (1160–1220 nm) played a dominant role in Trials 2 and 3. Protein-related absorption (1480–1500 nm) contributed significantly to Trials 2 and 3 but played a secondary role overall.

5.3.2. Analysis of ripened cheese samples

- NIRS analysis

This phase of analysis used Linear Discriminant Analysis (LDA) to classify ripened cheese samples within NIRS datasets based on feeding type (control Vs experimental from the feeding trial 2). Separate classification models were developed for each of the three storage periods (4, 8 and 12 weeks), reflecting variations in the cheese's chemical composition influenced by feeding and storage time. The goal was to identify feeding-related patterns in the data, assess the model's accuracy in distinguishing control and experimental samples after each storage period and understand how storage duration affected classification accuracies.

Figure 24 illustrates the LDA models employed to classify control and experimental ripened cheese samples across three storage periods: 4 weeks, 8 weeks, and 12 weeks. The figure also highlights the recognition and prediction accuracies achieved by the models. Remarkably, the models demonstrated high performance across all three ripening periods, achieving 100% recognition and prediction accuracies. These findings underscore the effectiveness of the NIRS

method in reliably distinguishing between control and experimental ripened cheese samples, regardless of the storage duration. The clear differentiation observed between the two groups at each storage period further confirms the robustness of this approach in identifying feeding-induced variations in the cheese samples, even as they undergo ripening over time.

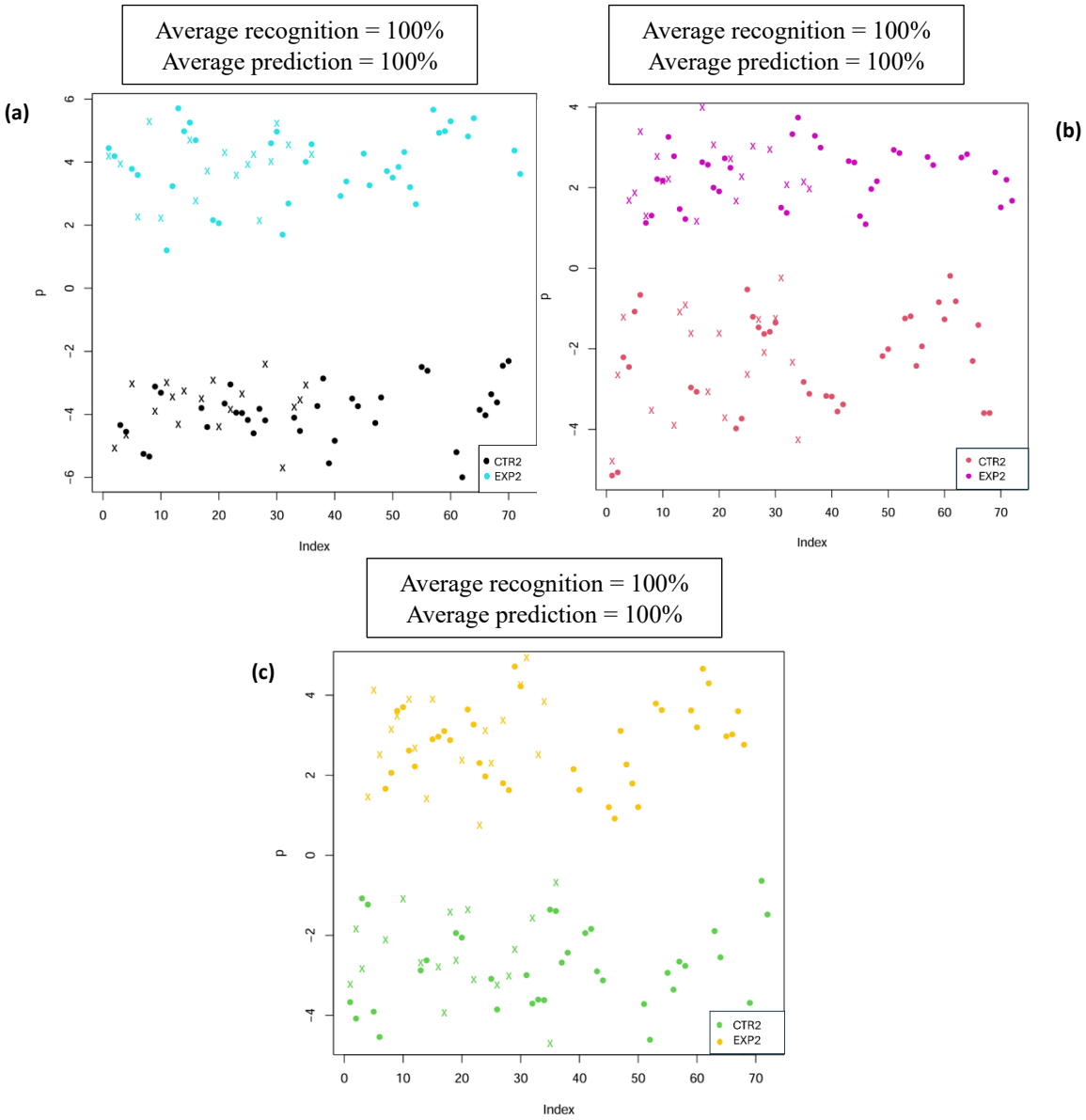

Figure 24. LDA models for the classification of experimental and control ripened cheese samples, over a storage period of 4 weeks (a), 8 weeks (b) and 12 weeks (c); Control ripened cheese samples (CTR), Experimental ripened cheese samples (EXP)

- Contributing wavelengths

During this phase of analysis, our primary objective is to identify the key wavelengths that most significantly improve the performance of the classification models. By identifying these wavelengths, we aim to gain a more comprehensive understanding of the chemical composition differences between control and experimental cheese samples throughout the three ripening periods. This detailed analysis will enable us to investigate how the ripening period influences the ability of the classification model to discriminate between the two sample groups. Figure 25 shows the contributing wavelength to the classification models presented in Figure 24.

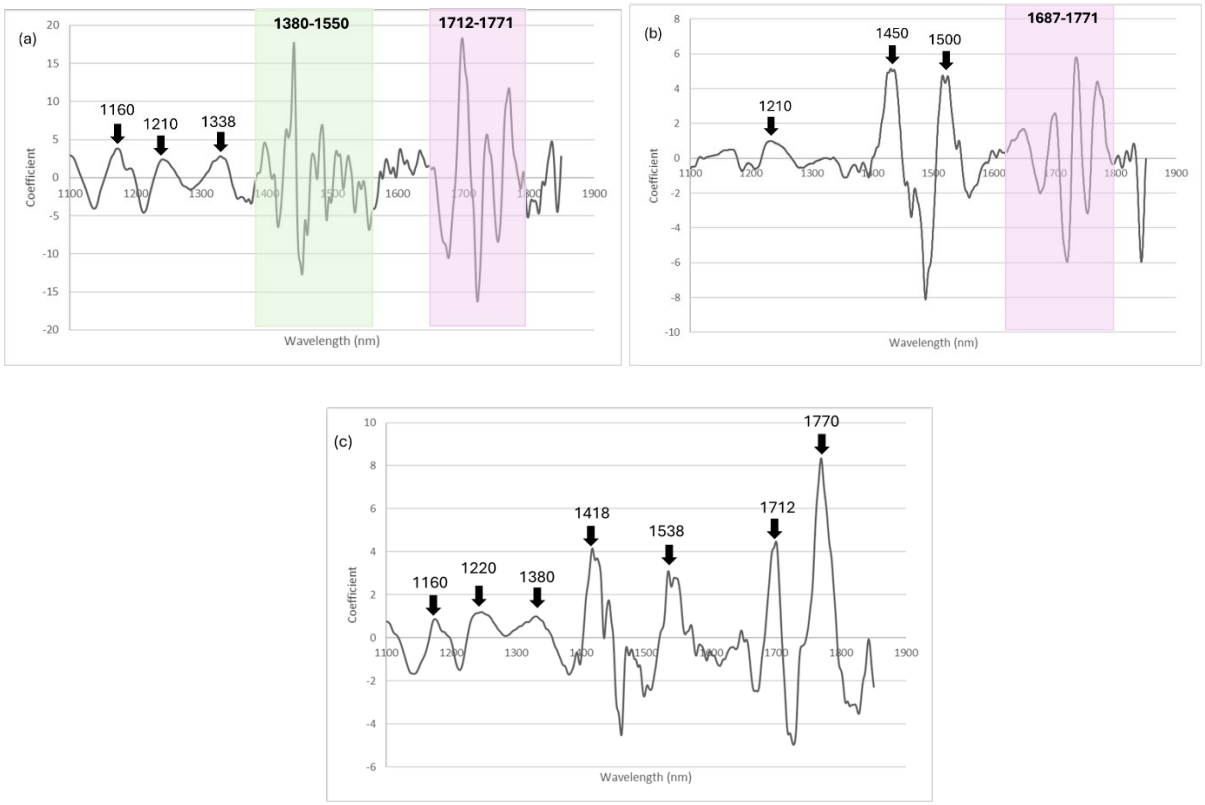

Figure 25. Contributing wavelengths to the classification of experimental and control ripened fresh cheese samples, over a storage period of 4 weeks (a), 8 weeks (b) and 12 weeks (c)

For the ripening period of 4 weeks, the wavelengths contributing to the classification of control and experimental groups were primarily concentrated in the spectral regions of 1380–1550 nm and 1712–1771 nm. Additional contributing wavelengths included 1160 nm and 1220 nm, both related to fat absorbance. The spectral region of 1380–1550 nm corresponds to water and protein absorption, while the region of 1712–1771 nm is primarily associated with the first overtone of C-H stretching vibrations and C=O (carbonyl) vibrations, which are linked to fat and fatty acids (Muncan, Kovacs, et al., 2021; Hourant et al., 2000). Among these, 1712 nm and 1450 nm were identified as key markers. The wavelength 1712 nm, along with 1726, was of particular interest

due to its assignment to the first overtone of C-H stretching vibrations in methyl ($–CH_3$), methylene ($–CH_2$), and ethenyl groups (–HC=CH–). These groups indicate the presence of double bonds, which are characteristic of unsaturated fatty acids, including oleic acid (C18:1), known for its strong absorption due to its cis double bond configuration, as well as linoleic acid and linolenic acid (Grabska et al., 2018; González-Martín et al., 2020). While 1771 nm was associated with the absorption of saturated components (Núñez-Sánchez et al., 2016). Another significant wavelength, 1450 nm, was linked to water absorption. Overall, the classification of the samples in the 4-week ripening period was driven by water absorption, fatty acids (primarily unsaturated), and their associated characteristics.

For the ripening period of 8 weeks, the main contributing wavelengths were 1450 nm, 1500 nm, 1726 nm, and 1771 nm. The 1500 nm peak was attributed to the first overtone of N-H stretching vibrations, which are related to proteins, while 1450 nm continued to represent water absorption (Downey et al., 2005; Sharma et al., 2023). Similar to the 4-week period, 1726 nm was associated with the absorption characteristics of unsaturated fatty acids. However, it is important to note that the absorption peak at 1712 nm was significantly less intense compared to the 4-week period. The 1771 nm peak, linked to saturated fatty acids, remained consistent in its contribution. This highlights a shift in the dominance of saturated components as the ripening process progresses.

By the 12-week ripening period, the most significant contributing wavelength was 1770 nm, indicating a strong relationship to saturated fatty acids. Peaks related to unsaturated fatty acids, such as 1726 nm, exhibited decreased intensity compared to earlier ripening stages. This decline can be attributed to the higher susceptibility of unsaturated fatty acids to oxidation and degradation due to their double bonds, whereas saturated fatty acids are more stable (You et al., 2024; M. K. Gupta, 2017). Nonetheless, traces of unsaturated fatty acid absorption remained evident, particularly at 1712 nm. Secondary contributions during this period were associated with fat, water, and protein absorption, albeit with reduced prominence compared to earlier stages.

In summary, the ripening process significantly influenced the spectral contributions of water, protein, and fatty acids. During the 4-week period, unsaturated fatty acids played a dominant role, as evidenced by the strong absorption peaks at 1712 nm and 1726 nm, alongside contributions from water and protein absorption. By the 8-week period, there was a notable reduction in unsaturated fatty acid absorption intensity, while contributions from saturated fat components and proteins became more pronounced. Finally, at the 12-week ripening period, saturated fatty acids dominated the spectral contributions, with their characteristic peak at 1770 nm, and the intensity of unsaturated fatty acid peaks diminished due to oxidation and degradation. The observed trends underscore the dynamic chemical changes occurring during ripening, with fatty acid stability and

oxidation playing critical roles in the classification of samples across ripening periods.

- Classification of ripened cheese samples according to the length of ripening period

Figure 26 and Figure 27 show the classification models of control and experimental ripened cheese samples across different ripening periods, emphasizing the most significant contributing wavelengths. For both groups, most of the contributing wavelengths were concentrated in the spectral range of 1380–1550 nm, a region strongly associated with the absorption characteristics of water and proteins. This spectral range includes the specific O-H stretching overtone, which is particularly sensitive to subtle changes in the structure of water or its interactions with other components (Visconti et al., 2024; Andueza et al., 2013).

During the ripening process, significant biochemical transformations occur, which can alter the microstructure of water in cheese and influence how water molecules interact with proteins, fats, and other macromolecules (Atasever, 2024). These changes are reflected in the absorption characteristics within the 1380–1550 nm range. For instance, modifications to the cheese matrix caused by fermentation or enzymatic activity may shift the way how water is bound to or distributed among components, leading to ripening-specific patterns in absorption (Stocco et al., 2024). This highlights the importance of water-related spectral features as key indicators of cheese ripening.

The most prominent difference, however, was observed in the spectral region of 1712–1770 nm, particularly in the experimental group. The wavelength 1712 nm showed a significant contribution and is specifically attributed to the absorption characteristics of unsaturated fatty acids. This suggests a considerable difference in unsaturated fatty acid content across the ripening periods. As previously established, unsaturated fatty acids are highly susceptible to oxidation due to their double bonds, leading to a progressive reduction in their content during the ripening process. This phenomenon aligns with the observation of a decreasing intensity at 1712 nm over time.

The pronounced contribution at 1712 nm in the case of the experimental group further emphasises the critical role of unsaturated fatty acids during the earlier stages of ripening. These fatty acids, including oleic, linoleic, and linolenic acids, are key markers for the biochemical changes of cheese during ripening. Their gradual degradation through oxidation and ripening-associated hydrolysis results in shifts in the cheese's fat composition, ultimately impacting its texture, flavor, and nutritional profile. In comparison, the control group exhibited a more uniform pattern in this spectral region, suggesting less variability in the unsaturated fatty acid content and molecular allocation (free and ester bound) across ripening stages.

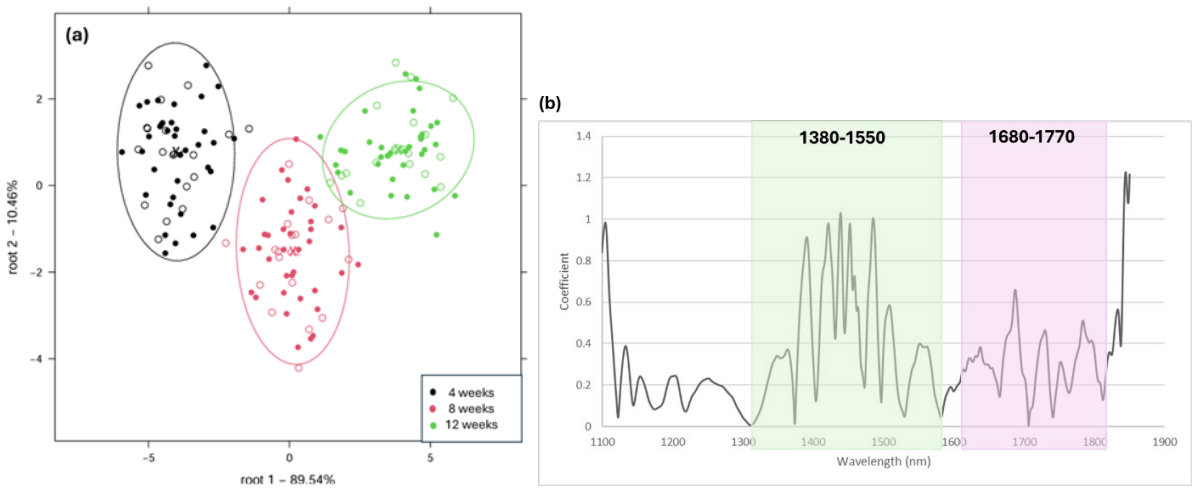

Figure 26. LDA model for the classification of the ripening period in the case of control cheese samples(a) and its corresponding contributing wavelengths (b)

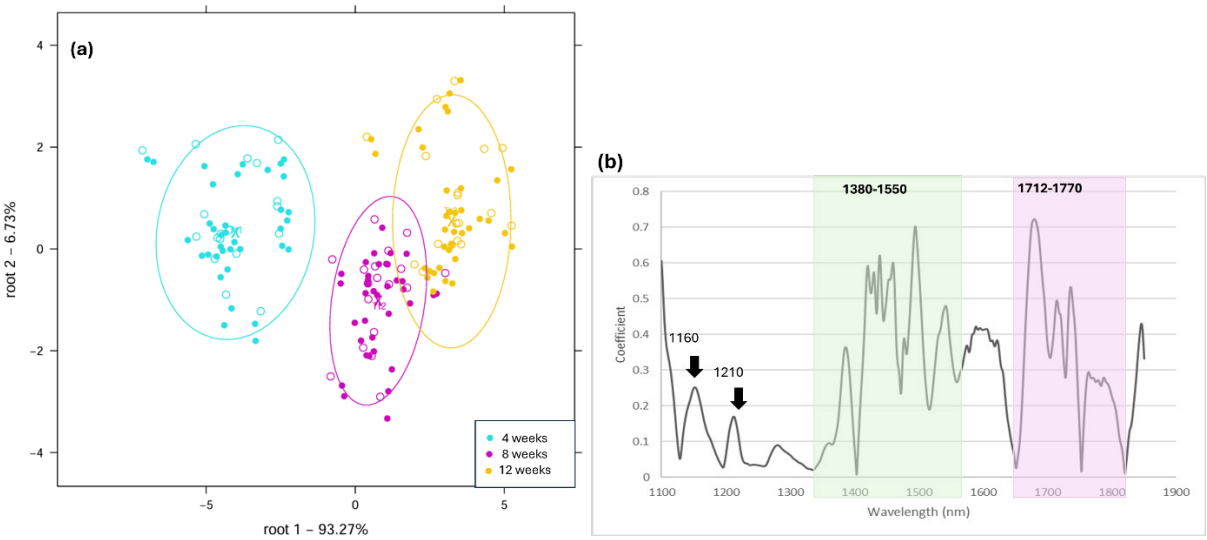

Figure 27. LDA model for the classification of the ripening period in the case of experimental cheese samples(a) and its corresponding contributing wavelengths (b)

These findings confirm that PUFA supplementation induces measurable molecular changes in cheese, which can be effectively detected with NIRS. Compared to literature, our results align with prior research demonstrating that spectroscopic techniques are powerful tools for characterizing cheese composition and monitoring ripening. For instance, Manuelian et al. (2017) used NIRS to predict fatty acid profiles in cheese, achieving moderate to high predictive accuracy, while Stocco et al. (2019) applied Bayesian models to estimate a range of chemical and physical traits, highlighting the method's versatility for dairy analysis. Similarly, Andueza et al. (2013) successfully discriminated pasture-fed from preserved-forage cheeses using reflectance spectroscopy, and Foschi et al. (2025) achieved 97% correct classification of cheese origin based on ATR-FTIR data. Our study builds upon these approaches by integrating both compositional

analysis and ripening dynamics, demonstrating that PUFA-rich feed supplementation not only alters initial cheese composition but also drives distinct molecular changes throughout storage. By achieving up to 100% classification accuracy with PCA-LDA models, this work surpasses some previous cheese-focused studies in discriminative performance.

From a practical perspective, these results provide a dual benefit: nutritionally, cheeses with higher PUFA levels may contribute to cardiovascular health, while industrially, the ability to rapidly classify and monitor ripening stages enables more precise quality control. This combined approach supports the production of premium, functional dairy products with clear labelling and traceability, expanding on earlier studies that focused solely on composition or origin. Ultimately, our findings highlight the value of coupling targeted nutritional interventions with advanced spectroscopic tools to optimize both the health properties and market value of cheese products.

6. CONCLUSIONS

This research demonstrates the robust potential of near-infrared spectroscopy (NIRS) as a versatile analytical tool for characterizing dairy products, spanning reconstituted milk powders, fermented milk, and cheese. Unlike previous studies that focus on individual matrices or isolated compositional traits, this work integrates three complementary studies, providing a holistic understanding of dairy product composition, processing effects, nutritional enhancement, and molecular-level differentiation. This integrated approach represents a novel contribution to dairy science by linking feeding strategies, processing conditions, and compositional changes with rapid, non-destructive analytical techniques.

In the first study, NIRS combined with advanced chemometric models accurately differentiated reconstituted milk samples derived from cow, camel, and mare milk across varying concentrations (5%, 10%, 12.5%) and reconstruction temperatures (25 °C, 40 °C, 65 °C). ANOVA analysis confirmed that milk type was the primary driver of compositional variation, a finding validated by PCA-LDA models achieving 100% classification accuracy. Further, SVR models outperformed PLSR in predicting key quality parameters, including pH, viscosity, dry matter, fat content, conductivity, and amino acid composition. These results confirm that NIRS can provide rapid, non-invasive, and precise assessment of reconstituted milk quality and composition, enabling effective industrial monitoring, standardization, and optimization of formulations tailored to specific nutritional requirements.

The second study explored fermented cow milk, integrating NIRS and electronic nose (e-nose) techniques to investigate the impact of cow feeding regimes on chemical composition and probiotic potential. NIRS effectively captured broad chemical attributes, such as water, fat, and protein content, while the e-nose detected subtle volatile compounds crucial for flavor differentiation. Key markers, such as hexanal and 1-hexen-3-one, indicated the oxidative breakdown of unsaturated fatty acids, providing insight into the biochemical processes influencing flavor and quality. Specific NIRS wavelengths (1600–1800 nm) associated with mono- and polyunsaturated fatty acids reliably distinguished samples by feeding type, while water-dominated wavelengths (1300–1600 nm) allowed differentiation based on LAB strains. These findings highlight the potential for combining NIRS and e-nose technologies to tailor fermented dairy products for dietary, nutritional, and probiotic optimization, enhancing both consumer health outcomes and product differentiation in the marketplace.

The third study investigated the impact of PUFA-rich feed supplementation on the biochemical

and compositional attributes of cheese during ripening. ANOVA analysis revealed consistent increases in crude fat content, with trial-dependent variations in protein, dry matter, and ash content, reflecting both feeding composition and environmental influences. Spectral analysis identified key wavelengths corresponding to water, protein, and fatty acid transformations. During ripening, unsaturated fatty acids dominated at early stages but decreased over 12 weeks due to reduction, while saturated fatty acids became more prominent. PUFA supplementation induced unique molecular signatures, enhancing both the nutritional profile and classification potential of the cheese. These findings illustrate how feed composition, ripening dynamics, and spectral markers collectively determine cheese quality, stability, and differentiation potential, offering a framework for designing dairy products with tailored fatty acid profiles for improved health benefits.

Collectively, these studies demonstrate the originality and broader impact of this research in advancing dairy science and industry practices. By integrating NIRS with chemometric modelling and complementary analytical techniques, this work provides a comprehensive approach for monitoring compositional, biochemical, and molecular changes in dairy products. The ability to rapidly identify and quantify critical parameters enables producers to ensure consistent quality, optimize nutritional content, and adapt products to specific consumer needs. Furthermore, this research illustrates the potential to use feeding strategies and processing conditions as tools to enhance the health profile of dairy products, particularly through modulation of PUFA content in milk and cheese.

Previous studies have often focused on isolated dairy matrices or single analytical techniques. This work advances the field by combining NIRS with multivariate analysis and e-nose techniques to achieve high-precision classification, predictive modelling, and biochemical tracking across multiple product types. It also provides clear evidence of how feeding strategies and ripening periods affect the molecular composition of dairy products, complementing and extending prior research on milk fatty acids, protein content, and flavor development.

The implications of this research are multifaceted. From a nutritional and health perspective, PUFA-enriched dairy products, as demonstrated, support cardiovascular health and improve overall dietary profiles, while the ability to monitor and optimize fatty acid content enables the production of functional dairy foods targeted toward specific health outcomes. Economically and for industry adoption, rapid, non-destructive NIRS analysis reduces reliance on time-consuming chemical assays, minimizes production losses, and facilitates large-scale quality control, thereby enhancing efficiency, product standardization, and market competitiveness. In terms of product innovation, the identification of spectral fingerprints associated with feeding and processing

strategies allows the design of tailored milk, fermented milk, and cheese products, expanding options for functional, fortified, or specialty dairy foods. Finally, from a sustainability standpoint, optimizing feed supplementation and tracking its effects on product quality can reduce waste, improve resource efficiency, and support environmentally sustainable dairy production.

Expanding calibration datasets to include diverse environmental, seasonal, and breed-related variations will improve the robustness of NIRS models. Advanced chemometric techniques, such as deep learning or hybrid models, could further enhance predictive accuracy. Integration with complementary tools such as E-nose, mass spectrometry, or metabolomics will allow more comprehensive profiling of dairy products, including flavor, nutritional, and health-relevant compounds. Additionally, longitudinal studies assessing consumer health outcomes from PUFA-enriched dairy consumption could provide further evidence of the practical benefits of these innovations.

By demonstrating the analytical power of NIRS across multiple dairy matrices and linking feeding strategies, processing conditions, and ripening dynamics to compositional and biochemical markers, this thesis advances the field of dairy science. It establishes a framework for rapid, reliable, and precise characterization of dairy products, enabling industry adoption, nutritional optimization, and innovative product development. This integrated approach contributes to improved food quality, health outcomes, and sustainable dairy production, highlighting NIRS as a transformative tool for the future of the dairy sector.

7. NEW SCIENTIFIC RESULTS

The scientific findings presented here are grounded in clearly defined dairy product origins and types, as well as carefully controlled instrumental setups. For the benchtop near infrared spectroscopy (NIRS) analysis the XDS Rapid Content Analyzer (XDS RCA) (Metrohm, Herisau, Switzerland) was utilized using a circular cuvette with 0.5 mm layer thickness for reconstituted and fermented milk samples and 1 cm for stored cheese samples, respectively. The handheld device used was the MicroNIR 1700 EC spectrometer (Viavi Solutions Inc., Chandler, AR, USA), which operates in diffuse reflectance mode with a circular glass cuvette optimized for NIRS, employing a 1 cm sample thickness for fresh cheese samples. The instrumental odour analysis of the fermented milk samples was performed with the Heracles 300 ultra-fast-GC analyser (Alpha MOS, Toulouse, France).

1. Combined statistical and chemometric analyses were used to characterize and predict the quality of reconstituted milk from different species. analysis of variance (ANOVA) and principal component analysis based linear discriminant analysis (PCA-LDA) models effectively distinguished cow, camel, and mare milk samples reconstituted from powders at specific concentrations (C1 = 5%, C2 = 10%, C3 = 12.5%) and temperatures (T1 = 25 °C, T2 = 40 °C, T3 = 65 °C) with significant differences in case of main quality parameters such as the viscosity, dry matter content, titratable acidity, conductivity, pH and the colour components L*, a*, b* ($p \leq 0.05$) and 100% classification accuracy in case of NIRS, respectively. Support vector regression (SVR) models demonstrated superior predictive performance ($R^2pr = 0.80–0.99$) compared to partial least squares regression (PLSR) for the main quality parameters and amino acid profile of milk.

2. NIRS and e-nose based principal component analysis–linear discriminant analysis (PCA-LDA) models were developed to distinguish fermented milk obtained from cows fed either a Total Mixed Ration (TMR) containing hydrogenated palm oil or TMR enriched with polyunsaturated fatty acids, fermented with *L. bulgaricus* S06, S04 or S09. The models, classifying samples according to feeding type and probiotic strain, achieved recognition accuracies of 97–99.5% and prediction accuracies of 97–98%. Milk fermented with *L. bulgaricus* S06 yielded 100% correct classification and exhibited distinct biochemical and volatile profiles independent of the feeding regime, highlighting the strain's metabolic activity in the overall fermentation signature.

3. Qualitative analysis of the key wavelengths of NIRS contributing to the classification of fermented milk from cows fed either a Total Mixed Ration (TMR) containing hydrogenated palm oil or TMR enriched with polyunsaturated fatty acids, fermented with *L. bulgaricus* S06, S04, or S09, revealed that the most significant features were concentrated in the 1600–1800 nm range.

Peaks at 1642, 1680, 1712, and 1726 nm, corresponding to C–H and C=O vibrational overtones, reflect bonds typical of saturated and unsaturated fatty acids, respectively. The consistent spectral patterns in this region across all strains indicate that fatty acid composition, particularly the double bonds of unsaturated fatty acids, serves as a robust, strain-independent marker for characterizing milk from different feeding regimes. Similarly, the 1300–1600 nm region, dominated by O–H overtone absorption, reflects water structure and its interactions with proteins and carbohydrates, driven by strain-specific metabolic activity.

4. The odour fingerprint of control and experimental fermented milk samples (fermented with *L. bulgaricus* S06*,* S04 or S09) obtained from cows fed with Total Mixed Ration (TMR) containing hydrogenated palm oil or TMR enriched with polyunsaturated fatty acids, respectively, revealed higher levels of 1-hexen-3-one, 1 hexen-3-ol, hexanal, and (Z)-4-heptenal in the experimental groups. These volatiles, products of unsaturated fatty acid oxidation, played a key role in differentiating strains. The e-nose showed strong sensitivity to these aroma compounds, effectively distinguishing samples based on fermentation and feed-induced aroma differences.

5. NIRS based principal component analysis–linear discriminant analysis (PCA-LDA) models for classifying Trappista cheeses produced from milk of cows fed either a Total Mixed Ration (TMR) containing hydrogenated palm oil or TMR enriched with polyunsaturated fatty acids, and aged for 4, 8, or 12 weeks under control storage, achieved 100% recognition and prediction accuracy. This highlights the model's effectiveness in detecting feed-induced molecular and age-dependent (ripening) changes in the respective cheeses. Specific spectral markers evolved: at 4 weeks, unsaturated fatty acids (1712, 1726 nm) and water (1450 nm) dominated; by 8 weeks, protein (1500 nm) and saturated fats (1771 nm) became more prominent; and at 12 weeks, saturated fats (1770 nm) prevailed, with reduced signals from unsaturated fats due to oxidation.

8. SUMMARY

The dairy industry has rapidly advanced with technology and growth. Consumers now seek safer, higher-quality food products and are willing to pay more than the normal price. Quality depends on factors like traceability, composition, and safety, shaped by processing and storage. This has increased the need for accurate testing of dairy products to ensure fairness and protect consumers.

This research combines findings from three comprehensive studies, collectively demonstrating the strong potential of near-infrared spectroscopy (NIRS), combined with chemometrics, as a powerful tool for characterizing dairy products, specifically reconstituted milk, fermented milk, and cheese.

In the first study, NIRS was applied to reconstituted cow, camel, and milk samples prepared at varying concentrations (5%, 10%, 12.5%) and temperatures (25 °C, 40 °C, 65 °C). Analysis of Variance (ANOVA) revealed that milk type was the most significant factor influencing compositional variation, surpassing both concentration and temperature. This was further supported by PCA-LDA models that achieved 100% classification accuracy. Spectral data, particularly in the 1300–1800 nm range, enabled the accurate prediction of key compositional parameters such as pH, fat content, viscosity, dry matter, conductivity, and amino acid levels. Among predictive methods, Support Vector Regression (SVR) outperformed Partial Least Squares Regression (PLSR), underscoring the superior capabilities of nonlinear modeling. These results demonstrate NIRS's value for rapid, non-destructive analysis and its potential for industrial quality control, nutritional formulation, and process monitoring.

The second study focused on fermented milk derived from cows subjected to different Total Mixed Ration (TMR) feeding regimens and fermented with various probiotic lactic acid bacteria (LAB) strains. Using both NIRS and E-nose technologies, the study identified robust spectral and volatile markers that differentiated samples based on feed type and microbial strain. NIRS effectively captured broad compositional differences, while the e-nose detected volatiles such as hexanal and 1-hexen-3-one, associated with the oxidation of polyunsaturated fatty acids. Wavelengths between 1600–1800 nm proved especially useful in identifying mono- and polyunsaturated fatty acids like oleic, linoleic, and linolenic acids. Meanwhile, the 1300–1600 nm range revealed strain-specific differences linked to water structure and interactions with proteins and carbohydrates. Strain P emerged as a standout, consistently producing distinct and reproducible spectral and volatile profiles across all feeding trials, independent of diet. These findings illustrate the synergy between NIRS and e-nose in assessing nutritional quality, probiotic functionality, and product differentiation in fermented dairy.

The third study examined the impact of PUFA-enriched feeds on Trappista cheese during ripening (4, 8, and 12 weeks). NIRS analysis revealed clear changes in spectral profiles corresponding to biochemical transformations. Early ripening was characterized by unsaturated fatty acid markers (1712 and 1726 nm), while later stages showed an increase in saturated fats (around 1770–1771 nm) and protein-associated bands (1500 nm), reflecting oxidation and maturation processes. Additional wavelengths in the 1380–1550 nm range indicated changes in water structure and macromolecular interactions during ripening. LDA classification models achieved 100% accuracy in distinguishing both feeding type and ripening stage. Experimental cheese groups consistently exhibited distinct molecular signatures tied to PUFA supplementation, which not only influenced nutritional profiles but also enhanced the ability to classify and standardize products based on feeding and processing history.

Together, these studies underscore NIRS's versatility and reliability in the dairy industry, highlighting its utility in identifying spectral fingerprints and quantifying key compositional parameters under varied conditions. Its rapid, non-invasive nature makes it ideal for quality assurance, research and development, and industrial standardization. Complementary technologies like the e-nose enhance analytical depth, particularly in capturing aroma profiles and flavor differentiation driven by feed and microbial interactions.

9. LIST OF PUBLICATIONS

- **List of publications in the field of studies:**

Majadi, M., Ali, O., Szabó, A., Tóth, T., Bazar, G., & Kovacs, Z. (2025). Uncovering key factors in differentiating fermented milk by feeding type and probiotic potential with E-nose and NIRS techniques. Food Control, 176, 111376. https://doi.org/10.1016/j.foodcont.2025.111376

Majadi, M., Barkó, A., Varga-Tóth, A., Suleimenova Maukenovna, Z., Dossimova, Z. B., Senkebayeva, D., Lukacs, M., Kaszab, T., Mednyánszky, Z., & Kovacs, Z. (2024). Quality assessment of reconstituted cow, camel and mare milk powders by near-infrared spectroscopy and chemometrics. Molecules, 29. https://doi.org/10.3390/molecules29173989

- **List of publications in the field of NIRS:**

Kovacs, Z., Lukacs, M., Bazar, G., Gillay, Z., Bosquez, Aguinaga, JP., **Majadi, M.**, Vitalis, F. (2025). Recent results of near infrared spectroscopy on the way "from farm to fork" or even further. In K. Bec & C. Huck (Eds.), Proceedings of the 21st International Conference on Near Infrared Spectroscopy. ICNIR 2023. Springer. https://doi.org/10.1007/978-3-031-84794-3_10

Aouadi, B., Laryea, D., Aguinaga Bósquez, J. P., **Majadi, M.**, Kertész, I., Bodor, Z., Zaukuu, J.-L. Z., & Kovacs, Z. (2024). Aquaphotomics based screening of tomato powder extracts reveals susceptibility to bulking and coloring agents. Food Control, 157, 110163. https://doi.org/10.1016/j.foodcont.2023.110163

Bodor, Z., **Majadi, M.**, Benedek, C., Zaukuu, J.-L. Z., Veresné Bálint, M., Csajbókné Csobod, É., & Kovacs, Z. (2023). Detection of low-level adulteration of Hungarian honey using near infrared spectroscopy. Chemosensors, 11(2), 89. https://doi.org/10.3390/chemosensors110200896

Aguinaga Bósquez, J. P., Oguz, E., Cebeci, A., **Majadi, M.**, Kiskó, G., Gillay, Z., & Kovacs, Z. (2022). Characterization and viability prediction of commercial probiotic supplements under temperature and concentration conditioning factors by NIR spectroscopy. Fermentation, 8(2), 66. https://doi.org/10.3390/fermentation8020066

References:

Aernouts, B., Polshin, E., Lammertyn, J., & Saeys, W. (2011). Visible and near-infrared spectroscopic analysis of raw milk for cow health monitoring: Reflectance or transmittance? *Journal of Dairy Science*, *94*(11), 5315–5329. https://doi.org/10.3168/jds.2011-4354

Agelet, L. E., & Hurburgh, C. R. (2010). A tutorial on near infrared spectroscopy and its calibration. *Critical Reviews in Analytical Chemistry*, *40*(4), 246–260. https://doi.org/10.1080/10408347.2010.515468

Alander, J. T., Bochko, V., Martinkauppi, B., Saranwong, S., & Mantere, T. (2013). A Review of Optical Nondestructive Visual and Near-Infrared Methods for Food Quality and Safety. *International Journal of Spectroscopy*, 1–36. https://doi.org/10.1155/2013/341402

Alvarez-Hess, P. S., Thomson, A. L., Williams, S. R. O., Logan, A., Taylor, C., Singh, T., Roque, B. M., O Neachtain, A. S., Kinley, R. D., & Jacobs, J. L. (2024). The influence of feeding canola oil steeped Asparagopsis armata on resulting fatty acid profile and dairy processing properties of cow's milk. *Animal Feed Science and Technology*, *310*, 115924. https://doi.org/10.1016/j.anifeedsci.2024.115924

AlYammahi, J., Rambabu, K., Thanigaivelan, A., Hasan, S. W., Taher, H., Show, P. L., & Banat, F. (2023). Production and characterization of camel milk powder enriched with date extract. *Lwt*, *179*(March), 114636. https://doi.org/10.1016/j.lwt.2023.114636

Andueza, D., Agabriel, C., Constant, I., Lucas, A., & Martin, B. (2013). Using visible or near infrared spectroscopy (NIRS) on cheese to authenticate cow feeding regimes. *Food Chemistry*, *141*(1), 209–214. https://doi.org/10.1016/j.foodchem.2013.02.086

Aouadi, B., Zaukuu, J. L. Z., Vitális, F., Bodor, Z., Fehér, O., Gillay, Z., Bazar, G., & Kovacs, Z. (2020). Historical evolution and food control achievements of near infrared spectroscopy, electronic nose, and electronic tongue—critical overview. *Sensors (Switzerland)*, *20*(19), 1–42. https://doi.org/10.3390/s20195479

Arango, O., Trujillo, A. J., & Castillo, M. (2020). Inline control of yoghurt fermentation process using a near infrared light backscatter sensor. *Journal of Food Engineering*, *277*(December 2019), 1–6. https://doi.org/10.1016/j.jfoodeng.2019.109885

Atasever, M., Mazlum, H. (2024). Biochemical Processes During Cheese Ripening. *Vet Sci Pract*,

19(3), 174–182. https://doi.org/10.17094/vetsci.1609184

Augustin, M. A., Clarke, P. T., & Craven, H. (2003). Characteristics of Milk Powders, in Cabellero, B. (eds), *Encyclopedia of Food Sciences and Nutrition*, 2nd edition. Elsevier: Amsterdam, The Netherlands, pp. 4703–4711. https://doi.org/10.1016/b0-12-227055-x/00956-1

Azad, T., & Ahmed, S. (2016). Common milk adulteration and their detection techniques. *International Journal of Food Contamination*, *3*(1). https://doi.org/10.1186/s40550-016-0045-3

Baeten, V., Rogez, H., Fernández Pierna, J. A., Vermeulen, P., & Dardenne, P. (2015). Vibrational spectroscopy methods for the rapid control of agro-food products. *Handbook of Food Analysis*, *2*, 591–614.

Balabin, R. M., & Lomakina, E. I. (2011). Support vector machine regression (SVR/LS-SVM) - An alternative to neural networks (ANN) for analytical chemistry? Comparison of nonlinear methods on near infrared (NIR) spectroscopy data. *Analyst*, *136*(8), 1703–1712. https://doi.org/10.1039/c0an00387e

Balabin, R. M., & Smirnov, S. V. (2011). Melamine detection by mid- and near-infrared (MIR/NIR) spectroscopy: A quick and sensitive method for dairy products analysis including liquid milk, infant formula, and milk powder. *Talanta*, *85*(1), 562–568. https://doi.org/10.1016/j.talanta.2011.04.026

Balivo, A., Sacchi, R., Di Francia, A., Masucci, F., & Genovese, A. (2024). E-nose analysis of milk to detect the inclusion of hydroponic barley forage in the buffalo diet. *Journal of Food Composition and Analysis*, *131*(January), 106230. https://doi.org/10.1016/j.jfca.2024.106230

Barkema, H. W., von Keyserlingk, M. A. G., Kastelic, J. P., Lam, T. J. G. M., Luby, C., Roy, J. P., LeBlanc, S. J., Keefe, G. P., & Kelton, D. F. (2015). Invited review: Changes in the dairy industry affecting dairy cattle health and welfare. *Journal of Dairy Science*, *98*(11), 7426–7445. https://doi.org/10.3168/jds.2015-9377

Barnes, R. J, Dhanoa, M. S, & Lister, Susan J. (1989). Standard Normal Variate Transformation and De-Trending of Near-Infrared Diffuse Reflectance Spectra. *Applied Spectroscopy*, *43*(5), 772–777. https://doi.org/10.1366/0003702894202201

Bintsis, T., & Papademas, P. (2022). The Evolution of Fermented Milks, from Artisanal to Industrial Products: A Critical Review. *Fermentation*, *8*(12), 1–24. https://doi.org/10.3390/fermentation8120679

Bista, A., McCarthy, N., O'Donnell, C. P., & O'Shea, N. (2021). Key parameters and strategies to control milk concentrate viscosity in milk powder manufacture. *International Dairy Journal*, 121, p. 105120. https://doi.org/10.1016/j.idairyj.2021.105120

Biswas, A., & Chaudhari, S. R. (2024). Exploring the role of NIR spectroscopy in quantifying and verifying honey authenticity : A review. *Food Chemistry*, *445*(November 2023), 138712. https://doi.org/10.1016/j.foodchem.2024.138712

Bittante, G., Patel, N., Cecchinato, A., & Berzaghi, P. (2022). Invited review: A comprehensive review of visible and near-infrared spectroscopy for predicting the chemical composition of cheese. *Journal of Dairy Science*, *105*(3), 1817–1836. https://doi.org/10.3168/jds.2021-20640

Bodkowski, R., Wierzbicki, H., Mucha, A., Cholewińska, P., Wojnarowski, K., & Sokoła, B. P. (2024). Composition and fatty acid profile of milk from cows fed diets supplemented with raw and n - 3 PUFA - enriched fish oil. *Scientific Reports*, 1–12. https://doi.org/10.1038/s41598-024-61864-z

Brereton, R. G. (2022). Graphical introduction to principal components analysis. *Journal of Chemometrics*, *36*(6), 1–8. https://doi.org/10.1002/cem.3404

Butler, G., Stergiadis, S., Chatzidimitriou, E., Franceschin, E., Davis, H. R., Leifert, C., & Steinshamn, H. (2019). Differing responses in milk composition from introducing rapeseed and naked oats to conventional and organic dairy diets. *Scientific Reports*, *9*(1), 1–12. https://doi.org/10.1038/s41598-019-44567-8

Buttriss, J. (1997). Nutritional properties of fermented milk products. *International Journal of Dairy Technology*, *50*(1), 21–27. https://doi.org/10.1111/j.1471-0307.1997.tb01731.x

Capuano, E., Boerrigter-Eenling, R., Koot, A., & van Ruth, S. M. (2015). Targeted and Untargeted Detection of Skim Milk Powder Adulteration by Near-Infrared Spectroscopy. *Food Analytical Methods*, *8*(8), 2125–2134. https://doi.org/10.1007/s12161-015-0100-3

Cen, H., & He, Y. (2007). Theory and application of near infrared reflectance spectroscopy in determination of food quality. *Trends in Food Science and Technology*, *18*(2), 72–83. https://doi.org/10.1016/j.tifs.2006.09.003

Chaudhary, V., Kajla, P., Dewan, A., Pandiselvam, R., Socol, C. T., & Maerescu, C. M. (2022). Spectroscopic techniques for authentication of animal origin foods. *Frontiers in Nutrition*, *9*(September). https://doi.org/10.3389/fnut.2022.979205

Chen, H., Tan, C., Lin, Z., & Wu, T. (2017). Detection of melamine adulteration in milk by near-infrared spectroscopy and one-class partial least squares. *Spectrochimica Acta - Part A: Molecular and Biomolecular Spectroscopy*, *173*, 832–836. https://doi.org/10.1016/j.saa.2016.10.051

Chen, H., Tan, C., Lin, Z., & Wu, T. (2018). Classification and quantitation of milk powder by near-infrared spectroscopy and mutual information-based variable selection and partial least squares. *Spectrochimica Acta - Part A: Molecular and Biomolecular Spectroscopy*, *189*, 183–189. https://doi.org/10.1016/j.saa.2017.08.034

Cheng, J.-H., & Sun, D.-W. (2017). Partial Least Squares Regression (PLSR) Applied to NIR and HSI Spectral Data Modeling to Predict Chemical Properties of Fish Muscle. *Food Engineering Reviews*, *9*(1), 36–49. https://doi.org/10.1007/s12393-016-9147-1

Chi, X., Yang, Q., Su, Y., Zhang, J., Sun, B., & Ai, N. (2024). Improvement of rheological and sensory properties of Lactobacillus helveticus fermented milk by prebiotics. *Food Chemistry: X*, *23*(June), 101679. https://doi.org/10.1016/j.fochx.2024.101679

Christie, W. W. (2003). Lipid analysis : isolation, separation, identification, and structural analysis of lipids (3rd ed). Oily Press.

Coleman, B., Van Poucke, C., De Witte, B., Casciaro, V., Moerdijk-Poortvliet, T., Muylaert, K., & Robbens, J. (2023). The effect of drying, cell disruption and storage on the sensory properties of Nannochloropsis sp. *Algal Research*, *71*(December 2022), 103092. https://doi.org/10.1016/j.algal.2023.103092

Coppa, M., Chassaing, C., Ferlay, A., Agabriel, C., Laurent, C., Borreani, G., Barcarolo, R., Baars, T., Kusche, D., Harstad, O. M., Verbič, J., Golecký, J., Delavaud, C., Chilliard, Y., & Martin, B. (2015). Potential of milk fatty acid composition to predict diet composition and authenticate feeding systems and altitude origin of European bulk milk. *Journal of Dairy Science*, *98*(3), 1539–1551. https://doi.org/10.3168/jds.2014-8794

Coppa, M., Ferlay, A., Leroux, C., Jestin, M., Chilliard, Y., Martin, B., & Andueza, D. (2010). Prediction of milk fatty acid composition by near infrared reflectance spectroscopy. *International Dairy Journal*, *20*(3), 182–189. https://doi.org/10.1016/j.idairyj.2009.11.003

Coppa, M., Martin, B., Agabriel, C., Chassaing, C., Sibra, C., Constant, I., Graulet, B., & Andueza, D. (2012). Authentication of cow feeding and geographic origin on milk using visible and near-infrared spectroscopy. *Journal of Dairy Science*, *95*(10), 5544–5551. https://doi.org/10.3168/jds.2011-5272

Cowe, Ian A, & McNicol, James W. (1985). The Use of Principal Components in the Analysis of Near-Infrared Spectra. *Applied Spectroscopy*, *39*(2), 257–266. https://doi.org/10.1366/0003702854248944

Czaja, T. P., Vickovic, D., Pedersen, S. J., Hougaard, A. B., & Ahrné, L. (2023). Spectroscopic characterisation of acidified milk powders. *International Dairy Journal*, *142*. https://doi.org/10.1016/j.idairyj.2023.105664

da Silva Medeiros, M. L., Moreira de Carvalho, L., Madruga, M. S., Rodríguez-Pulido, F. J., Heredia, F. J., & Fernandes Barbin, D. (2024). Comparison of hyperspectral imaging and spectrometers for prediction of cheeses composition. *Food Research International*, *183*(January), 114242. https://doi.org/10.1016/j.foodres.2024.114242

Darvishi, P., Mirzaee-Ghaleh, E., Ramedani, Z., Karami, H., & Wilson, A. D. (2025). A novel approach for identifying melamine adulteration in powdered milk with E-nose and AI. *Food and Chemical Toxicology*, *202*(March), 115521. https://doi.org/10.1016/j.fct.2025.115521

de Almeida, V. E., de Sousa Fernandes, D. D., Diniz, P. H. G. D., de Araújo Gomes, A., Véras, G., Galvão, R. K. H., & Araujo, M. C. U. (2021). Scores selection via Fisher's discriminant power in PCA-LDA to improve the classification of food data. *Food Chemistry*, *363*. https://doi.org/10.1016/j.foodchem.2021.130296

Demarigny, Y., Legrand, E., Sanchez, J., Hallier, A., Laurent, N., Slimani, S., Livache, T., & Picque, D. (2021). Utilisation of a Portable Electronic Nose, NeOse Pro, to Follow the Microbial Fermentation of a Yoghurt. *Food and Nutrition Sciences*, *12*(01), 90–105. https://doi.org/10.4236/fns.2021.121008

De Knegt, R. J., & Van Den Brink, H. (1998). Improvement of the drying oven method for the determination of the moisture content of milk powder. *International Dairy Journal*, *8*(8), 733–738. https://doi.org/10.1016/S0958-6946(97)00110-6

de la Roza-Delgado, B., Garrido-Varo, A., Soldado, A., González Arrojo, A., Cuevas Valdés, M., Maroto, F., & Pérez-Marín, D. (2017). Matching portable NIRS instruments for in situ monitoring indicators of milk composition. *Food Control*, *76*, 74–81.

https://doi.org/10.1016/j.foodcont.2017.01.004

De Marchi, M., Penasa, M., Zidi, A., & Manuelian, C. L. (2018). Invited review: Use of infrared technologies for the assessment of dairy products—Applications and perspectives. *Journal of Dairy Science*, *101*(12), 10589–10604. https://doi.org/10.3168/jds.2018-15202

Dhanoa, Mewa Singh, Lister, Susan Jane, Sanderson, Ruth, Barnes, Ralph James, Lopez, Secundino, & France, James. (2024). A critique of multiplicative scatter correction pre-treatment of NIR spectra. *NIR News*, *35*(7–8), 7–11. https://doi.org/10.1177/09603360241313184

Di Rosa, A. R., Leone, F., Cheli, F., & Chiofalo, V. (2017). Fusion of electronic nose, electronic tongue and computer vision for animal source food authentication and quality assessment – A review. *Journal of Food Engineering*, *210*, 62–75. https://doi.org/10.1016/j.jfoodeng.2017.04.024

Dias, C. M., Nunes, H., Borba, A., & Wetzel, D. (2024). Near-Infrared Spectroscopy in Animal Nutrition : Historical Insights , Technical Principles , and Practical Applications. *Analytica*, 5(4), 481–498. https://doi.org/10.3390/analytica5040033

Diaz-Olivares, J. A., Adriaens, I., Stevens, E., Saeys, W., & Aernouts, B. (2020). Online milk composition analysis with an on-farm near-infrared sensor. *Computers and Electronics in Agriculture*, *178*(May), 105734. https://doi.org/10.1016/j.compag.2020.105734

Downey, G., Sheehan, E., Delahunty, C., O'Callaghan, D., Guinee, T., & Howard, V. (2005). Prediction of maturity and sensory attributes of Cheddar cheese using near-infrared spectroscopy. *International Dairy Journal*, *15*(6–9), 701–709. https://doi.org/10.1016/j.idairyj.2004.06.013

Ding, H., Li, B., Boiarkina, I., Wilson, D. I., Yu, W., & Young, B. R. (2020). Effects of morphology on the bulk density of instant whole milk powder. *Foods*, *9*(8), 1–19. https://doi.org/10.3390/foods9081024

Duncan, S. E., & Webster, J. B. (2010). Oxidation and protection of milk and dairy products, in Decker, E.A., Elias, R.J., McClements, D.J. (eds), *Oxidation in Foods and Beverages and Antioxidant Applications: Management in Different Industry Sectors*. Woodhead Publishing Limited: Cambridge, UK, pp. 121–155. https://doi.org/10.1533/9780857090331.1.121

Ehlayel, M. S., Hazeima, K. A., Al-Mesaifri, F., & Bener, A. (2011). Camel milk: An alternative for cow's milk allergy in children. *Allergy and Asthma Proceedings*, *32*(3), 255–258.

https://doi.org/10.2500/aap.2011.32.3429

Ejeahalaka, K. K., & On, S. L. W. (2020). Characterisation of the quality alterations in model fat-filled milk powders under inclement conditions and the prediction of the storage time using near infrared spectroscopy. *Food Chemistry*, *323*(April), 126752. https://doi.org/10.1016/j.foodchem.2020.126752

Ellis, D. I., Muhamadali, H., Haughey, S. A., Elliott, C. T., & Goodacre, R. (2015). Point-and-shoot: Rapid quantitative detection methods for on-site food fraud analysis-moving out of the laboratory and into the food supply chain. *Analytical Methods*, *7*(22), 9401–9414. https://doi.org/10.1039/c5ay02048d

Eriksson, Å., Persson Waller, K., Svennersten-Sjaunja, K., Haugen, J.-E., Lundby, F., & Lind, O. (2005). Detection of mastitic milk using a gas-sensor array system (electronic nose). *International Dairy Journal*, *15*(12), 1193–1201. https://doi.org/https://doi.org/10.1016/j.idairyj.2004.12.012

Escribano, S., Biasi, W. V., Lerud, R., Slaughter, D. C., & Mitcham, E. J. (2017). Non-destructive prediction of soluble solids and dry matter content using NIR spectroscopy and its relationship with sensory quality in sweet cherries. *Postharvest Biology and Technology*, *128*, 112–120. https://doi.org/10.1016/j.postharvbio.2017.01.016

Esen, Mustafa Kadir, & Güzeler, N. (2023). The effects of the use of whey protein as a fat replacer on the composition, proteolysis, textural, meltability, microstructural, and sensory properties of reduced-fat Boru- type Künefe cheese during storage. *International Dairy Journal*, *137*. https://doi.org/10.1016/j.idairyj.2022.105519

Ezenarro, J., & Schorn-García, D. (2025). How Are Chemometric Models Validated? A Systematic Review of Linear Regression Models for NIRS Data in Food Analysis. *Journal of Chemometrics*, *39*(6). https://doi.org/10.1002/cem.70036

Fabro, M. A., Milanesio, H. V., Robert, L. M., Speranza, J. L., Murphy, M., Rodríguez, G., & Castañeda, R. (2006). Technical Note: Determination of acidity in whole raw milk: Comparison of results obtained by two different analytical methods. *Journal of Dairy Science*, *89*(3), 859–861. https://doi.org/10.3168/jds.S0022-0302(06)72149-X

Falih, M. A., Altemimi, A. B., Hamed, Q., Awlqadr, H., Gamal, T., Amjadi, S., & Hesarinejad, A. (2024). Heliyon Enhancing safety and quality in the global cheese industry : A review of innovative preservation techniques. *Heliyon*, *10*(23), e40459. https://doi.org/10.1016/j.heliyon.2024.e40459

Fantuz, F., Salimei, E., & Papademas, P. (2016). Macro-and Micronutrients in Non-cow Milk and Products and Their Impact on Human Health, in Tsakalidou, E., Papadimitriou, K. (eds), *Non-Bovine Milk and Milk Products*. Elsevier: Amsterdam, The Netherlands, pp. 209–261

Ferreira, M. M., Marins-Gonçalves, L., & De Souza, D. (2024). An integrative review of analytical techniques used in food authentication: A detailed description for milk and dairy products. *Food Chemistry*, *457*(March), 140206. https://doi.org/10.1016/j.foodchem.2024.140206

Fodor, M., Matkovits, A., Benes, E. L., & Jókai, Z. (2024). The Role of Near-Infrared Spectroscopy in Food Quality Assurance: A Review of the Past Two Decades. *Foods*, *13*(21). https://doi.org/10.3390/foods13213501

Folch, J., Lees, M., & Sloane Stanley, G. H. (1957). A simple method for the isolation and purification of total lipides from animal tissues. *The Journal of Biological Chemistry*, *226*(1), 497–509. https://doi.org/10.1016/s0021-9258(18)64849-5

Forchetti, D. A. P., & Poppi, R. J. (2017). Use of NIR hyperspectral imaging and multivariate curve resolution (MCR) for detection and quantification of adulterants in milk powder. *Lwt*, *76*, 337–343. https://doi.org/10.1016/j.lwt.2016.06.046

Foschi, M., Biancolillo, A., Reale, S., Poles, F., & D'Archivio, A. A. (2025). Classification of "Ricotta" whey cheese from different milk and Designation of Origin-protected samples through infrared spectroscopy and chemometric analysis. *Journal of Food Composition and Analysis*, *138*(September 2024), 107019. https://doi.org/10.1016/j.jfca.2024.107019

Fox, P. F., & McSweeney, P. L. H. (2017). Chapter 1 - Cheese*:* An Overview, in P. L. H. McSweeney, P. F. Fox, P. D. Cotter, & D. W. B. T.-C. (eds), Cheese (4th ed). Academic Press, pp. 5–21

Gebreyowhans, S., Lu, J., Zhang, S., Pang, X., & Lv, J. (2019). Dietary enrichment of milk and dairy products with n-3 fatty acids: A review. *International Dairy Journal*, *97*, 158–166. https://doi.org/10.1016/j.idairyj.2019.05.011

Glasser, F., Ferlay, A., & Chilliard, Y. (2008). Oilseed lipid supplements and fatty acid composition of cow milk: A meta-analysis. *Journal of Dairy Science*, *91*(12), 4687–4703. https://doi.org/10.3168/jds.2008-0987

González-Martín, M. I., Vivar-Quintana, A. M., Revilla, I., & Salvador-Esteban, J. (2020). The determination of fatty acids in cheeses of variable composition (cow, ewe's, and goat) by means of near infrared spectroscopy. *Microchemical Journal*, *156*(February), 104854.

https://doi.org/10.1016/j.microc.2020.104854

Grabska, J., Beć, K. B., Ishigaki, M., Huck, C. W., & Ozaki, Y. (2018). NIR Spectra Simulations by Anharmonic DFT-Saturated and Unsaturated Long-Chain Fatty Acids. *Journal of Physical Chemistry B*, *122*(27), 6931–6944. https://doi.org/10.1021/acs.jpcb.8b04862

Grabska, J., Huck, C. W., & Bec, K. B. (2021). Principles and Applications of Miniaturized Near-Infrared (NIR) Spectrometers. *Chemistry*, 27(5), 1514–1532. https://doi.org/10.1002/chem.202002838

Davies, AMC., Grant, A. (1987). Review: Near infra-red analysis of food. *International Journal of Food Science and Technology*, 22 (3), 191–207. https://doi.org/10.1111/j.1365-2621.1987.tb00479.x

Gunun, N., Kaewpila, C., Khota, W., Kimprasit, T., Cherdthong, A., & Gunun, P. (2024). The effect of supplementation with rubber seed kernel pellet on in vitro rumen fermentation characteristics and fatty acid profiles in swamp buffalo. *BMC Veterinary Research*, *20*(1), 1–8. https://doi.org/10.1186/s12917-024-04017-8

Gupta, M. K. (2017). Chapter 2 - Basic Oil Chemistry, in Gupta, M. K. (ed), guide to vegetable oil processing (2nd ed). AOCS Press, pp. 7-25 . https://doi.org/https://doi.org/10.1016/B978-1-63067-050-4.00002-7

Haider, A., Iqbal, S. Z., Bhatti, I. A., Alim, M. B., Waseem, M., Iqbal, M., & Mousavi Khaneghah, A. (2024). Food authentication, current issues, analytical techniques, and future challenges: A comprehensive review. *Comprehensive Reviews in Food Science and Food Safety*, *23*(3). https://doi.org/10.1111/1541-4337.13360

Hair, J. F., Black, W. C., Babin, B. J., & Anderson, R. E. (2013). *Multivariate Data Analysis*. Pearson Education Limited. https://books.google.hu/books?id=VvXZnQEACAAJ

Hammam, A. R. A., & Ahmed, M. S. I. (2019). Technological aspects , health benefits , and sensory properties of probiotic cheese. *SN Applied Sciences*, *1*(9), 1–9. https://doi.org/10.1007/s42452-019-1154-4

He, Y., Chen, L., Zheng, L., Cheng, F., Deng, Z. Y., Luo, T., & Li, J. (2022). A comparative study of volatile compounds in breast milk and infant formula from different brands, countries of origin, and stages. *European Food Research and Technology*, *248*(11), 2679–2694. https://doi.org/10.1007/s00217-022-04077-w

Hebling e Tavares, J. P., da Silva Medeiros, M. L., & Barbin, D. F. (2022). Near-infrared

techniques for fraud detection in dairy products: A review. *Journal of Food Science*, *87*(5), 1943–1960. https://doi.org/10.1111/1750-3841.16143

Hernández-Jiménez, M., Revilla, I., Hernández-Ramos, P., & Vivar-Quintana, A. M. (2024). Prediction of the Fatty Acid Profiles of Iberian Pig Products by Near Infrared Spectroscopy: A Comparison Between Multiple Regression Tools and Artificial Neural Networks. *Food and Bioprocess Technology*, *0123456789*. https://doi.org/10.1007/s11947-024-03486-x

Hew, P. S., Jinap, S., Jambari, N. N., Murugesu, S., Sanny, M., Khatib, A., & Sukor, R. (2024). Quality and safety of food product – Current assessment, issues, and metabolomics as a way forward. *Food Chemistry Advances*, *4*(June 2023), 100632. https://doi.org/10.1016/j.focha.2024.100632

Hoppe, C., Andersen, G. S., Jacobsen, S., Mølgaard, C., Friis, H., Sangild, P. T., & Michaelsen, K. F. (2008). The use of whey or skimmed milk powder in fortified blended foods for vulnerable groups. *Journal of Nutrition*, 138 (1). https://doi.org/10.1093/jn/138.1.145s

Hourant, P., Baeten, V., Morales, M. T., Meurens, M., & Aparicio, R. (2000). Oil and Fat Classification by Selected Bands of Near-Infrared Spectroscopy. *Applied Spectroscopy*, *54*(8), 1168–1174. https://opg.optica.org/as/abstract.cfm?URI=as-54-8-1168

Jollife, I. T., & Cadima, J. (2016). Principal component analysis: A review and recent developments. *Philosophical Transactions of the Royal Society A: Mathematical, Physical and Engineering Sciences*, *374*(2065). https://doi.org/10.1098/rsta.2015.0202

Kalyankar, S. D., Deshmukh, M. A., Chopde, S. S., Khedkar, C. D., Lule, V. K., & Deosarkar, S. S. (2015). Milk Powder, in Caballero, B., Finglas, P and Toldra, F.(eds), *Encyclopedia of Food and Health (1st ed)*. Elsevier Ltd, pp. 724–728. https://doi.org/10.1016/B978-0-12-384947-2.00465-7

Kamal, M., & Karoui, R. (2015). Analytical methods coupled with chemometric tools for determining the authenticity and detecting the adulteration of dairy products: A review. *Trends in Food Science and Technology*, *46*(1), 27–48. https://doi.org/10.1016/j.tifs.2015.07.007

Kapaj, A., & Deci, E. (2017). World Milk Production and Its Consumption and socio economic factors effecting its consumption, in Watson, RR., Collier, R J., Preedy, V R. (eds), *Dairy in Human Health and Disease across the Lifespan*. Academic Press, pp. 107-115. https://doi.org/10.1016/B978-0-12-809868-4.00007-8

Kasemsumran, S., Thanapase, W., & Kiatsoonthon, A. (2007). Feasibility of near-infrared spectroscopy to detect and to quantify adulterants in cow milk. *Analytical Sciences*, *23*(7), 907–910. https://doi.org/10.2116/analsci.23.907

Kholif, A. E., & Olafadehan, O. A. (2022). Dietary strategies to enrich milk with healthy fatty acids - A review. *Annals of Animal Science*, *22*(2), 523–536. https://doi.org/10.2478/aoas-2021-0058

Kiteto, M. K., & Mecha, C. A. (2024). Insight into the Bouguer-Beer-Lambert Law : A review. *Sustainable Chemical Engineering*, *5*(2), 567–587. https://doi.org/10.37256/fce.5220245325

Kokić, B., Rakita, S., & Vujetić, J. (2024). Impact of Using Oilseed Industry Byproducts Rich in Linoleic and Alpha-Linolenic Acid in Ruminant Nutrition on Milk Production and Milk Fatty Acid Profile. *Animals*, *14*(4), 1–19. https://doi.org/10.3390/ani14040539

Kuzmenko, A. V, Tverjanovich, A. S., Ilyushin, M. A., & Tveryanovich, Y. S. (2019). The effect of the concentration of high-absorbing inclusions on the laser initiation threshold of energetic materials: model and experiment. *Journal of Energetic Materials*, *37*(4), 420–432. https://doi.org/10.1080/07370652.2019.1630028

Lasalvia, M., Capozzi, V., & Perna, G. (2022). A Comparison of PCA-LDA and PLS-DA Techniques for Classification of Vibrational Spectra. *Applied Sciences (Switzerland)*, *12*(11). https://doi.org/10.3390/app12115345

Lerch, S., Ferlay, A., Graulet, B., Cirié, C., Verdier-Metz, I., Montel, M. C., Chilliard, Y., & Martin, B. (2015). Extruded linseeds, vitamin E and plant extracts in corn silage-based diets of dairy cows: Effects on sensory properties of raw milk and uncooked pressed cheese. *International Dairy Journal*, *51*, 65–74. https://doi.org/10.1016/j.idairyj.2015.07.006

Lerch, S., Ferlay, A., Shingfield, K. J., Martin, B., Pomiès, D., & Chilliard, Y. (2012). Rapeseed or linseed supplements in grass-based diets: Effects on milk fatty acid composition of Holstein cows over two consecutive lactations. *Journal of Dairy Science*, *95*(9), 5221–5241. https://doi.org/10.3168/jds.2012-5337

Li, H., Yang, X., Tang, D., Xi, B., Li, W., Chen, Z., Bao, Y., Dingkao, R., Gao, Y., Wang, P., & Wang, H. (2024). Exploring the link between microbial community structure and flavour compounds of traditional fermented yak milk in Gannan region. *Food Chemistry*, *435*(September 2023), 137553. https://doi.org/10.1016/j.foodchem.2023.137553

Li, L., Shao, X., Feng, Z., Ni, W., Jiang, H., Gong, X., & Xiao, G. (2024). Effects of Dendrobium

officinale on physicochemical and flavor properties of yogurt during different fermentation time. *Food Bioscience*, *57*(October 2023), 103579. https://doi.org/10.1016/j.fbio.2024.103579

Li, B., Morris, J., & Martin, E. B. (2002). Model selection for partial least squares regression. *Chemometrics and Intelligent Laboratory Systems*, *64*(1), 79–89. https://doi.org/https://doi.org/10.1016/S0169-7439(02)00051-5

Liu, S., Lei, T., Li, G., Liu, S., Chu, X., Hao, D., Xiao, G., Khan, A. A., Haq, T. U., Sameeh, M. Y., Aziz, T., Tashkandi, M., & He, G. (2023). Rapid detection of micronutrient components in infant formula milk powder using near-infrared spectroscopy. *Frontiers in Nutrition*, *10*(September), 1–12. https://doi.org/10.3389/fnut.2023.1273374

Liu, Z.-P. (2013). *Linear Discriminant Analysis BT - Encyclopedia of Systems Biology* (W. Dubitzky, O. Wolkenhauer, K.-H. Cho, & H. Yokota (eds.); pp. 1132–1133). Springer New York. https://doi.org/10.1007/978-1-4419-9863-7_395

Lohumi, S., Lee, S., Lee, H., & Cho, B. K. (2015). A review of vibrational spectroscopic techniques for the detection of food authenticity and adulteration. *Trends in Food Science and Technology*, *46*(1), 85–98. https://doi.org/10.1016/j.tifs.2015.08.003

Loudiyi, M., Temiz, H. T., Sahar, A., Haseeb Ahmad, M., Boukria, O., Hassoun, A., & Aït-Kaddour, A. (2022). Spectroscopic techniques for monitoring changes in the quality of milk and other dairy products during processing and storage. *Critical Reviews in Food Science and Nutrition*, *62*(11), 3063–3087. https://doi.org/10.1080/10408398.2020.1862754

Lu, C., Xiang, B., Hao, G., Xu, J., Wang, Z., & Chen, C. (2009). Rapid detection of melamine in milk powder by near infrared spectroscopy. *Journal of Near Infrared Spectroscopy*, *17*(2), 59–67. https://doi.org/10.1255/jnirs.829

Mafra, I., Honrado, M., & Amaral, J. S. (2022). Animal Species Authentication in Dairy Products. *Foods*, *11*(8), 1–31. https://doi.org/10.3390/foods11081124

Magan, J. B., O′Callaghan, T. F., Kelly, A. L., & McCarthy, N. A. (2021). Compositional and functional properties of milk and dairy products derived from cows fed pasture or concentrate-based diets. *Comprehensive Reviews in Food Science and Food Safety*, *20*(3), 2769–2800. https://doi.org/10.1111/1541-4337.12751

Manikas, I., & Manos, B. (2009). Design of an integrated supply chain model for supporting traceability of dairy products. *International Journal of Dairy Technology*, *62*(1), 126–138.

https://doi.org/10.1111/j.1471-0307.2008.00444.x

Manley, M. (2014). Near-infrared spectroscopy and hyperspectral imaging: Non-destructive analysis of biological materials. *Chemical Society Reviews*, *43*(24), 8200–8214. https://doi.org/10.1039/c4cs00062e

Manley, M., & Baeten, V. (2018). Spectroscopic Technique : Near Infrared (NIR) Spectroscopy, in Sun D.W. (ed), *Modern Techniques for Food Authentication (2nd ed)*. Elsevier Inc, pp. 65-116. https://doi.org/10.1016/B978-0-12-814264-6.00003-7

Manuelian, C. L., Currò, S., Penasa, M., Cassandro, M., & De Marchi, M. (2017). Prediction of minerals, fatty acid composition and cholesterol content of commercial cheeses by near infrared transmittance spectroscopy. *International Dairy Journal*, *71*, 107–113. https://doi.org/10.1016/j.idairyj.2017.03.011

Martin .A, K. (1992). Recent Advances in Near- Infrared Reflectance Spectroscopy. *Applied Spectroscopy Reviews,* 27 (4). https://doi.org/10.1080/05704929208018109

Martins, M., Marins-gonçalves, L., & Souza, D. De. (2024). An integrative review of analytical techniques used in food authentication : A detailed description for milk and dairy products. *Food Chemistry*, *457*(March), 140206. https://doi.org/10.1016/j.foodchem.2024.140206

Maryniak, N. Z., Hansen, E. B., Ballegaard, A. S. R., Sancho, A. I., & Bøgh, K. L. (2018). Comparison of the allergenicity and immunogenicity of Camel and cow's milk—A study in brown Norway rats. *Nutrients*, *10*(12). https://doi.org/10.3390/nu10121903

Maryniak, N. Z., Sancho, A. I., Hansen, E. B., & Bøgh, K. L. (2022). Alternatives to Cow's Milk-Based Infant Formulas in the Prevention and Management of Cow's Milk Allergy. *Foods*, *11*(7). https://doi.org/10.3390/foods11070926

McClure, W. F. (2003). 204 Years of near infrared technology: 1800-2003. *Journal of Near Infrared Spectroscopy*, *11*(6), 487–518. https://doi.org/10.1255/jnirs.399

McDermott, A., Visentin, G., De Marchi, M., Berry, D. P., Fenelon, M. A., O'Connor, P. M., Kenny, O. A., & McParland, S. (2016). Prediction of individual milk proteins including free amino acids in bovine milk using mid-infrared spectroscopy and their correlations with milk processing characteristics. *Journal of Dairy Science*, *99*(4), 3171–3182. https://doi.org/10.3168/jds.2015-9747

Mendoza-martinez, G. D., Diaz, L., Le, D., Relling, A. E., Vazquez-valladolid, A., Palacios-mart, M., Abel, P., Chay-canul, A. J., Flores-ramirez, R., & Roque-jim, A. (2022). Application of

an Electronic Nose and HS-SPME / GC-MS to. *Foods*, *11*(1887).

Michael, N. A., Al Ibrahim, M. A., Scheibe, C., & Craigie, N. (2025). Best practices of utilizing principal component analysis in chemostratigraphic studies. *Applied Geochemistry*, *186*(November 2024), 106355. https://doi.org/10.1016/j.apgeochem.2025.106355

Moatsou, G. (2024). Emerging Technologies for Improving Properties , Shelf Life , and analysis of dairy products. *Foods,* 13(7), 1078. https://doi.org/10.3390/foods13071078

Mohammadi, S., Gowen, A., Luo, J., & O'Donnell, C. (2024). Prediction of milk composition using multivariate chemometric modelling of infrared, Raman, and fluorescence spectroscopic data: A review. *Food Control*, *165*(June), 110658. https://doi.org/10.1016/j.foodcont.2024.110658

Muncan, J., Kovacs, Z., Pollner, B., Ikuta, K., Ohtani, Y., Terada, F., & Tsenkova, R. (2021). Near infrared aquaphotomics study on common dietary fatty acids in cow's liquid, thawed milk. *Food Control*, *122*(June 2020), 107805. https://doi.org/10.1016/j.foodcont.2020.107805

Muncan, J., Tei, K., & Tsenkova, R. (2021). Real-time monitoring of yogurt fermentation process by aquaphotomics near-infrared spectroscopy. *Sensors (Switzerland)*, *21*(1), 1–18. https://doi.org/10.3390/s21010177

Nasralla, N. N., Gomah, N. H., Aly, M. M., Abdel-aleem, J. A., Hammam, A. R. A., Osman, D. M., & El-derwy, Y. M. A. (2022). Compositional characteristics of dairy products and their potential nondairy applications after shelf-life Current Research in Food Science Compositional characteristics of dairy products and their potential nondairy applications after shelf-life. *Current Research in Food Science*, *5*(January), 150–156. https://doi.org/10.1016/j.crfs.2021.12.017

Núñez-Sánchez, N., Martínez-Marín, A. L., Polvillo, O., Fernández-Cabanás, V. M., Carrizosa, J., Urrutia, B., & Serradilla, J. M. (2016). Near Infrared Spectroscopy (NIRS) for the determination of the milk fat fatty acid profile of goats. *Food Chemistry*, *190*, 244–252. https://doi.org/10.1016/j.foodchem.2015.05.083

Okparanma, R. N., Araka, P. P., Ayotamuno, J. M., Mouazen, A. M., & Harcourt, P. (2018). Towards enhancing sustainable reuse of pre-treated drill cuttings for construction purposes by near-infrared analysis : A review. *Journal of civil engineering and construction technology*, *9*(3), 19–39. https://doi.org/10.5897/JCECT2018.048

Osborne, B. G., Fearn, T., Hindle, P. H., & Hindle, P. T. (1993). Practical NIR Spectroscopy with

Applications in Food and Beverage Analysis. Longman Scientific & Technical. https://books.google.hu/books?id=HkawxwEACAAJ

Parson, W. W. (2015). Modern Optical Spectroscopy With Exercises and Examples from biophysics and biochemistry (2nd ed). Springer: Berlin. 10.1007/978-3-662-46777-0

Pasquini, C. (2017). Near Infrared Spectroscopy : Fundamentals , Practical Aspects and Analytical Applications. *Journal of the Brazilian Chemical Society*, 14(2). https://doi.org/10.1590/S0103-50532003000200006

Pasquini, C. (2018). Analytica Chimica Acta Near infrared spectroscopy : A mature analytical technique with new perspectives e A review. *Analytica Chimica Acta*, *1026*, 8–36. https://doi.org/10.1016/j.aca.2018.04.004

Patil, G. B., Wani, S. P., Bafna, P. S., Bagul, V. S., Kalaskar, M. G., & Mutha, R. E. (2024). Milk adulteration : From detection to health impact. *Food and Humanity*, *3*(June), 100339. https://doi.org/10.1016/j.foohum.2024.100339

Peinado, I., Miles, W., & Koutsidis, G. (2016). Odour characteristics of seafood flavour formulations produced with fish by-products incorporating EPA, DHA and fish oil. *Food Chemistry*, *212*, 612–619. https://doi.org/10.1016/j.foodchem.2016.06.023

Pellicer, A., & Bravo, C. (2011). Seminars in Fetal & Neonatal Medicine Near-infrared spectroscopy : A methodology-focused review. *Seminars in Fetal and Neonatal Medicine*, *16*(1), 42–49. https://doi.org/10.1016/j.siny.2010.05.003

Pieszka, M., Łuszczyński, J., Zamachowska, M., Augustyn, R., Długosz, B., & Hędrzak, M. (2016). Is mare milk an appropriate food for people? - A review. *Annals of Animal Science*, *16*(1), 33–51. https://doi.org/10.1515/aoas-2015-0041

Porep, J. U., Kammerer, D. R., & Carle, R. (2015). On-line application of near infrared (NIR) spectroscopy in food production. *Trends in Food Science and Technology*, *46*(2), 211–230. https://doi.org/10.1016/j.tifs.2015.10.002

Porwal, G., Jain, K., Mohapatra, S., Dhayal, V., & Chopra, I. (2024). A Comprehensive Analysis and Detection Methodology Using Near-Infrared (NIR) Spectroscopy to Unveil the Deceptive Practice of Milk Adulteration . *Eng. Proc*, 59, 196.

Praveen, M. (2025). Microbial Fermentation in Food and Beverage Industries : Innovations , Challenges , and Opportunities. *Foods*, 14(1), 114.https://doi.org/10.3390/foods14010114

Priyashantha, H., & K.Vidanarachchi, J. (2024). Advancements in Dairy Research : Exploring

Nutritional. *Animals*, *14*. https://doi.org/https://doi.org/10.3390/ani14131870

Pu, Y. Y., O'Donnell, C., Tobin, J. T., & O'Shea, N. (2020). Review of near-infrared spectroscopy as a process analytical technology for real-time product monitoring in dairy processing. *International Dairy Journal*, *103*, 104623. https://doi.org/10.1016/j.idairyj.2019.104623

Pugliese, A., Cabassi, G., Chiavaro, E., Paciulli, M., Carini, E., & Mucchetti, G. (2017). Physical characterization of whole and skim dried milk powders. *Journal of Food Science and Technology*, *54*(11), 3433–3442. https://doi.org/10.1007/s13197-017-2795-1

Qiao, L., Mu, Y., Lu, B., & Tang, X. (2023). Calibration Maintenance Application of Near-infrared Spectrometric Model in Food Analysis. *Food Reviews International*, *39*(3), 1628–1644. https://doi.org/10.1080/87559129.2021.1935999

Rashidinejad, A., Bremer, P., Birch, J., & Oey, I. (2017). and Disease, in Watson, RR., Collier, R J., Preedy, V R. (eds), *Nutrients in Dairy and Their Implications for Health and Disease*. Academic Press. https://doi.org/10.1016/B978-0-12-809762-5.00014-0

Rațu, R. N., Cârlescu, P. M., Usturoi, M. G., Lipșa, F. D., Veleșcu, I. D., Arsenoaia, V. N., Florea, A. M., Ciobanu, M. M., Radu-Rusu, R. M., Postolache, A. N., & Simeanu, D. (2023). Effects of Dairy Cows Management Systems on the Physicochemical and Nutritional Quality of Milk and Yogurt, in a North-Eastern Romanian Farm. *Agriculture (Switzerland)*, *13*(7), 1–20. https://doi.org/10.3390/agriculture13071295

Ray, S. (2023). Sensory Properties of Foods and Their Measurement Methods, in Khan, MS., Rahman, MS.(eds), Techniques to Measure Food Safety and Quality. Springer. https://doi.org/10.1007/978-3-030-68636-9

Sager, M., Mcculloch, C. R., & Schoder, D. (2018). Heavy metal content and element analysis of infant formula and milk powder samples purchased on the Tanzanian market : International branded versus black market products. *Food Chemistry*, *255*(June 2017), 365–371. https://doi.org/10.1016/j.foodchem.2018.02.058

Sarita, B., & Kovaleva, E. G. (2025). A comprehensive review of probiotics and human health-current prospective and applications. *Front. Microbiol*. https://doi.org/10.3389/fmicb.2024.1487641

Savitzky, A., & Golay, M. J. E. (1964). Smoothing and Differentiation of Data by Simplified Least Squares Procedures. *Analytical Chemistry*, *36*(8), 1627–1639. https://doi.org/10.1021/ac60214a047

Schuck, P. (2011). Milk powder: Physical and functional properties of milk powders, in Fuquay, J.W. (Ed), *Encyclopedia of dairy sciences (2nd ed)*. Elsevier: Amsterdam, The Netherlands, pp. 117–124. https://doi.org/978-0-12-374402-9

Seifu, E. (2023). Camel milk products: innovations, limitations and opportunities. *Food Production, Processing and Nutrition*, *5*(1). https://doi.org/10.1186/s43014-023-00130-7

Sghaier, L., Cordella, C. B. Y., Rutledge, D. N., Watiez, M., Breton, S., Kopczuk, A., Sassiat, P., Thiebaut, D., & Vial, J. (2015). Comprehensive Two-dimensional Gas Chromatography for Analysis of the Volatile Compounds and Fishy Odor Off-flavors from Heated Rapeseed Oil. *Chromatographia*, *78*(11–12), 805–817. https://doi.org/10.1007/s10337-015-2897-8

Shahidi, F., & Ambigaipalan, P. (2018). Omega-3 Polyunsaturated Fatty Acids and Their Health Benefits. *Annual Review of Food Science and Technology*, *9*, 345–381. https://doi.org/10.1146/annurev-food-111317-095850

Sharma, A., Jana, A. H., & Chavan, R. S. (2012). Functionality of Milk Powders and Milk-Based Powders for End Use Applications-A Review. *Comprehensive Reviews in Food Science and Food Safety,* 11(5), 518–528). https://doi.org/10.1111/j.1541-4337.2012.00199.x

Sharma, S., Sirisomboon, P., K.C, S., Terdwongworakul, A., Phetpan, K., Kshetri, T. B., & Sangwanangkul, P. (2023). Near-infrared hyperspectral imaging combined with machine learning for physicochemical-based quality evaluation of durian pulp. *Postharvest Biology and Technology*, *200* (October 2022), 112334. https://doi.org/10.1016/j.postharvbio.2023.112334

Shen, F., Niu, X., Yang, D., Ying, Y., Li, B., Zhu, G., & Wu, J. (2010). Determination of amino acids in Chinese rice wine by fourier transform near-infrared spectroscopy. *Journal of Agricultural and Food Chemistry*, *58*(17), 9809–9816. https://doi.org/10.1021/jf1017912

Shawky, E., Nahar, L., Nassief, S. M., Sarker, S. D., & Ibrahim, R. S. (2024a). Dairy products authentication with biomarkers: A comprehensive critical review. *Trends in Food Science and Technology*, *147*(December 2023), 104445. https://doi.org/10.1016/j.tifs.2024.104445

Shawky, E., Nahar, L., Nassief, S. M., Sarker, S. D., & Ibrahim, R. S. (2024b). Spice authentication by near-infrared spectroscopy: Current advances, limitations, and future perspectives. *Trends in Food Science and Technology*, *148* (April), 104522. https://doi.org/10.1016/j.tifs.2024.104522

Singh, S., Szostak, R., & Czarnecki, M. A. (2021). Vibrational intensities and anharmonicity in

MIR , NIR and Raman theoretical study. *Journal of Molecular Liquids*, 336, 116277. https://doi.org/10.1016/j.molliq.2021.116277

Singh, P., Habiba, U., Shafi, Z., Noor, A., Pandey, V. K., & Singh, R. (2025). Understanding the Concepts of Smart E-nose Technology in Combination With Machine Learning for New Era of Food Safety: An Advanced Review. *Food Safety and Health*, 1–17. https://doi.org/10.1002/fsh3.70029

Soares, F., & Anzanello, M. J. (2018). Support vector regression coupled with wavelength selection as a robust analytical method. *Chemometrics and Intelligent Laboratory Systems*, *172*, 167–173. https://doi.org/https://doi.org/10.1016/j.chemolab.2017.12.007

Štefániková, J., Nagyová, V., Hynšt, M., Vietoris, V., Martišová, P., & Nagyová, Ľ. (2019). Application of electronic nose for determination of Slovak cheese authentication based on aroma profile. *Potravinarstvo Slovak Journal of Food Sciences*, *13*(1), 262–267. https://doi.org/10.5219/1076

Skeie, S., Feten, G., Almøy, T., Østlie, H., & Isaksson, T. (2006). The use of near infrared spectroscopy to predict selected free amino acids during cheese ripening. *International Dairy Journal*, *16*(3), 236–242. https://doi.org/10.1016/j.idairyj.2005.03.008

Sørensen, K. M., Khakimov, B., & Engelsen, S. B. (2016). The use of rapid spectroscopic screening methods to detect adulteration of food raw materials and ingredients. *Current Opinion in Food Science*, *10*(Figure 2), 45–51. https://doi.org/10.1016/j.cofs.2016.08.001

Stocco, G., Cipolat-Gotet, C., Ferragina, A., Berzaghi, P., & Bittante, G. (2019). Accuracy and biases in predicting the chemical and physical traits of many types of cheeses using different visible and near-infrared spectroscopic techniques and spectrum intervals. *Journal of Dairy Science*, *102*(11), 9622–9638. https://doi.org/10.3168/jds.2019-16770

Stocco, G., Gómez-Mascaraque, L. G., Deshwal, G. K., Sanchez, J. C., Molle, A., Pizzamiglio, V., Berzaghi, P., Gergov, G., & Cipolat-Gotet, C. (2024). Exploring the use of NIR and Raman spectroscopy for the prediction of quality traits in PDO cheeses. *Frontiers in Nutrition*, *11*(February). https://doi.org/10.3389/fnut.2024.1327301

Suksangpanomrung, P., Ritthiruangdej, P., Hiriotappa, A., & Therdthai, N. (2024). Rapid, non-destructive prediction of coconut composition for sustainable UHT milk production via near-infrared spectroscopy. *Journal of Food Composition and Analysis*, *128*(January), 106009. https://doi.org/10.1016/j.jfca.2024.106009

Sutariya, S. G., Huppertz, T., & Patel, H. A. (2017). Influence of milk pre-heating conditions on casein–whey protein interactions and skim milk concentrate viscosity. *International Dairy Journal*, *69*, 19–22. https://doi.org/10.1016/j.idairyj.2017.01.007

Swelum, A. A., El-Saadony, M. T., Abdo, M., Ombarak, R. A., Hussein, E. O. S., Suliman, G., Alhimaidi, A. R., Ammari, A. A., Ba-Awadh, H., Taha, A. E., El-Tarabily, K. A., & Abd El-Hack, M. E. (2021). Nutritional, antimicrobial and medicinal properties of Camel's milk: A review. *Saudi Journal of Biological Sciences*, *28*(5), 3126–3136. https://doi.org/10.1016/j.sjbs.2021.02.057

Tang, Y., Yu, M., Liu, C., Gao, X., & Song, H. (2024). Sensory-directed characterization of key odor-active compounds in fermented milk. *Journal of Food Composition and Analysis*, *126*(December 2023), 105904. https://doi.org/10.1016/j.jfca.2023.105904

Teixeira Dos Santos, C. A., Lopo, M., Páscoa, R. N. M. J., & Lopes, J. A. (2013). A review on the applications of portable near-infrared spectrometers in the agro-food industry. *Applied Spectroscopy*, *67*(11), 1215–1233. https://doi.org/10.1366/13-07228

Tian, H., Chen, B., Lou, X., Yu, H., Yuan, H., Huang, J., & Chen, C. (2022). Rapid detection of acid neutralizers adulteration in raw milk using FGC E-nose and chemometrics. *Journal of Food Measurement and Characterization*, *16*(4), 2978–2988. https://doi.org/10.1007/s11694-022-01403-4

Tian, H., Liu, H., He, Y., Chen, B., Xiao, L., Fei, Y., Wang, G., Yu, H., & Chen, C. (2020). Combined application of electronic nose analysis and back-propagation neural network and random forest models for assessing yogurt flavor acceptability. *Journal of Food Measurement and Characterization*, *14*(1), 573–583. https://doi.org/10.1007/s11694-019-00335-w

Tian, H., Shen, Y., Yu, H., He, Y., & Chen, C. (2017). Effects of 4 Probiotic Strains in Coculture with Traditional Starters on the Flavor Profile of Yogurt. *Journal of Food Science*, *82*(7), 1693–1701. https://doi.org/10.1111/1750-3841.13779

Tian, H., Wu, D., Chen, B., Yuan, H., Yu, H., Lou, X., & Chen, C. (2023). Rapid identification and quantification of vegetable oil adulteration in raw milk using a flash gas chromatography electronic nose combined with machine learning. *Food Control*, *150*, 109758. https://doi.org/https://doi.org/10.1016/j.foodcont.2023.109758

Tirgarian, B., Yadegari, H., Bagheri, A., Neshagaran, E., Mardani, M., & Farmani, J. (2023). Reduced-fat chocolate spreads developed by water-in-oleogel emulsions. *Journal of Food Engineering*, *337*, 111233. https://doi.org/10.1016/J.JFOODENG.2022.111233

Tóth, T., Mwau, P. J., Bázár, G., Andrássy-Baka, G., Hingyi, H., Csavajda, É., & Varga, L. (2019). Effect of feed supplementation based on extruded linseed meal and fish oil on composition and sensory properties of raw milk and ultra-high temperature treated milk. *International Dairy Journal*, *99*. https://doi.org/10.1016/j.idairyj.2019.104552

Tominaga, Y. (1999). Comparative study of class data analysis with PCA-LDA, SIMCA, PLS, ANNs, and k-NN. *Chemometrics and Intelligent Laboratory Systems*, *49*(1), 105–115. https://doi.org/https://doi.org/10.1016/S0169-7439(99)00034-9

Trout, G. M., & Lucas, P. S. (1947). A Comparison of the Babcock, Gerber, Minnesota, Pennsylvania, and Mojonnier Methods for Determining the Percentage of Fat in Homogenized Milk. *Journal of Dairy Science*, *30*(3), 145–159. https://doi.org/10.3168/jds.S0022-0302(47)92332-1

Tsenkova, R., Atanassova, S., Itoh, K., Ozaki, Y., & Toyoda, K. (2000). Near infrared spectroscopy for biomonitoring: Cow milk composition measurement in a spectral region from 1,100 to 2,400 nanometers. *Journal of Animal Science*, *78*(3), 515–522. https://doi.org/10.2527/2000.783515x

Tsenkova, R., Atanassova, S., Morita, H., Ikuta, K., Toyoda, K., Iordanova, I. K., & Hakogi, E. (2006). Near infrared spectra of cows' milk for milk quality evaluation: Disease diagnosis and pathogen identification. *Journal of Near Infrared Spectroscopy*, *14*(6), 363–370. https://doi.org/10.1255/jnirs.661

Valenti, B., Martin, B., Andueza, D., Leroux, C., Labonne, C., Lahalle, F., Larroque, H., Brunschwig, P., Lecomte, C., Brochard, M., & Ferlay, A. (2013). Infrared spectroscopic methods for the discrimination of cows' milk according to the feeding system, cow breed and altitude of the dairy farm. *International Dairy Journal*, *32*(1), 26–32. https://doi.org/10.1016/j.idairyj.2013.02.014

Varga-Visi, É., Jócsák, I., Kozma, V., Lóki, K., Ali, O., & Szabó, A. (2022). Effects of Surface Treatment with Thymol on the Lipid Oxidation Processes, Fatty Acid Profile and Color of Sliced Salami during Refrigerated Storage. *Foods*, *11*(23). https://doi.org/10.3390/foods11233917

Veena, V. B. N. (2024). Understanding the role of pH in cheese manufacturing : general aspects of cheese quality and safety. *Journal of Food Science and Technology*, *61*(1), 16–26. https://doi.org/10.1007/s13197-022-05631-w

Visconti, L. G., Diniz, P. H. G. D., de Sousa Fernandes, D. D., Rodriguez, M. S., & Di Anibal, C.

V. (2024). Authentication of grated hard cheeses and quantification of adulteration by FT-NIR spectroscopy and multivariate analysis. *International Dairy Journal*, *158*(December 2023), 106035. https://doi.org/10.1016/j.idairyj.2024.106035

Wang, C., Reis, M. G., Waterhouse, G. I. N., Hemar, Y., & Reis, M. M. (2021). Prediction of dairy powder functionality attributes using diffuse reflectance in the visible and near infrared (Vis-NIR) region. *International Dairy Journal*, *117*, 104981. https://doi.org/10.1016/j.idairyj.2021.104981

Wang, Y., Yu, M., Tang, Y., Wang, B., Song, H., Hou, B., & Li, B. (2024). Study on the flavor of brown milk fermented by Lactobacillus paracasei K56 in different strain states. *Journal of Food Composition and Analysis*, *125*(July 2023), 105777. https://doi.org/10.1016/j.jfca.2023.105777

Wang, M., & Chen, Y. (2024). Electronic nose and its application in the food industry: a review. In *European Food Research and Technology* (Vol. 250, Issue 1). Springer Berlin Heidelberg. https://doi.org/10.1007/s00217-023-04381-z

Wasana, W. P., Waterland, M., & Everett, D. W. (2025). Functional Significance of Probiotic Bacterial Interactions with Milk Fat Globules in a Human Host. *Microrganisms*, 13(2), 223. https://doi.org/10.3390/microorganisms13020223

Wei, F., & Seng, K. (2021). A review on recent near infrared spectroscopic measurement setups and their challenges. *Measurement*, *171*(November 2020), 108732. https://doi.org/10.1016/j.measurement.2020.108732

Wetzel, D. L. B. (1998). Analytical near infrared spectroscopy. *Developments in Food Science*, *39*(C), 141–194. https://doi.org/10.1016/S0167-4501(98)80009-5

Weyer, L. G., Lo, S., & Point, W. (2006). Spectra – Structure Correlations in the Near-infrared, in *Handbook of Vibrational Spectroscopy*. John Wiley & Sons, Ltd.: Hoboken, NJ, USA. https://doi.org/10.1002/9780470027325.s4102

Williams, P. C., & Stevensen, S. G. (1990). Near-infrared reflectance analysis: food industry applications. *Trends in Food Science and Technology*, *1*(C), 44–48. https://doi.org/10.1016/0924-2244(90)90030-3

Woodcock, T., Downey, G., & O'Donnell, C. P. (2008). Better quality food and beverages: The role of near infrared spectroscopy. *Journal of Near Infrared Spectroscopy*, *16*(1), 1–29. https://doi.org/10.1255/jnirs.758

Wu, D., He, Y., & Feng, S. (2008). Short-wave near-infrared spectroscopy analysis of major compounds in milk powder and wavelength assignment. *Analytica Chimica Acta*, *610*(2), 232–242. https://doi.org/10.1016/j.aca.2008.01.056

Wu, T., Chen, H., Lin, Z., & Tan, C. (2016). Identification and Quantitation of Melamine in Milk by Near-Infrared Spectroscopy and Chemometrics. *Journal of Spectroscopy*, *2016*. https://doi.org/10.1155/2016/6184987

Yang, Y., & Wei, L. (2021). Application of E-nose technology combined with artificial neural network to predict total bacterial count in milk. *Journal of Dairy Science*, *104*(10), 10558–10565. https://doi.org/10.3168/jds.2020-19987

Yakubu, H. G., Ali, O., Szabó, A., Tóth, T., & Bazar, G. (2023). Feeding Mixed Silages of Winter Cereals and Italian Ryegrass Can Modify the Fatty Acid and Odor Profile of Bovine Milk. *Agriculture (Switzerland)*, *13*(2). https://doi.org/10.3390/agriculture13020381

Yakubu, H. G., Kovacs, Z., Toth, T., & Bazar, G. (2022). The recent advances of near-infrared spectroscopy in dairy production—a review. *Critical Reviews in Food Science and Nutrition*, *62*(3), 810–831. https://doi.org/10.1080/10408398.2020.1829540

Yang, S., Bai, M., Kwok, L., Zhong, Z., & Sun, Z. (2025). The intricate symbiotic relationship between lactic acid bacterial starters in the milk fermentation ecosystem. *Critical Reviews in Food Science and Nutrition*, *65*(4), 728–745. https://doi.org/10.1080/10408398.2023.2280706

Yang, X., & Berzaghi, P. (2024). Near-Infrared Spectroscopy, in A. M. Jiménez-Carvelo, A. Arroyo-Cerezo, & L. Cuadros-Rodríguez (eds), *Non-invasive and Non-destructive Methods for Food Integrity*. Springer Nature Switzerland, pp. 41–59. https://doi.org/10.1007/978-3-031-76465-3_3

Yang, X., Guang, P., Xu, G., Zhu, S., Chen, Z., & Huang, F. (2020). Manuka honey adulteration detection based on near-infrared spectroscopy combined with aquaphotomics. *Lwt*, *132*(June), 109837. https://doi.org/10.1016/j.lwt.2020.109837

Yerlikaya, O. (2023). A review of fermented milks: potential beneficial effects on human nutrition and health. *African Health Sciences*, *23*(4), 498–507. https://doi.org/10.4314/ahs.v23i4.54

You, L. Q., Wang, Y. R., Bai, S., Wang, X. Y., & Wei, Z. J. (2024). Impact of ripening periods on the key volatile compounds of Cheddar cheese evaluated by sensory evaluation, instrumental analysis and chemometrics method. *Applied Food Research*, *4*(2), 100578.

https://doi.org/10.1016/j.afres.2024.100578

Yu, H., Liu, H., Erasmus, S. W., Zhao, S., Wang, Q., & van Ruth, S. M. (2020). Rapid high-throughput determination of major components and amino acids in a single peanut kernel based on portable near-infrared spectroscopy combined with chemometrics. *Industrial Crops and Products*, *158*(July), 112956. https://doi.org/10.1016/j.indcrop.2020.112956

Yu, X., Sun, Y., Shen, X., Li, W., Cai, H., Guo, S., & Sun, Z. (2024). Effect of different isolation sources of Lactococcus lactis subsp. lactis on volatile metabolites in fermented milk. *Food Chemistry: X*, *21*(October 2023), 101224. https://doi.org/10.1016/j.fochx.2024.101224

Zouari, A., Perrone, Í. T., Schuck, P., Gaucheron, F., Dolivet, A., Attia, H., & Ayadi, M. A. (2019). Effect of outlet drying temperature and milk fat content on the physicochemical characteristics of spray-dried camel milk powder. *Drying Technology*, *37*(13), 1615–1624. https://doi.org/10.1080/07373937.2018.1526189

Zouari, A., Schuck, P., Gaucheron, F., Triki, M., Delaplace, G., Gauzelin-Gaiani, C., Lopez, C., Attia, H., & Ayadi, M. A. (2020). Microstructure and chemical composition of camel and cow milk powders' surface. *Lwt*, *117*(May 2019), 108693. https://doi.org/10.1016/j.lwt.2019.108693

Zou, Z., Duley, J. A., Cowley, D. M., Reed, S., Arachchige, B. J., Bhandari, B., Shaw, P. N., & Bansal, N. (2022). Physicochemical Properties and Whey Proteomes of Camel Milk Powders Produced by Different Concentration and Dehydration Processes. *Foods*, *11*(5). https://doi.org/10.3390/foods11050727

Zifarelli, A., Giglio, M., Menduni, G., Sampaolo, A., Patimisco, P., Passaro, V. M. N., Wu, H., Dong, L., & Spagnolo, V. (2020). Partial Least-Squares Regression as a Tool to Retrieve Gas Concentrations in Mixtures Detected Using Quartz-Enhanced Photoacoustic Spectroscopy. *Analytical Chemistry*, *92*(16), 11035–11043. https://doi.org/10.1021/acs.analchem.0c00075

ACKNOWLEDGMENT

First and foremost, all thanks for **God Almighty**

I would like to express my sincere gratitude to the **Tempus Public Foundation** and the **Stipendium Hungaricum Program** for their generous support throughout my doctoral studies. My heartfelt thanks go to my **family and friends** for their unwavering encouragement, patience, and love during this journey.

I am deeply thankful to my **supervisors**, as well as the **professors and colleagues** at the **Department of Food Measurements and Process Control, MATE**, whose guidance, expertise, and support were invaluable to my academic and personal growth.